2 cy

HEDL-TME 71-41
UC-80, REACTOR
TECHNOLOGY

ANALYSIS OF FTR PHASE B CRITICAL EXPERIMENTS PART 4 ZPR-III ASSEMBLY 56B

MAY 1971

HANFORD ENGINEERING DEVELOPMENT LABORATORY
UNITED STATES ATOMIC ENERGY COMMISSION

Operated by
WADCO CORPORATION

CONTRACT AT(45-1)-2170

HEDL-TME-71-41
UC-80, REACTOR
TECHNOLOGY

ANALYSIS OF FTR PHASE B CRITICAL EXPERIMENTS PART 4 ZPR-III ASSEMBLY 56B

MAY 1971

S. L. Engstrom

R. A. Bennett

HANFORD ENGINEERING DEVELOPMENT LABORATORY
UNITED STATES ATOMIC ENERGY COMMISSION

Operated by
WADCO CORPORATION

CONTRACT AT(45-1)-2170

ANALYSIS OF FTR PHASE B CRITICAL EXPERIMENTS

PART 4

ZPR-III ASSEMBLY 56B

S. L. Engstrom and R. A. Bennett

ABSTRACT

Critical experiments in support of the design of the Fast Flux Test Reactor have been carried out in ZPR-III Assemblies 48, 48A, 51, 52 a through f, and 56B, by personnel of Argonne National Laboratory. This report presents the results and analysis of the experiments performed in Assembly 56B. Measured and calculated values are presented of critical mass, control rod worths, fuel column worths, central fission ratios, and spatial reaction rates. Two dimensional diffusion theory is used with a 26 energy group basic cross section set.

TABLE OF CONTENTS

LIST OF FIGURES

LIST OF TABLES

INTRODUCTION

A critical experiments program is being carried out in support of the design of the Fast Test Reactor (FTR) of the Fast Flux Test Facility (FFTF). The experiments are being conducted at the Argonne National Laboratories in their "Zero Power Facilities". The program is two fold: first, experiments are being conducted to obtain data for use in evaluation of calculational models being used in the design and determination of FTR neutronics characteristics; second, engineering mockup experiments are to be performed to verify the preliminary design of FTR.

To achieve the first objective the program initially had two phases, A and B. The phase A experiments dealt primarily with control rod experiment-theory correlations. Analyses, using few group diffusion and transport theory were made and reported[1]. The phase B experiments were originally designed to progressively investigate the neutronics of the dispersed core concept of FTR, specifically the split core concept. A large number of experiments were performed and analyzed, and are reported as Parts 1[2] and 2[3] and 3[4] of the phase B program. The present report describes the results of an analysis of Part 4 or the phase B experiments which consisted of measurements of critical mass, peripheral and central rod and fuel worths, reaction rate traverses and central fission ratios in a non-dispersed, 600 liter, Pu-fueled, reflected assembly; ZPR-III, Assembly 56B.

SUMMARY

A brief summary is presented here of the conclusions reached in the analysis of the ZPR-III, Assembly 56B experiments and their correlations with results obtained from the analysis of earlier experiments. Subjects summarized are experiment-theory correlations on critical mass and multiplication constants, control strengths, central fission rate ratios, and spatial power density distributions.

MULTIPLICATION CONSTANTS

Asymmetries in the reference configuration of Assembly 56B were removed, using differential experimental data, to provide a symmetric system for analysis. The adjusted assembly had a fissile mass of 334.4 kg of $^{239}Pu + ^{241}Pu + ^{235}U$ and a multiplication constant of 1.00135. The calculated multiplication constant for this adjusted assembly was 1.00413, which yields an experiment-to-calculation ratio of 1.00278. This value is approximately 1% higher than that found in the Analyses of ZPR-III Assembly 52a[3], which had a fissile mass of 200.7 kg and core volume of approximately 300ℓ. One may expect a slight dependence upon reactor size and hence a slightly higher C/E for the 1000ℓ, 500 kg fissile, FTR. If the larger FTR criticals, FTR-2 and FTR-3, verify this trend to over-calculate the multiplication constant, then the initial calculated design enrichment for FTR will have to be increased slightly to provide the desired excess reactivity.

LARGE IN-CORE CONTROL STRENGTHS

Experiments and analyses indicate an estimate of the bias in the FTR design model for in-core B_4C control rods of +10%, i.e., the model overestimates the control strength of a central rod by 10%. This value is larger than that found in ZPR-III Assembly 48 and 51 analyses by as much as 5%.

Earlier models had fewer broad energy groups (5 and 8) compared to the 13-group model used here and in design calculations. Since one would actually expect this model to be better, it must be concluded that 5 and 10% overestimates are from a statistical distribution whose mean is in the

vicinity of 5 to 10%. A more precise statement can be made following the completion of analyses of other in-core rod experiments later in the FTR Critical Experiments program.

LARGE PERIPHERAL CONTROL ROD STRENGTHS

The bias in the model for calculating peripheral control rod strengths, similar in strength to those anticipated for the FTR, is +2% based upon the analyses reported here. This value is in agreement with the lower limit found on the analysis of ZPR-III Assembly 48A[1] experiments. The upper limit on the calculational bias in those earlier experiments was +11%. One must conclude, therefore, that this calculation model, and hence the present model used in FTR design could overestimate peripheral control strenghts by as much as +11%. FTR 2 and 3 experiment analyses are expected to provide sufficient data for a statistical assessment of this bias.

REACTIVITY WORTHS OF CORE MATERIALS

Reactivity shimming with fuel drivers in FTR and changes in test loop compositions were simulated in these experiments to test models for calculating spatially distributed large reactivity perturbations. The central matrix tube of Assembly 56B was replaced with a sodium-stainless mixture. The reactivity worth was $-0.459\% \Delta k/_k$ and the C/E value was calculated to be 1.25. This C/E value is larger than that obtained for Pu + U worth experiments performed in Assembly 51[2] where the C/E value was 1.15. The latter C/E value is believed to be the best in view of the spatial dependence of C/E values for plutonium and uranium worth distributions. For example, the small sample C/E values as a function of axial position vary from 1.25 at the center to 1.00 near the axial core-reflector interface in Assembly 51, hence the C/E for a whole column of fuel should be less than 1.25 and greater than 1.0. These results are based on Keepen's[6] data and the C/E values could be reduced[7] by approximately 15% through the use of Master's data[8].

REACTION RATE TRAVERSES AND FISSION RATIOS

Calculated and measured reaction rate distributions for ^{239}Pu and ^{238}U fission and ^{10}B capture, when mutually normalized to the core center, do not show large disagreement within the core boundary. The measured and calculated ^{238}U fission curves generally agree throughout the core. For both ^{239}Pu fission and ^{10}B capture, the calculation underestimates the experimental values at the core-reflector interface. A further discrepancy is seen for ^{10}B capture in the radial reflector region. From this it may be concluded that:

(1) The calculated core-reflector interface spectrum may be defective.

(2) Either the low-energy calculated spectrum in the reflector, or the low-energy ^{10}B cross sections are in error.

The calculated and measured fission ratios for ^{233}U, ^{234}U, ^{236}U will respect to ^{235}U are in good agreement. While the disagreement for fission ratios of ^{238}U and ^{239}Pu with respect to ^{235}U is less than 10%, the discrepancy is greater than was expected from the analysis of fission ratios in other assemblies with the same codes and data. The calculated ^{240}Pu fission ratio with respect to ^{235}U is in very poor agreement with the experimental result. The experimental results are suspect, based upon measurements reported for Assembly ZPPR-1 (FTR-2)[25].

III. DETAILED EXPERIMENT AND ANALYSIS DESCRIPTIONS

All experiments in this portion of the Phase B Critical Experiments program were conducted in the ZPR III, Assembly 56B.[9-11] The core, approximating a 615 liter right circular cylinder, was fueled with plutonium and uranium metal and uranium oxide. Oxygen was added in the form of carbonates and oxides to simulate a PuO_2-UO_2 composition and Na was added to approximate a homogenized Na cooled FTR. The reflector was a Ni, Na and steel mixture.

In general, the core is composed of alternate columns of "A" and "B" drawers, containing differing amounts of fissile material. The assembly control requirements are met with eighteen control and safety drawers. The composition of the safety and control matrix cells are only slightly different from the typical "B", or high fuel content drawers of the columns in which they reside.

A. REFERENCE LOADING DESCRIPTION

Loading 56-17 is the reference loading for the 56B experiments. Areal profiles of halves one and two are shown in Figure 3.1. Core asymmetries in the two halves are as follows:

- o The lowest row containing core material has only three core matrix tubes compared to five on the left and top;
- o In half #2, the furthest column to the right in the core has only four matrix tubes of core material, hence half #2 has one less core drawer than half #1.
- o Safety rods, labelled S, are symmetric in both halves; however, the control rods, labelled C, are only in the lower portion of each half.
- o Vertical and horizontal asymmetries in the reflectors are denoted in Figure 3.1. Asymmetries in the boundary between reflectors 1 and 2 are not important as the compositions are nearly equivalent.

For purposes of calculation an inferred equivalent cylinder has been determined to have a core radius of 45.89 cm. and a height of 91.6 cm.

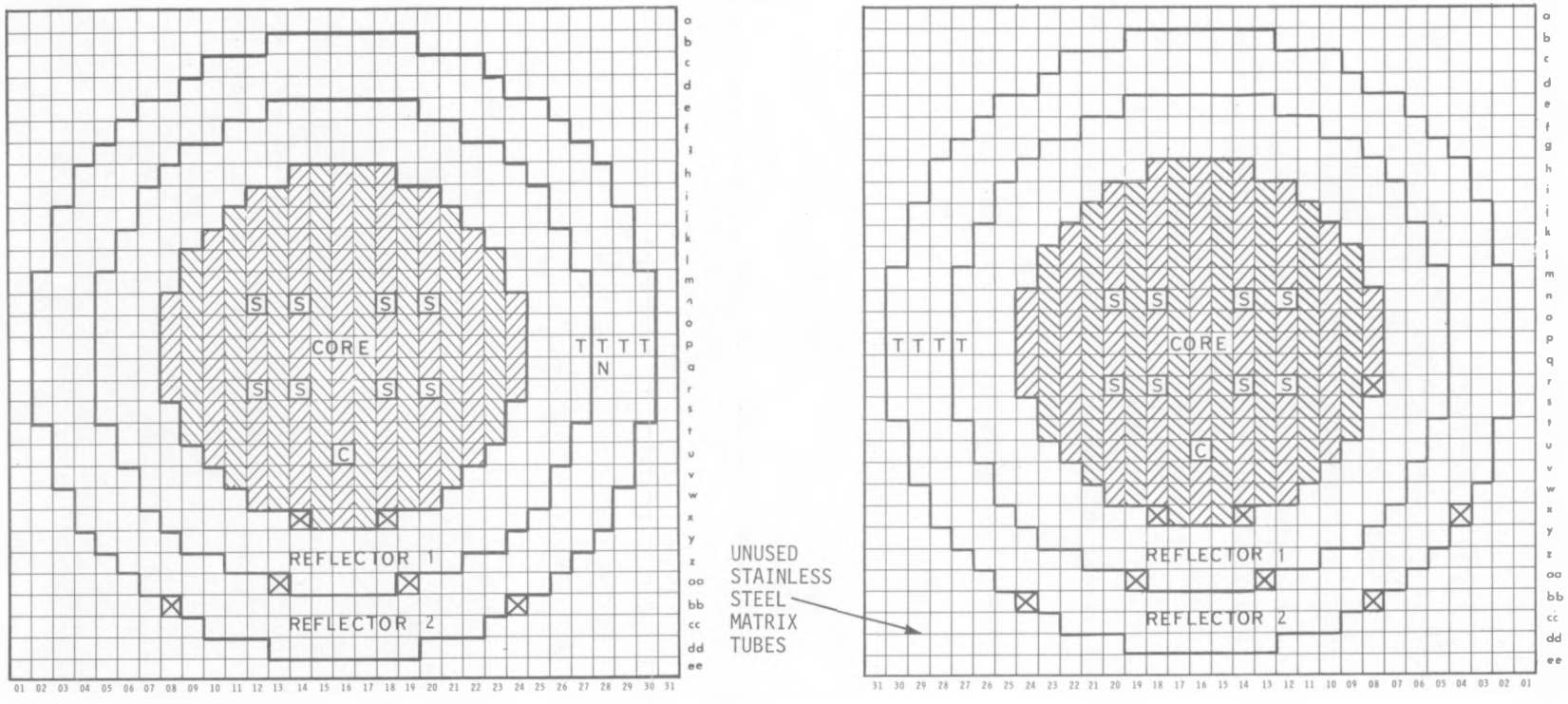

FIGURE 3.1 Reference Loading 56-17, Assembly 56B

The details of cylindricizing the assembly are given in Appendix A. Detailed dimensions, given on an axial cross section, are shown in Figure 3.2. The as-built atom densities for each zone are listed in Table 3.1. These atom densities reflect the air space and additional steel of the spring gaps. The latter is denoted in Figure 3.2 with dotted lines.

A close approximation to the average FTR fuel composition is arrived at through the platelet pattern represented in Figure 3.3 which extends over an "A" and "B", two drawer unit cell. The "B" drawers of this two drawer cell have the higher enrichment of ^{239}Pu. This zoning of alternate fuel column types will subsequently be referred to as a "striped core". The dimensions of a single matrix tube and drawer are given in Figure 3.4.

Of the three radial reflector zones, two are shown in Figure 3.1 and three in Figure 3.2. For calculational purposes, zones numbered two and three, Figure 3.2, are averaged as a single zone, denoted as, Reflector 2 in Figure 3.1 and Table 3.1, because the atom densities for the two zones are only slightly different. The unused portion of the stainless steel matrix tubes is shown in Figure 3.1. Where this region is included in calculations, it is referred to as Stainless Steel Mesh, and has the composition, listed under that heading, in Table 3.1.

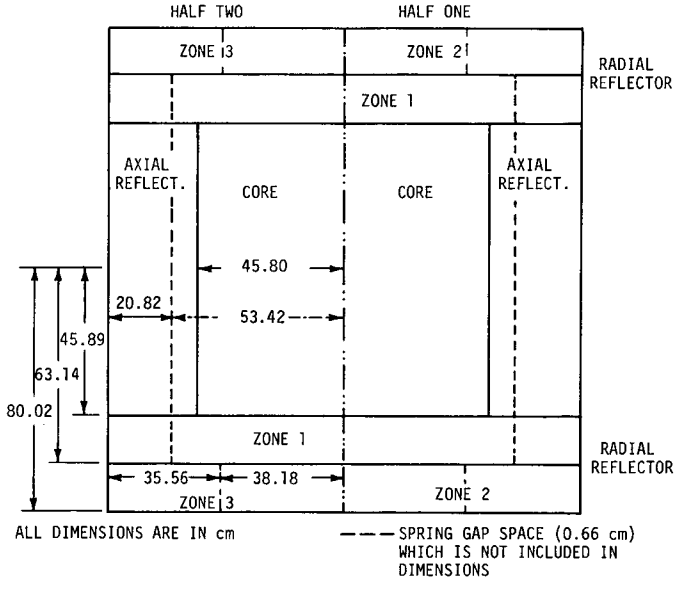

FIGURE 3.2 Equivalent Cylindrical Loading for Reference Core of Assembly 56B (Loading 56-17)

TABLE 3.1

ATOM DENSITIES FOR 56B EXPERIMENT ANALYSIS

ATOMS/BARN-CM FOR GIVEN ZONE

ISOTOPE	CORE, R-Z AVERAGE	CORE, X-Y AVERAGE	"A" DRAWER	"B" DRAWER	SAFETY & CONTROL
^{239}Pu	0.001332	0.001315	0.000886	0.001771	0.001708
^{240}Pu	0.000177	0.000175	0.000118	0.000235	0.000227
^{241}Pu	0.000025	0.000025	0.000017	0.000033	0.000031
^{238}U	0.006193	0.006176	0.005762	0.006617	0.006426
^{235}U	0.000014	0.000013	0.000012	0.000015	0.000014
O	0.015192	0.015183	0.014970	0.015410	0.012530
Fe	0.013757	0.013631	0.010370	0.017100	0.019490
Cr	0.002492	0.002496	0.002579	0.002406	0.003480
Ni	0.001090	0.001092	0.001129	0.001053	0.001523
Na	0.008669	0.008749	0.010760	0.006609	0.006546
Mo	0.000343	0.000339	0.000228	0.000457	0.000440
Si	0.000122	0.000122	0.000126	0.000118	0.000171
Mn	0.000104	0.000104	0.000108	0.000101	0.000145
C	0.001030	0.001070	0.002075	--	--

ISOTOPE	RADIAL REFLECTOR I	RADIAL REFLECTOR II	STAINLESS STEEL MESH	AXIAL REFLECTOR
Fe	0.007613	0.007728	0.004389	0.008825
Cr	0.001882	0.001917	0.001030	0.002188
Ni	0.047440	0.047710	0.000475	0.019480
Na	0.006535	0.006576	--	0.013460
Si	0.000113	0.000132	0.000030	0.000107
Mn	0.000294	0.000288	0.000043	0.000181

ISOTOPE	P-16, CENTRAL CONTROL ROD	PERIPHERAL CONTROL ROD
^{10}B	0.007124	0.007145
^{11}B	0.028890	0.028970
C	0.009331	0.009358
Fe	0.009642	0.010540
Cr	0.002470	0.002651
Ni	0.001115	0.001177
Na	0.009250	0.008736
Si	0.000139	0.000140
Mn	0.000120	0.000119

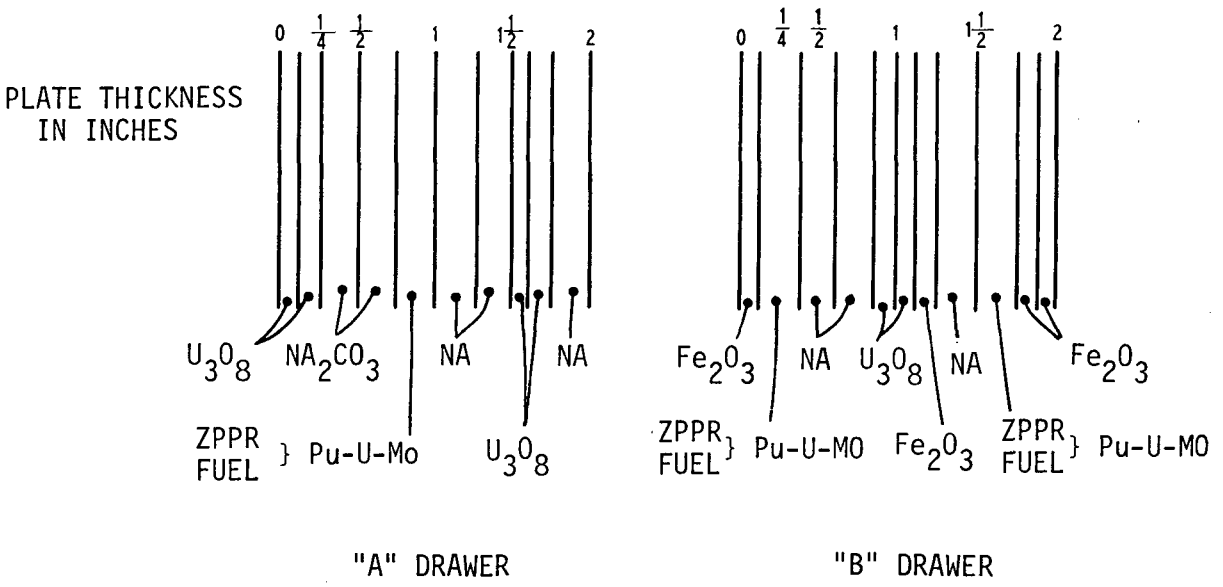

FIGURE 3.3 Assembly 56-B Drawer

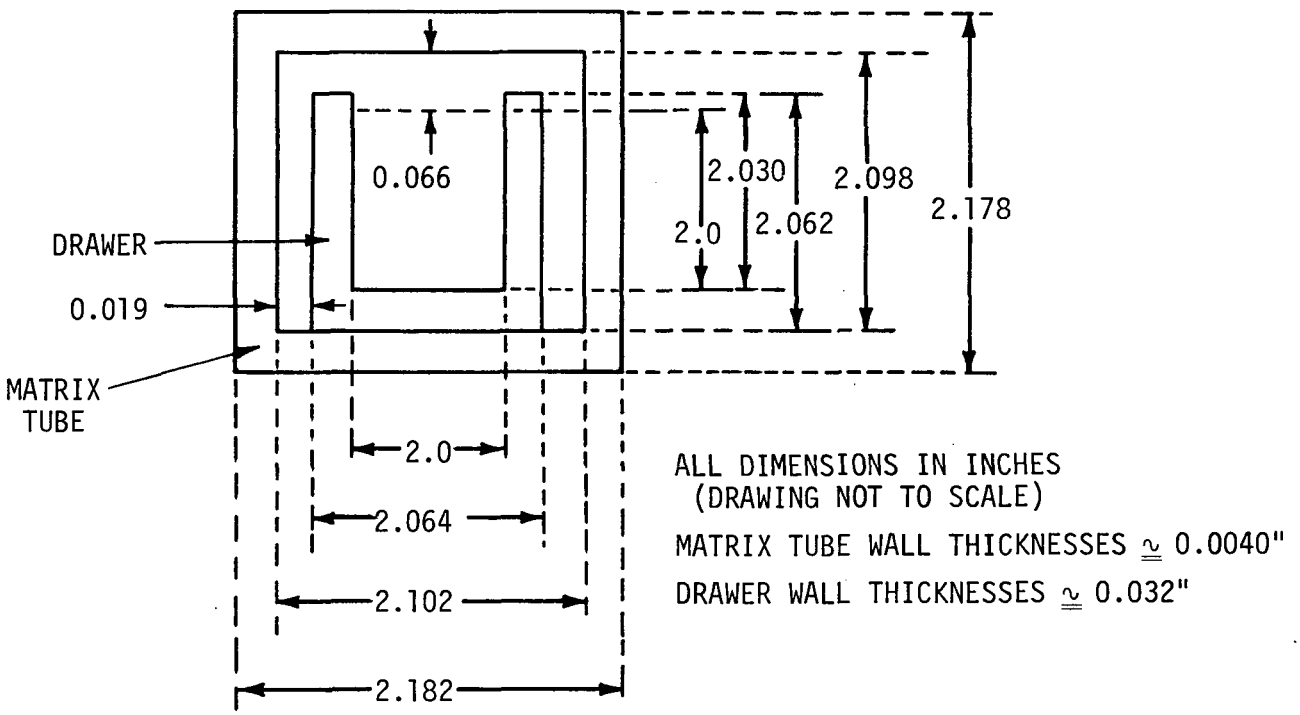

FIGURE 3.4 ZPR III Matrix Tube and Drawer Dimensions

B. DESCRIPTION OF CALCULATIONAL MODEL

A general calculational model was used for the analysis of the 56B experiments. Where alternate schemes or options are used, they will be described separately. Figure 3.5 is a flow diagram of the analytical method employed. The individual components of this diagram are described below, as they were specifically used in the 56B analysis. No attempt is made to describe all options available in the codes involved.

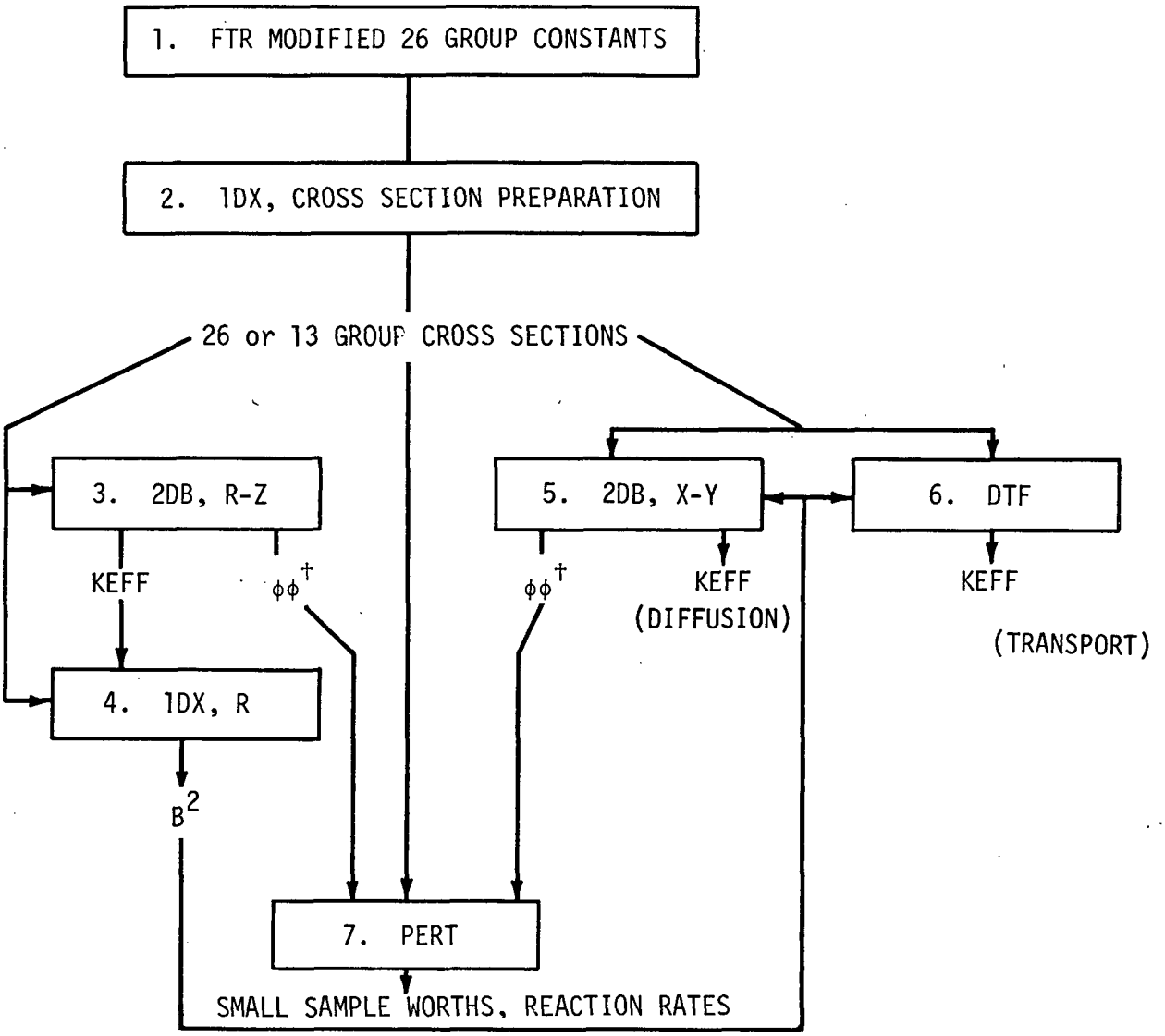

FIGURE 3.5 Flow Diagram of Calculational Model

1. FTR modified 26 group constants:[12] this is the original Bondarenko[13] set with some additional modifications. A list of the specific isotopes selected from the full set for use in the calculations is given in Appendix D.

2. IDX:[14] This is a diffusion theory program used for one-dimensional k_{eff} calculations, cross section preparation and buckling searches. The following IDX options were used:

   - o The 26 group cross sections were collapsed to 13 groups over zone averaged spectra;
   - o All cross sections were adjusted to 40°C;
   - o The transport cross section was reciprocally weighted in the collapsing process;
   - o Input buckling guess was $5.9 \times 10^{-4} cm^{-2}$.

3. 2DB:(15) This is a two-dimensional diffusion theory code. It was used as follows:

   - o In R-Z geometry, to calculate the k_{eff} of the cylindricized reference core;
   - o With 13 and 26 group cross sections;
   - o For the calculation of critical mass of a cylindricized core, for reactivity changes resulting from large central perturbations, and production of fluxes and adjoints for perturbation calculations.

4. 1DX: This is a diffusion theory program (described above) with buckling search option, given an input k_{eff} from step 3, calculates B^2 to be used for the axial leakage term in the following X-Y calculations.

5. 2DB: This is the same code as described above but in X-Y geometry, for accurate boundary descriptions:

   - o Uses B^2_z from 1DX to calculate DB^2_z for each material zone for leakage simulation;
   - o Uses either 13 or 26 group cross sections;
   - o Used usually with a quarter core description of the 56B assembly;

- o Calculates the critical mass of the as-built reference core, reactivity changes resulting from large perturbations, and produces fluxes and adjoints for perturbation calculations.

6. DTF-IV:[16] This is a one-dimensional transport theory code, similar in structure to 1DX, which is used for diffusion-transport approximation comparisons and platelet heterogeneity correction calculations.

7. PERT-V:[17] This is a first order perturbation theory program used in conjunction with fluxes and adjoints from 2DB and 26 or 13 group cross section sets to produce zero sample size worth distributions and reaction rates.

Detailed descriptions of these codes can be found in the reference documents. Specific calculational options selected are listed in the summary sheets in Appendix B.

C. CALCULATION CORRECTION FACTORS

The following corrections should be made for all reported calculations.

Transport Correction

From calculations of equivalent volume spheres in DTF-IV, S_4 quadrature, and 1DX, the correction required to convert a diffusion theory k_{eff} to transport S_4 is +0.00746 Δk and to transport $S\infty$ is extrapolated[18] to be +0.00634 Δk.

Heterogeneity Correction[19]

The calculations in this analysis are made with homogeneous smears of the platelet structure within the cell. Heterogeneous calculations were made in DTF-IV, S_{12} to account for spatial and resonance self-shielding. The Bell correction and leakage cross sections were used. The correction is +0.0106 Δk.

Normalized Reciprocal Weighting Correction

While the analysis was made with transport cross sections reciprocally weighted in the callapsing process, an improved, normalized reciprocal

weighting option has been added. The correction which should be added to all two-dimensional calculated k_{eff}'s is +0.0019[4] Δk.

D. MULTIPLICATION CONSTANT

The effective multiplication constant of the reference loading 56-17 was measured to be 0.999964 with a fueled control drawer withdrawn 8.62 inches. The total fissile mass inventory was 333.41 kg of ^{239}Pu + ^{241}Pu + ^{235}U, of which 332.94 kg were within the core boundary for the above measurement. The in-core fissile materials inventory is listed in Table 3.2.

TABLE 3.2

IN-CORE FISSILE MATERIALS INVENTORY
CRITICAL ASSEMBLY 56-17

DRAWER TYPE	NUMBER	FISSILE MASS, Kg ^{239}Pu + ^{241}Pu + ^{235}U
"A" DRAWER	216.00	110.069
"B" DRAWER	203.00	205.738
SAFETY DRAWER	16.00	15.645
CONTROL DRAWER	1.52	1.487
TOTAL	436.52	332.939

As shown in Figure 3.1, the core profile of this loading is asymmetric about both the X and Y axes. Revisions, using experimental data, have been made to form two modified hypothetical cores which can more readily be calculated; one in R-Z geometry and the other in X-Y geometry.

R-Z Model Analysis

The revisions required to form the cylindricized core are described in detail in Appendix A, and summarized in Table A-3. This cylindrical core has an inferred experimental k_{eff} of 1.00000 $\pm$ 0.00014, a core radius of 45.89 cm, a core height of 91.59 cm, and a fissile mass of 328.991 kg of ^{239}Pu + ^{241}Pu + ^{235}U.

The calculated k_{eff} for this system is 0.98221 $\pm$ 0.00006 (Appendix B-2). This value was obtained from an R-Z, 2DB calculation using 26 energy groups and the physical model and mesh structure shown in Figure 3.6. Because of a minor difference between the calculation and the inferred experimental cylinder, a total correction of 0.126 $\Delta k/k$ is included in this value to account for 0.01 cm radius difference and a 0.987 kg mass. The latter is the dominant effect. It arises from inappropriate averaging of "A" and "B" drawer atom densities to form the homogenized R-Z core averaged atom densities.

The radius correction was made using the average measured edge worth of 0.043% $\Delta k/k$ per kg fissile. The remaining mass correction was made by uniformly adjusting enrichment using the calculated expression for this assembly of $\Delta k/k = 0.49\ dm/m$, where m is the fissile mass.

Since the experimental multiplication constant is unity, the ratio of the calculated to experimental value for this diffusion approximation, uncorrected for heterogeneity, $(C/E)_{diffusion,}$ is 0.98211 $\pm$ 0.00014. Also shown in Appendix B-2 is the corresponding transport value, corrected for platelet heterogeneity of 0.99861 $\pm$ 0.00017 for the S_∞ transport option. Calculational uncertainties which have been used in this section and will be used in the remainder of the report are explained in the introduction to Appendix B.

X-Y Model Analysis

An X-Y loading of the 56-17 reference assembly which is symmetric about the Y axis could be formed by adding a "B" fuel drawer in matrix location R-8 of half 2. The measured reactivity worth of replacing a single drawer of reflector with fuel at this location is +0.048% dk/k. This is an interpolated value from the drawer worth versus distance from core center curve. Figure A-2 in Appendix A. This adjusted core has a fissile mass of 334.428 kg, and an inferred experimental k_{eff} of 1.001347 $\pm$ 0.00012. As noted in Table 3.3, this includes core gap and temperature corrections.

TABLE 3.3

SUMMARY OF MASS AND REACTIVITY CHANGES INVOLVED IN CONVERTING TO A SYMMETRIC REPRESENTATION OF ASSEMBLY 56B[a]

	FISSILE MASS KG.	MULTIPLICATION
INITIAL VALUES:	333.415 [b]	0.999964±0.0000015
CHANGES:	Δkg	Δρ, %ΔK/K
1. CONTROL DRAWER INSERTION	0	+0.0719 ± 0.0007
2. TEMPERATURE, 37.6°-40.0°C	0	-0.0056 ± 0.00007
3. REMOVE INTERFACE GAP	0	+0.024 ± 0.012
4. ADD DRAWER 2-R-8	1.013	+0.048 ± 0.001
TOTALS	334.428	1.001347± 0.000120[c]

(a) This is a conversion of the asymmetric loading, 56-17, to the profile of the symmetric loading 56-34.

(b) Uncertainties in fissile mass have not been made available.

(c) The final uncertainty in k_{eff} is a result of the uncertainty in the core gap which is explained in Appendix A.

The multiplication constant of this system has been calculated with 2DB in X-Y geometry with the twenty-six group cross section set. The areal profile and mesh structure for a half core homogeneous calculation are shown in Figure 3.7. The multiplication constant for this calculation is 0.98768 ± 0.00006. See Appendix B-1. The homogeneous diffusion-theory correlation, $(C/E)_{diffusion}$ is 0.98630 ± 0.00013.

Including corrections for heterogeneity and transport theory, the k_{eff} of this X-Y calculation becomes 1.00413 ± 0.00009. The C/E for this value is 1.00278 ± 0.00015.

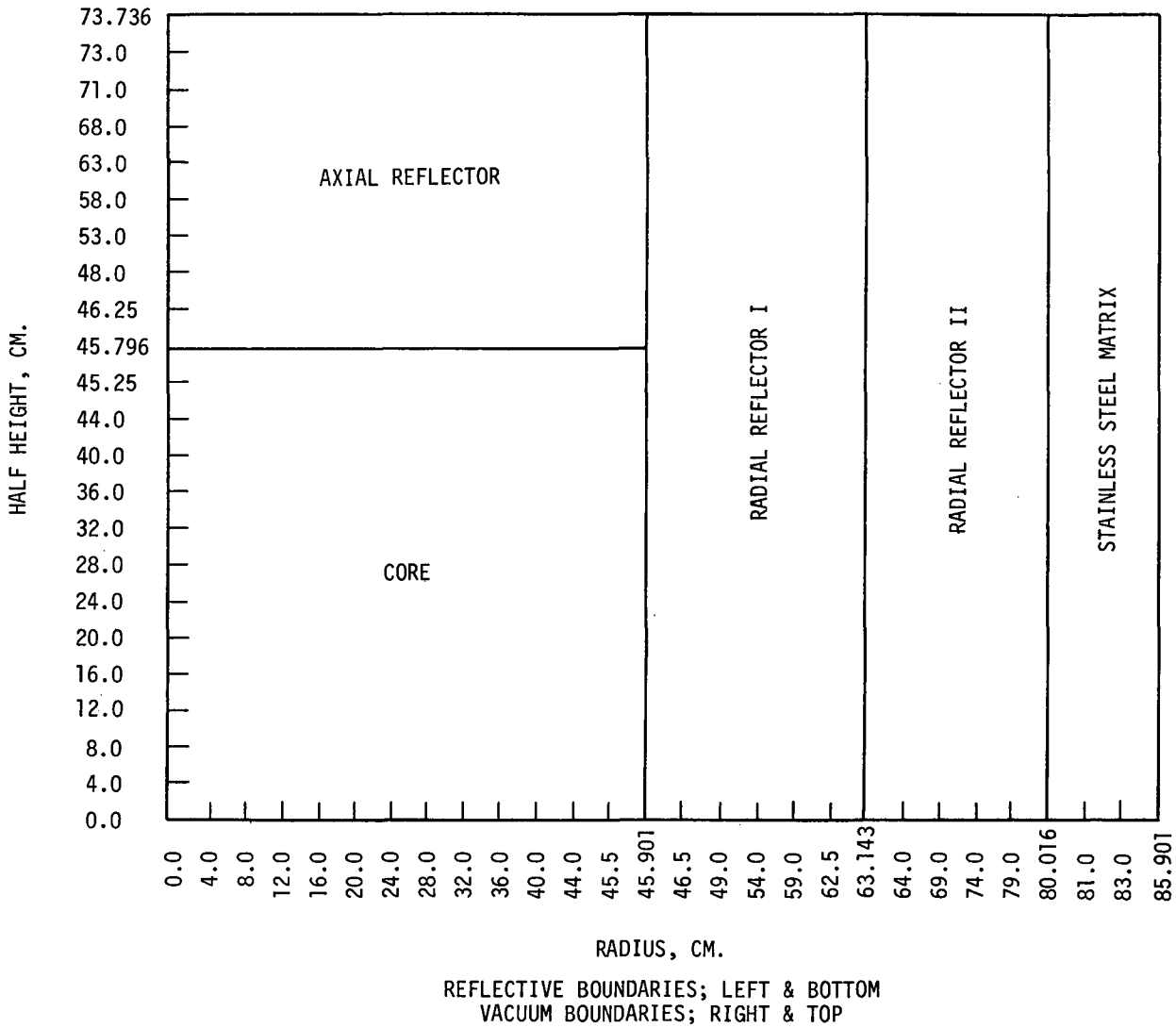

FIGURE 3.6 R-Z Geometric Calculational Model
Assembly 56-B, Loading 56-17

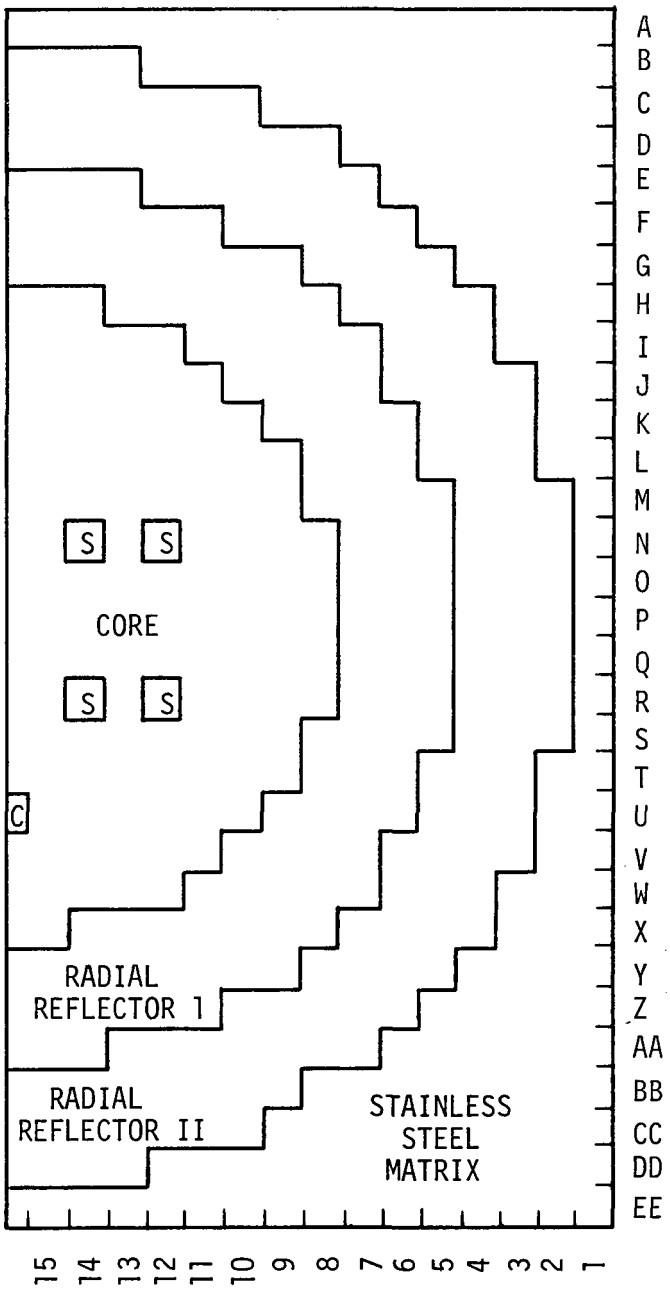

S = SAFETY DRAWER

C = CONTROL DRAWER

Columns, Interval cm	#
0.000	
1.386	16
2.771-	
5.542	15
8.313-	
11.084	14
13.855-	
16.626	13
19.397-	
22.168	12
24.939-	11
30.481-	10
36.032-	
40.565	9
41.565-	
44.363	8
47.107-	
48.107	7
52.649-	6
58.191-	5
63.733-	4
69.275-	3
74.817-	2
80.359-	1
85.901-	

Rows, Interval cm	#
0.000	
5.532-	EE
11.064-	DD
16.596-	CC
22.128-	BB
27.660-	AA
33.192-	Z
38.724-	Y
44.256-	X
49.788-	W
54.320	V
55.320-	
58.086	U
60.852-	
61.852	T
66.384-	
70.916	S
71.916-	
74.682	R
77.448-	
78.448	Q
82.980-	P
88.512-	
93.044	O
94.044-	
96.810	N
99.576-	
100.576	M
105.108-	L
110.640-	K
116.172-	J
121.704-	I
127.236-	H
132.768-	G
138.300-	F
143.832	E
149.364-	D
154.896-	C
160.428	B
165.960-	A
171.492-	

FIGURE 3.7 Assembly 56B; 1/2 Core, X-Y Geometric Model

E. RESULTS OF VARIATIONS IN THE CALCULATIONAL MODEL

The multiplication constant of the revised core, having half core symmetry as described in the preceding section, has also been calculated in 2DB using X-Y geometry with thirteen as well as twenty-six group cross sections, with both coarse and fine mesh structures, with half and quarter core symmetries, and with homogeneous and striped core zoning structure. The results are summarized in Tables 3.4 and 3.5. The appendices describing the calculations are listed in Table 3.4.

The first variation of the calculational model is the use of a 13 energy group structure. As previously described, the cross sections for the core were collapsed from the original twenty-six group set to the new thirteen group set by averaging over the volume averaged core spectrum as determined from a one dimensional radial model of the reactor profile. Reflector cross sections were similarly collapsed over the volume averaged radial reflector spectrum. This technique of collapsing over an average spectrum does, in principle, yield cross sections that are not best for any position within their respective regions. Interest in the thirteen group set stems from a desire to minimize costs of analysis and survey work associated with design.

The 26 group k_{eff} for this 1/2 core X-Y calculation, as listed in Table 3.4, is 0.99779 ± 0.00006. The buckling used was $6.35 \times 10^{-4} cm^{-2}$. The equivalent 13 group calculation, also using a buckling of 6.35×10^{-4} cm^{-2}, gives a k_{eff} of 0.99625 ± 0.00006. From a separate set of calculations, it was determined that the 13 group B_Z^2 that should be used is 6.46×10^{-4} cm^{-2}. $\Delta k/\Delta B^2$ for Assembly 56B is 178.5. Hence, the correction that must be applied to the 13 group calculation is -0.00196, giving a k_{eff} of 0.99429 ± 0.00008. The change in k_{eff} resulting from a reduction in energy groups from 26 to 13 is, therefore, 0.00350 ± 0.00004 Δk.

The use of a quarter core calculational model is the second variation of the analysis. The symmetry of the quarter core model was achieved by using half drawers where there was lack of symmetry either across the

TABLE 3.4

SUMMARY OF X-Y GEOMETRY CALCULATIONS OF K_{eff}

Appendix #	Symmetry	Core Zoning	Mesh Structure	X-Section Groups	Homogeneous Diffusion Theory K_{eff}(a)
B-1	1/2 core	homog.	coarse	26	0.99779 ± 0.00006
B-5	1/2 core	homog.	coarse	13	0.99429 ± 0.00008
B-15	1/4 core	homog.	coarse	13	0.99434 ± 0.00008(b)
B-8	1/4 core	homog.	fine	13	0.99416 ± 0.00008
B-7	1/4 core	striped	fine	13	0.98892 ± 0.00008

(a)Corrections for normalized reciprocal weighting and correct B_z^2 variations in fissile mass, and heterogeneity have been added.

(b)This value was inferred from a similar set of calculations.

TABLE 3.5

RESULTS OF CALCULATIONAL OPTION VARIATIONS

X-Y Calculational Option	Change in Calculational Model From	To	Resulting ΔK_{eff}
Cross section groups	26 groups	13 groups	-0.00350 ± 0.00004
Core symmetry	half core	quarter core	+0.00005 ± 0.00004
Mesh structure	coarse mesh	fine mesh	-0.00018 ± 0.00004
Core zoning	homog. zoning	striped zoning	-0.00544 ± 0.00004

X axis or between half one and half two of the critical assembly. A diagram of the quarter core model is shown in Figure 3.8. A multiplication constant is listed in Table 3.4 for a quarter core which is compatible with the previous half core calculation. This calculation, having a k_{eff} of 0.99434 $\pm$ 0.00008, is described in detail in Appendix B-15. This value of k_{eff} for the quarter core, thirteen group calculation differs from the half core, thirteen group calculation by only 0.005 $\pm$ 0.004% $\Delta k/k$, which is negligible.

The quarter core model was then used to calculate the k_{eff} of the 56B core using thirteen groups, X-Y averaged core atom densities as listed in Table 3.1, but with a finer mesh structure than was previously used. The k_{eff} of 0.99416 $\pm$ 0.00008 resulting from this calculation with fine mesh structure differs by only 0.018 $\pm$ 0.004% $\Delta k/k$ from the result which was inferred using coarse mesh structure. While the finer mesh structure is advisable for more detailed analysis, for example striping and central drawer worths, the small difference between fine and coarse mesh structure in this instance justifies the use of coarse mesh structure for the analysis of the homogenized reference core.

A final comparison is made, between the use of a single set of averaged atom densities throughout the core and using striped zoning. These two calculations, described in Appendices B-8 and B-7, differ from one another by 0.544 $\pm$ 0.004% $\Delta k/_k$. In view of the fact that accounting for heterogeneities usually causes an increase in the k_{eff} of a calculation, it is interesting that a striped zoning calculation of the core has a lower multiplication constant than the homogeneous calculation. A tentative explanation is that the striped zoning of the calculational model is less representative of the actual structure than is the homogenized core. Although there are two fuel platelets in each "B" drawer and only one in each "A" drawer, the fuel platelets are arranged, within the two drawer cell, to allow nearly equal spacing between fuel platelets, hence, an even distribution of fuel. Striped zoning of the core does not infer an even distribution of fuel throughout the core. Rather, the fuel

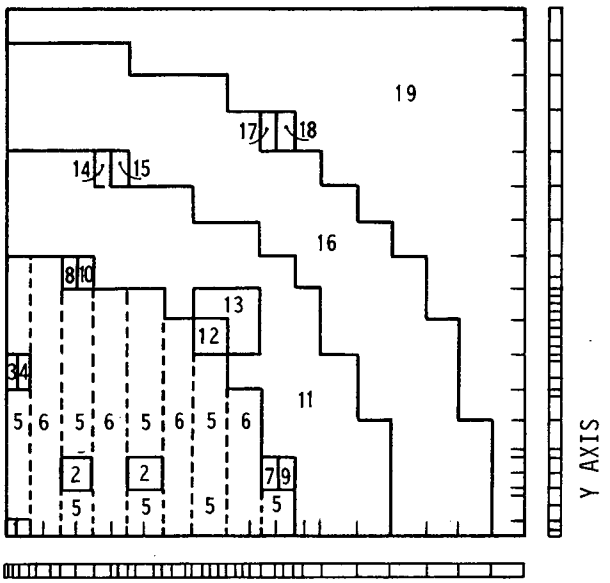

COARSE MESH STRUCTURE

COLUMN	X (CM.)	Y (CM.)	ROW
	0.0	0.0	
	1.3860	2.766-	P
16	- 2.7710	7.298	
	5.542	8.298-	O
15	- 8.313	11.064	
14	11.084	13.830-	N
	-13.855	14.830	
	16.626	19.362-	M
13	-19.397	24.894-	L
12	22.168	30.426-	K
	-24.939	35.958-	J
11	-30.481	41.490-	I
10	-36.032	47.022-	H
9	40.565	52.554-	G
	-41.565	58.086-	F
8	44.336	63.618-	E
	-47.107	69.150-	D
7	48.107	74.682-	C
	-52.649	80.214-	B
6	-58.191	85.746-	A
5	-63.733		
4	-69.275		
3	-74.817		
2	-80.359		
1	-85.901		

FINE MESH STRUCTURE

COLUMN	X (CM.)	Y (CM.)	ROW
	0.0	0.0	
	.6928	1.766	P
16	1.386	2.766-	
	2.0784	5.532	O
	- 2.771	8.298-	
15	3.771	11.064	N
	7.313	13.830-	
	- 8.313	14.830	M
14	11.084	19.362-	
	-13.855	23.894	L
13	16.626	24.894-	
	18.397	25.894	K
	-19.397	29.426	
12	20.392	30.426-	
	23.939	31.426	
	-24.939	33.192	J
11	25.939	34.958	
	29.481	35.958-	
	-30.481	36.958	
	31.867	38.724	I
10	33.252	40.490	
	34.683	41.490-	
	-36.032	42.490	H
	37.409	47.022-	
9	38.795	49.788	G
	40.180	52.554-	F
	-41.565	58.086-	E
8	44.336	63.618-	D
	46.4145	69.150-	C
	-47.107	74.682-	B
7	48.107	80.214-	A
6	-52.649	85.746-	
5	-58.191		
4	-63.733		
3	-69.275		
2	-74.817		
1	-80.359		
	-85.901		

FIGURE 3.8 56B 1/4 Core, X-Y Model Zone and Mesh Structure

is inferred to be in locations of, possibly, lower worth than is actually the case. This can be of particular significance on the core edge. The magnitude of this effect appears to be related to the arrangement of "A" and "B" drawers on the core edge. Preliminary analysis of the reference cores FTR-1 and FTR-2,[5] which have the same cell arrangement, show the same tendency as do the core edge drawer arrangements.

G. CENTRAL DRAWER EXCHANGE WORTHS

Reactivity worths were measured for replacement of a full column of "B" type core material with first, a full column of reflector material; second, with a full column of B_4C, NA and stainless steel mixture. From the corresponding measured values of the reactor multiplication constants,[11] the experimental value of the reactivity worth of an exchange of B_4C, Na and stainless steel for axial reflector was also inferred. The experimental values and corresponding calculated results are presented in Table 3.6.

As indicated in the column headings, the reactivities, p, both calculated and experimental, are inferred from the expression:

$$\rho = \frac{k_2 - k_1}{k_1 k_2} \equiv \frac{\Delta k}{k_1 k_2}$$

where both of the multiplication constants k_1 and k_2 are less than unity and $k_1 > k_2$.

The Reference Column entries, e.g., B-3, refer to the Appendix B-3 calculational summary sheets that describe each calculation and give the specific calculated multiplication constants.

It should be noted that in inferring the experimental results, it was assumed that the effective source of the system was unaltered by removal of the central core material column and subsequent addition of the B_4C column. Since each of these changes actually reduces the effective source, the experimental reactivities must be considered maximum values. It is estimated that the systematic errors introduced are of the order of a percent of the reactivity worths. Finally, the calculated

results are k-difference values and hence source independent.

As noted in Table 3.6, the calculated worths are essentially independent of the model used, w.g., X-Y or R-Z, and 13 or 26 energy groups.

Cross sections for the 13 energy group model were collapsed over 26 group neutron spectra as follows:

- Core material cross sections as well as those for the "B" column of core material on the core axis were collapsed over the volume-averaged, unperturbed core spectrum, using a one-dimensional, radial diffusion model.
- Cross sections for the axial reflector material in the test column were similarly collapsed, using the same diffusion model.
- For the control column cross sections, the central column of the above one dimensional model was filled with control material and the cross sections were collapsed over the volume-weighted average spectrum in the control column. The radius of the central column was 3.124 cm.

TABLE 3.6

LARGE CENTRAL REACTIVITY WORTHS

Experiment Description	Experimental Worth, $\%\Delta k/1_1k_2$	Calculational Worth R-Z - $\%\Delta k/k_1k_2$	Appendix	Calculational Worth X-Y - $\%\Delta k/k_1k_2$	Appendix	C/E R-Z	C/E X-Y
Replace "B: drawer fuel with axial reflector	-0.459 ± 0.004	-0.575 ± 0.005[a] (13 group) -0.569 ± 0.005 (26 group)	B-3 B-4 B-16 B-17	-0.588 ± 0.005	B-7 B-9	1.25 ± 0.015 (13 group) 1.24 ± 0.015 (26 group)	1.28 ± 0.015
Replace "B" fuel with B_4C control rod	-1.515 ± 0.015	-1.771 ± 0.009	B-3 B-4	1.758 ± 0.009	B-7 B-10	1.17 ± 0.016	1.16 ± 0.016
Replace axial reflector with B_4C control rod	1.056 ± 0.016	1.196 ± 0.007	B-4	1.170 ± 0.007	B-9 B-10	1.13 ± 0.018	1.11 ± 0.018

Ih/ $\%\rho$ = 1039.1

(a) Calculational precision for worths derived from an accuracy of 3ε on convergence of K_{eff}.[15] All calculations are converged to an $\varepsilon = 10^{-5}$.

As illustrated in Figure 3.9, the plate arrangement in the B_4C, Na, and stainless steel column is quite heterogeneous, i.e., two half inch thick stainless steel clad B_4C plates, spaced alternately with half-inch thick stainless steel clad sodium plates. Appendix C presents the results of a detailed diffusion theory and transport theory study of cylindrical models of similar control rods. From these results, it is estimated the homogeneous calculational approximation in the experimental configuration of Figure 3.9 used here overestimates the reactivity worth by approximately 1%. Hence, the C/E values in Table 3.6 for B_4C are approximately 1% high.

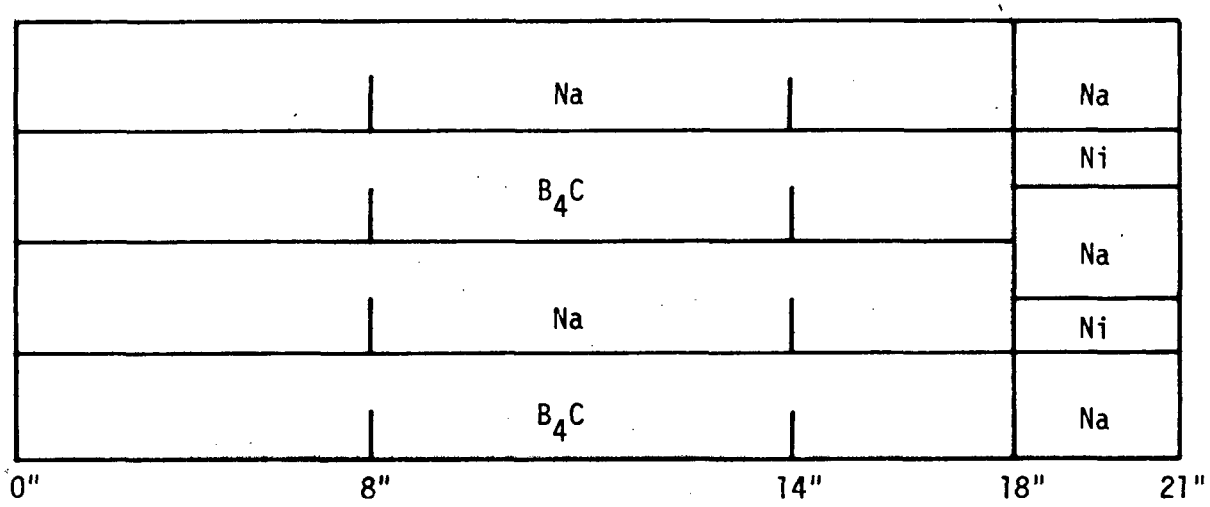

FIGURE 3.9 Drawer Loading Used For Central Worth Measurements

From the C/E values given in Table 3.6, and earlier work on ZPR-III Assemblies 48A[1] and 51[2], the following observations may be made.

- The C/E value for B_4C reported here, 1.11, is higher by about 3 - 5 % than that found in the earlier work and should be considered the upper limit on the bias of this diffusion model;
- The C/E value for core material of 1.25 is 10% higher than that obtained in analyses of similar Assembly 51[2] experiments, and should also be considered the upper limit on the bias.

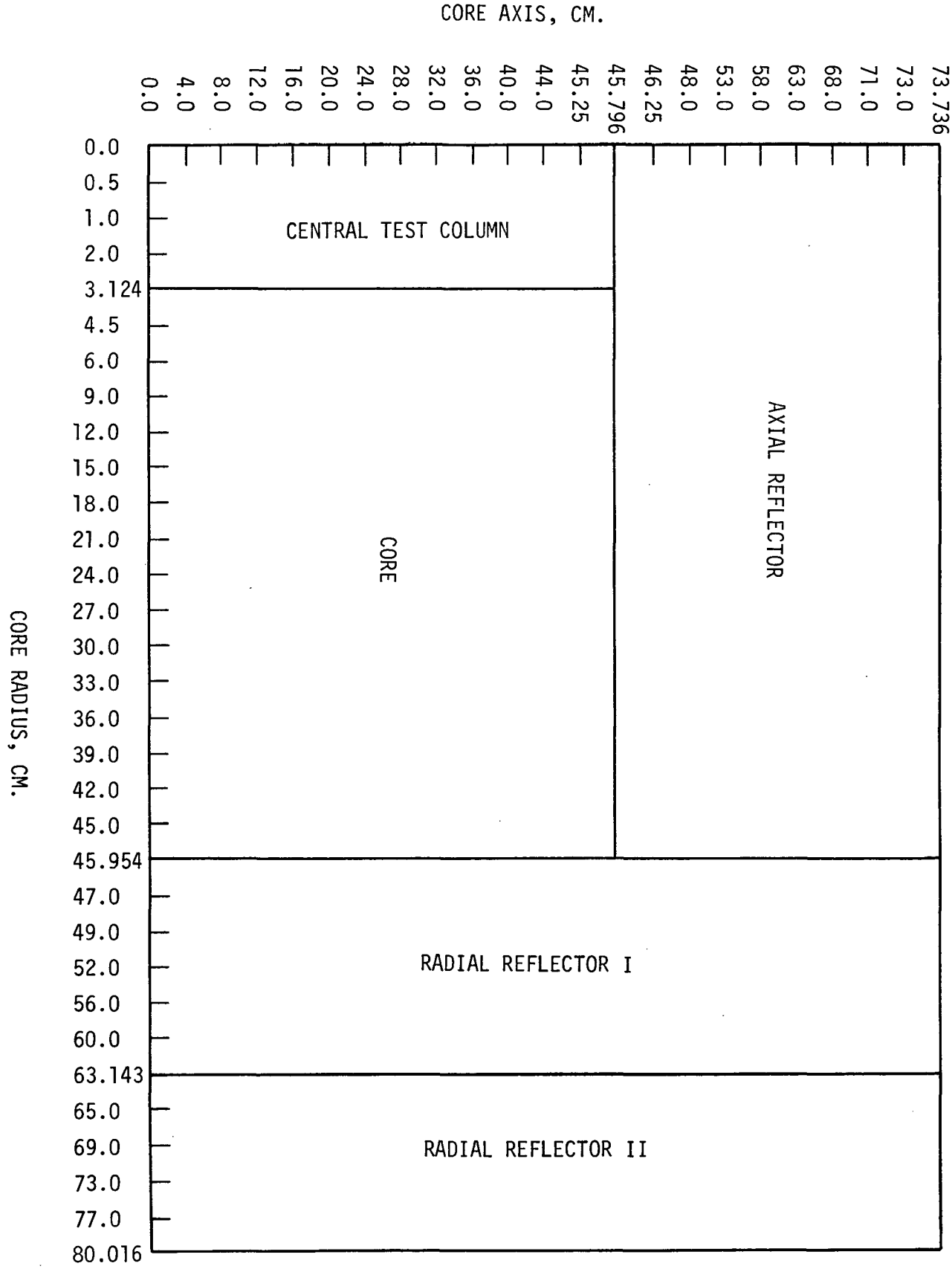

FIGURE 3.10 2DB, R-Z Geometry Model, Cylindricized Assembly 56-B, Central Column Replacement Worth Calculations

The latter result is somewhat higher than one would expect. Small sample worth biases, or the degree of overcalculation seems to diminish as one approaches the core-reflector interface (see Reference 2, small sample plutonium worth distribution) and seldom exceeds a central bias of 25%.

The 13 group calculated worths of axial reflector replacing fuel exceeds the experimental value by 25% and 28% in R-Z and X-Y geometry, respectively. While the fuel worth estimation is high, it is typically found to be so for this code and cross section set.[27] To assure that a substantial portion of this overestimation is not due to collapsing techniques, the worth of fuel-axial reflector exchange was calculated with the uncollapsed 26 group set in R-Z geometry. The 2% improvement is solely a result of using a larger denominator in the calculation of $\% \Delta k/k_1 k_2$, as the $k_{eff's}$ produced in 26 group calculations are 0.0036 Δk higher than the 13 group results.

The 3% disagreement between thirteen group X-Y and R-Z calculations for both fuel and control worths is probably a result of the use of a single B_Z^2 term for the entire core, regardless of perturbations, in the X-Y calculation. As this is not too large, it would appear, here, as in the analysis of central worths in Assembly 48,[1] that it is adequate to use a B_Z^2 term in X-Y geometry calculations to approximate the axial leakage.

G. PERIPHERAL DRAWER EXCHANGE WORTHS

Two control configurations were investigated at the core-reflector interface. For the first measurement, four matrix tubes of control material were substituted for reflector, one column in each quadrant. The columns of control material, composed of natural B_4C, Na, and stainless steel extended only along the height of the core. The locations of these rods are marked with a single vertical "cross" hatching on the drawings of Figure 3.11A. The drawer loading pattern of stainless steel clad B_4C and Na plates is shown in Figure 3.12, and the homogenized rod composition is given in Table 3.1. A second rod configuration was formed by adding three more matrix columns of control material to each existing column, giving a total of four 2 x 2 drawer arrays of control composition. The additions are marked with two vertical "cross" hatchings on Figure 3.11A. The worths of these control configurations were measured by the subcritical neutron multiplication technique.

Detectors used to determine changes in the neutron flux levels in the above worth measurements were four BF_3 gas filled chambers. Their locations within the assembly are shown in Figure 3.11 and descriptions are listed in Table 3.7.

Reactivity worths derived separately from each of these detectors vary by 7% for the four control columns and by 12.6% for the 16 columns. These values are listed in Table 3.8. This variation in the inferred experimental values of reactivity worths results from the relatively long relaxation distances of the neutron flux perturbations caused by insertions of the control materials. Separate, preliminary calculational studies[28] of this problem indicate that the centrally located sensors are less perturbed than the similarly remote but more peripherally located sensors, e.g., 4a and b.

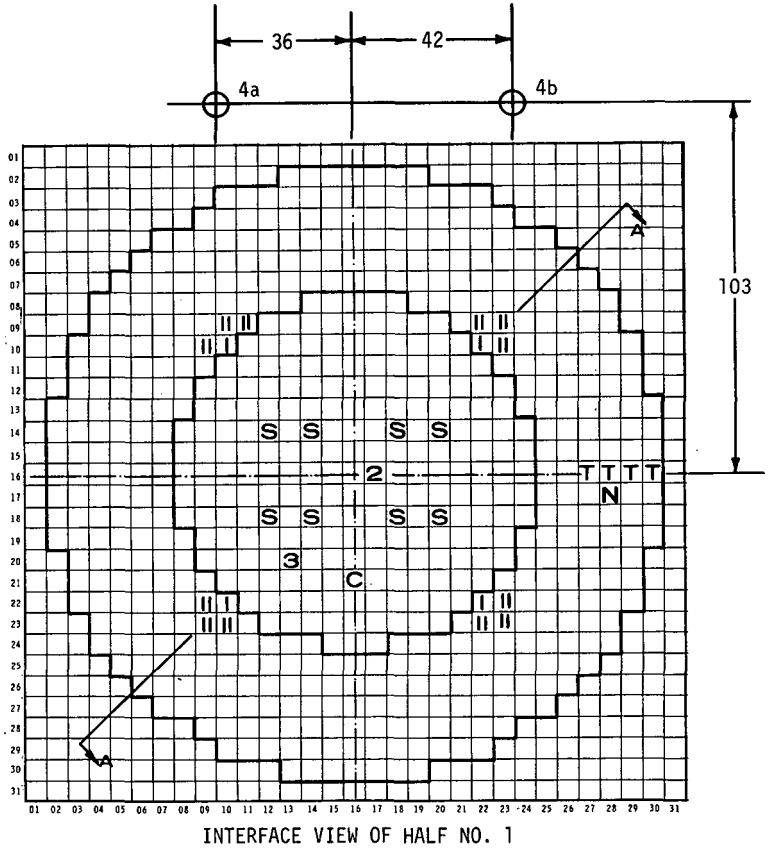

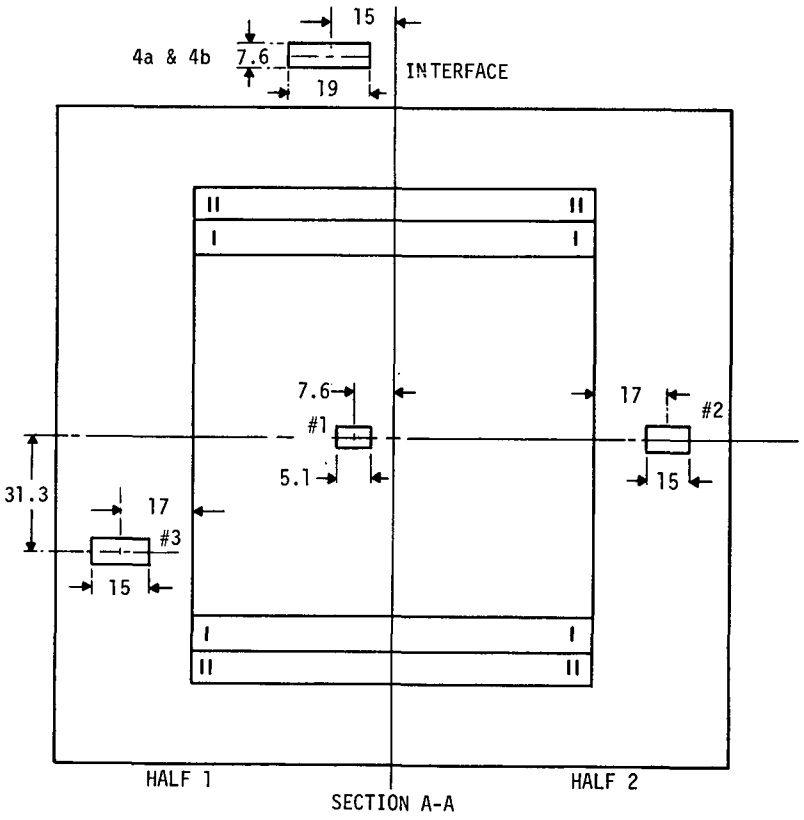

S - SAFETY ROD
C - CONTROL ROD
T - SOURCE TUBE
N - NEUTRON LEVEL DETECTOR

I POISON CONTROL I LOCATIONS
II POISON CONTROL II LOCATIONS
1, 2, 3, 4a AND 4b ARE DETECTOR LOCATIONS

NOTE: ALL DIMENSIONS IN CENTIMETERS

FIGURE 3.11 Detector and Control Rod Matrix Locations for the Peripheral Poison Control Worth Measurements

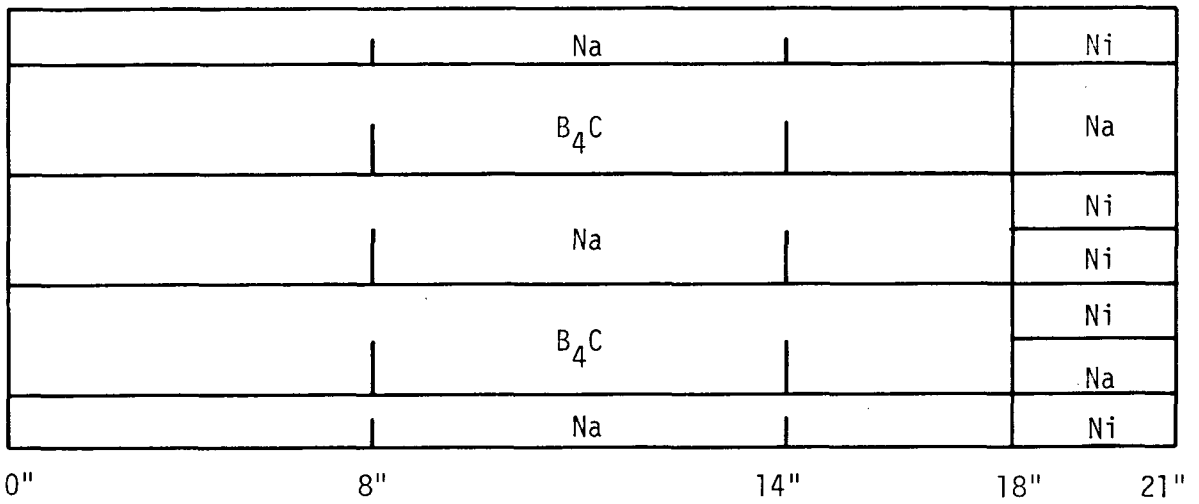

FIGURE 3.12 Drawer Loading Used for Measurements in the Radial Reflector

TABLE 3.7

DETECTOR LOCATIONS FOR THE CENTRAL DRAWER SUBSTITUTIONS AND THE PERIPHERAL BORON ROD WORTH EXPERIMENTS

			Geometric Location		
Detector No.	Type[a]	Signal	Matrix Element	Radius, cm[b]	Distance from Midplane, cm[b]
1	PC	Pulse	1-P-16	0	7.6
2	PC	Pulse	2-P-16	0	63
3	PC	Pulse	1-T-12	31.3	63
4a + 4b	IC	Current	External	∿110	15

(a) All detectors were BF_3 gas filled chambers

PC - proportional counter
IC - ion chamber

(b) Distance to center of the active volume

TABLE 3.8

PERIPHERAL DRAWER EXCHANGE WORTH

Experiment Description	Experimental Worth Counter	%Δk/k	Calculational Worth, %Δk/k	APPENDIX	C/E
Replace 4 reflector columns with B_4C rods	1	-0.932 ± 0.010	-0.923 ± 0.006[a]	B-11 B-13	0.990 ± 0.012
	2	-0.890 ± 0.010			1.037 ± 0.012
	3	-0.939 ± 0.010			0.983 ± 0.012
	4a + b	-0.962 ± 0.010			0.959 ± 0.012
Replace 16 reflector columns with B_4C rods	1	-1.736 ± 0.020	-1.770 ± 0.009	B-11 B-14	1.020 ± 0.013
	2	-1.700 ± 0.018			1.041 ± 0.012
	3	-1.727 ± 0.018			1.025 ± 0.012
	4a + b	-1.945 ± 0.020			0.910 ± 0.010

(a) Calculational precision for worths derived from accuracy of 3ε on convergence of K_{eff}[15]. All calculations are converged on $\varepsilon = 10^{-5}$.

The reference calculational model for the analysis of these peripheral control rod worths is the quarter core model, using striped zoning, as described in Figure 3.8 and in Appendix B-11. Compositions for the 19 zones of Figure 3.8 are as given below:

Striped Loading - 56B

Composition	Zones
"B" Drawer	1,4,5,7,8
"A" Drawer	6
Control and Safety Drawer	2,3
Radial Reflector I	10-14,9
Radial Reflector II	15-17
Stainless Steel Mesh	18,19

Cross sections for these calculations were collapsed to thirteen groups, from the original twenty-six group set over zone average spectra for two 1DX cylindrical models of 56B. The B_4C, Na, and stainless steel cross sections, used in the peripheral control rod locations, were collapsed to thirteen groups over the volume averaged spectrum in a B_4C control ring, 5.54 cm. wide, located just outside the core-reflector boundary. All other cross sections are from a thirteen group cross section set collapsed over core or reflector spectra in an unperturbed model of 56B.

The calculational model, shown in Figure 3.8, describes the core with the two separate configurations of control rods, as are depicted in Figure 3.11.

The configuration of four control rods is identified as zone 13 in the calculational model in Figure 3.8. The sixteen control rod pattern is identified as zones 12 and 13. Multiplication constant calculations were made with control rod atom densities, as listed in Table 3.1, in the appropriate zones. The reactivity worth of the rods was calculated with reference to the multiplication of the unperturbed configuration. The calculated worths are listed in Table 3.8 and compared with the experimental values. Additional details of these calculations are described in Appendices B-13 and B-14.

There are four different experimental results for both control rod measurements, corresponding to the four counter positions in the core described in Figure 3.11. Counter 1, located on the axis of the core, should give the best worth value for this experiment, as noted earlier.

Counter 2, located in the axial reflector on the core axis, tends to record the change in axial leakage, only, while detectors 4a and b, located outside the radial reflector would tend, predominately, to measure radial leakage. Counter 3 is located off axis and outside of the core in such a position that it would tend to measure the local effects of the perturbation rather than the reactivity change of the system as a whole.

Both four and sixteen column control rod worth results are in best agreement with the experimental worth associated with counter 1, and the agreement is very good. The calculation of the four control rod columns slightly underestimates the experimental worth while, for sixteen control rod columns, the calculation is an overestimate. The calculation of the single column control rods differs slightly from the results of the Assembly 48, 48A analyses[1] in which the worth of a series of single peripheral control columns were measured and the analysis resulted in an overestimation of the worths by 2 to 11%.

The worth of the four sets of four control rod columns is less than twice the worth of the four sets of single control columns. This is an obvious result of rod shadowing. Also, the three added columns in each set are in a lower worth region. This would suggest that a more advantageous use of boron would be in single column sizes placed on an optimum worth radius. Eight judiciously placed columns could be of equal worth to the sixteen columns located as they were in this experiment.

Peripheral Fuel Worths

The worths of exchanging core drawers for reflector drawers were measured for matrix positions U-10, U-23, V-11, V-22, W-12, X-17, and X-18. These worths, which were measured using a calibrated control rod, are listed in Table 3.9. These edge worths are plotted in Figure A-2 of Appendix A. From these curves, and methods described in Appendix A, the worth of all core edge drawers has been evaluated. The worth of drawer R-8 is of particular interest to this analysis as it is the only core asymmetry with respect to the Y axis. The extrapolated worth of this drawer is 0.048 $\pm$ 0.0005% $\Delta k/k$.

The reference calculational model for the analysis of the worth of the peripheral fuel drawer, R-8, is also the quarter core model, described in Figure 3.8, using the striped core loading. This base calculation is described in detail in Appendix B-7. The zone loading for this calculation differs from the striped loading description for the control rod reference in that Zone 9 contains "B" drawer fuel rather than reflector.

TABLE 3.9

WORTH OF CORE DRAWERS AT CORE-REFLECTOR INTERFACE

Drawer	Fissile Mass, kg $^{239}Pu + ^{241}Pu + ^{235}U$	Worth[(a)] % Δk/k
2-X-17	0.5097	0.02219
2-U-10	1.0136	0.05573
2-X-18	1.0136	0.04801
2-V-11	0.5097	0.02348
2-U-23	0.5097	0.01859
2-W-12	1.0136	0.04980
2-V-22	1.0136	0.04574

(a) Experimental uncertainties $\tilde{\sim} \pm$ 0.00024% Δk/k

The cross sections used to determine the worth of the peripheral fuel drawer, R-8, are from a thirteen group set collapsed from the original twenty-six groups over average core and reflector spectra in a one dimensional cylindrical 1DX calculation. Any spectrum shift resulting from the replacement of fuel by radial reflector material is not taken into account in the collapsing of the cross sections.

The calculation of the multiplication constant of the core, in which the fuel in drawer R-8 is replaced with radial reflector (zones 7 and 9 in the model shown in Figure 3.8) is described in Appendix B-12. The difference between the k_{eff} of this calculation and the calculation in which those zones contain fuel, results in the calculated worth of one fuel drawer of "B" composition in position R-8. This worth is listed in Table 3.10 and compared to the experimental value. The calculational model overestimates the experimental worth by 15%.

TABLE 3.10

PERIPHERAL FUEL DRAWER REPLACEMENT WORTH

Replacement	Experiment, % Δk/k	Calculation, % Δk/k	C/E
Replace fuel drawer R-8 with reflector	-0.048 ± 0.0005	-0.055 ± 0.001(a)	1.15 ± 0.02

(a) Calculational precision for worths derived from accuracy of 3ε on convergence of K_{eff}[15]. All calculations are converged on $\varepsilon = 10^{-5}$.

H. CENTRAL REACTION RATE RATIOS

Central fission rate ratios were measured for ^{239}Pu, ^{240}Pu, ^{233}U, ^{234}U, ^{236}U, and ^{238}U with respect to ^{235}U, by using gas flow spherical counters.[29] The measurements were made in both "B" and "A" drawers at positions chosen to be equally spaced from the central column, while no measurements were actually made in the core center position.

Calculations of these ratios have been made using core-center, twenty-six group fluxes from a one dimensional diffusion (1DX) analysis of 56B and twenty-six group homogeneous cross sections. Measured and calculated values, as well as the ratios of these values are listed in Table 3.11. The experimental values for the fission rate ratios are averages of values measured in "A" and "B" drawers, as these values differed by less than 1%.

The calculated fission ratios of ^{233}U, ^{234}U, ^{239}Pu, with respect to ^{235}U agree with the experimental values within approximately 5%. These results are consistent with a survey study of fission rate ratios in five previous ZPR-III cores[7], using the same cross section sets. The calculated $^{236}U/^{235}U$ fission rate ratio differs by 10% from the experimental value. In the above mentioned study, this was found to be true in the other five cores as well. It could then be concluded that the ^{236}U fission cross sections are in error.

The calculated ratio of the ^{238}U fission rate to the ^{235}U fission rate is also, nearly 10% lower than the experimental ratio. While the survey of the five previous cores shows an average C/E value for this ratio of 1.03, there is a spread of 10% in the C/E values. However, the C/E values for Assembly 56B, $^{238}U/^{235}U$ fission rate ratio is outside the spread of these values.

The calculated fission rate ratio for $^{240}Pu/^{235}U$ is 30% lower than the experimental value. This discrepancy is a factor of two larger than the worst value of the survey of the other five cores, and a factor of 5 worse than the average discrepancy.

The poor $^{238}U/^{235}U$ fission rate ratio agreement is a result of an inadequate calculational model. However, the ^{240}Pu results point to a probable experimental error. Consequently, the ratio of $^{240}Pu/^{235}U$ fission rates were scheduled to be remeasured in FTR design core, FTR-II; ZPPR core 1.

TABLE 3.11

REACTION RATIOS

Central Fission Ratio Measurements[a][b]

	$\bar{\sigma}f_i$ / σf_{U-235}		
Isotope, i	Calculation (C)	Experiment (E)	C/E[c]
U-233	1.448	1.478	0.979
U-234	0.189	0.195	0.968
U-236	0.0575	0.0639	0.899
U-238	0.0282	0.0309	0.913
Pu-239	0.9746	1.028	0.948
Pu-240	0.2017	0.2825	0.714

(a) Experimental uncertainty ± 1% of ratio

(b) Calculational uncertainties as a result of convergence criterion are negligible.[7]

(c) As the precision in the calculation is negligible, the total uncertainty in C/E is also ± 1% of the ratio.

I. REACTION RATE TRAVERSES

Axial and radial reaction rate distributions of ^{239}Pu, ^{238}U, and ^{10}B were measured. Gas filled counters were used for ^{239}Pu and ^{238}U, and the ^{10}B reaction rates were measured with a $^{10}BF_3$ proportional counter.

The reaction rate traverses were computed using the twenty-six group cross sections and fluxes from the X-Y and R-Z geometry 2DB calculations described in Appendices B-1 and B-2. The calculated ^{239}Pu reaction rates are in fair agreement with the experiment, as shown in Figures 3.13 through 3.15, except in the region of the core-reflector interface. Calculated and experimental ^{238}U fission rates, as shown in Figures 3.13 through 3.18, are in good agreement throughout the core. The calculated ^{10}B region rates, when normalized at the core center to the experimental data, as shown in Figures 3.19 through 3.21, are too low at the core-reflector interface and too high in the radial reflector but in good agreement elsewhere.

With the exception of the ^{238}U axial fission rate distribution, all calculated and experimental curves are normalized to 1.0 at the core center. The experimental ^{238}U fission rate shows a dip in the axial distribution at the core center -- a result of the core gap. Consequently, the experimental data is normalized to the calculated data at a position of 5cm removed from the core gap.

The discrepancies that occur between calculation and experiment in the reaction rate distributions within the core near the core-reflector boundary are not unique to the Assembly 56B analysis. They have appeared consistently in the analysis of previous experiments.[1,2] The calculation is consistently lower than the experiment. An example is the ^{10}B reaction rate comparison shown in Figure 3.20. Several possible explanations of this problem for investigation are listed below:

1. Cross sections being collapsed over inappropriate neutron spectra.
2. Need of flux and volume weighting of cross sections to approximate the effects resulting from heterogeneous platelet patterns.

3. Inability of diffusion or low S_n approximation transport theory to produce the correct spectrum at the boundaries.
4. Erroneous values of group constants including basic cross sections.
5. Inconsistency between experimental method and its description in the calculational model.

The discrepancies mentioned above appeared not only in the analysis of the 56B experiments, but in the analysis of the critical experiments performed in Assemblies 48, 48A,[2] 51,[3] and 52.[6] As a variety of methods has been used in the analyses of the above mentioned experiments, the first three of the possible explanations enumerated can be discarded as discussed below:

1. In the analyses of the five assemblies noted above, calculations were made with five and eight group collapsed cross section sets as well as with twenty-six groups. In the latter instance no spectrum weighing is involved. The calculated reaction rate distributions produced by the two collapsed group sets are little different from the results of the twenty-six group set.
2. Flux and volume weighting of the cross sections used to produce the fluxes with which the activity distributions were calculated is a technique used only in the analysis of the Assembly 51[2] and 52[6] experiments. There is no improvement in the calculated reaction rate distributions which used flux and volume weighting.
3. The fluxes used in the analysis of all the assemblies mentioned above were computed by codes using either diffusion or a low order S_n approximation to transport theory. It is possible that these models could not properly predict the correct space and energy distribution of the neutrons at the core-reflector boundary. A study was made, however, of the ratio of the ^{10}B reaction rate at the core center to the reaction rate at a position within the core near the core-reflector interface in other transport models. These ratios were calculated for S_n quadratures of 2,4,8 and 12. The difference in the calculated ratios using fluxes resulting from S_2 and S_{12} quadrature transport calculations was 0.3%. This is a negligible change.

It would appear, therefore, that the discrepancy between calculation and experiment in the activity distributions is a result of erroneous values of the group constants in the basic twenty-six group set, or the description of the experiment in the calculational model is inadequate to describe the actual experiment. Further investigation of both possibilities is recommended.

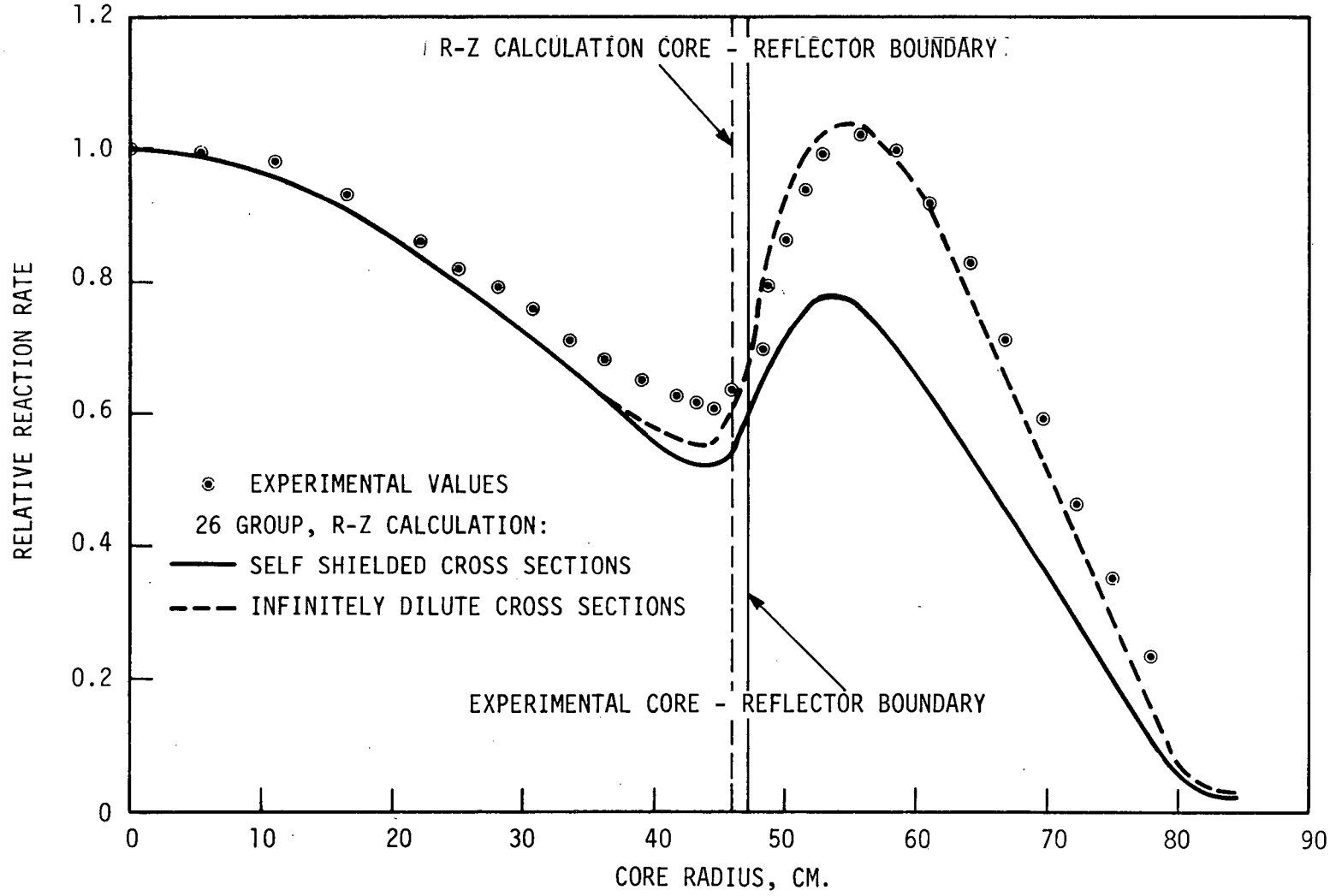

FIGURE 3.13 ^{239}Pu Radial Fission Rate Distribution

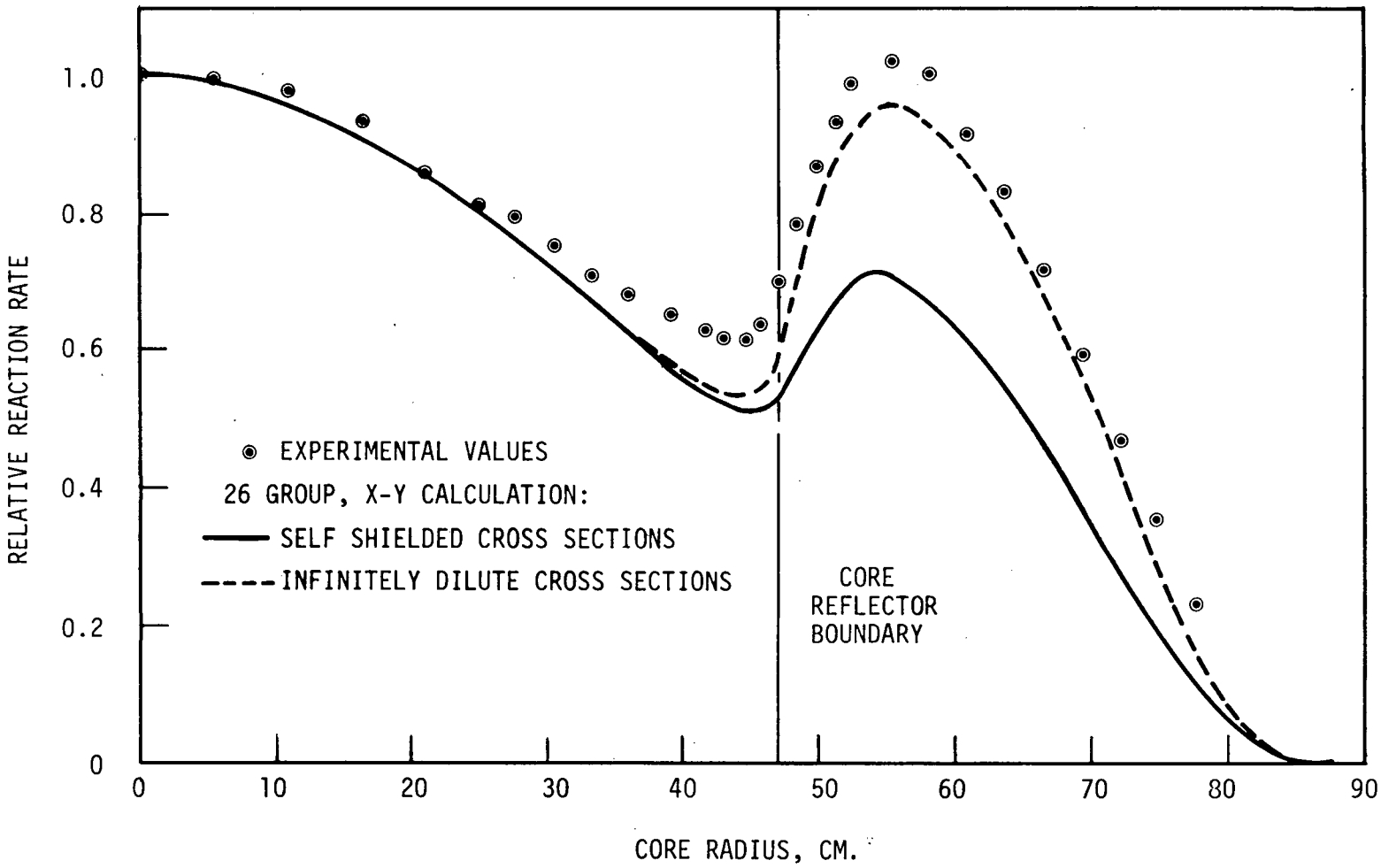

FIGURE 3.14 ^{239}Pu Radial Fission Rate Distribution

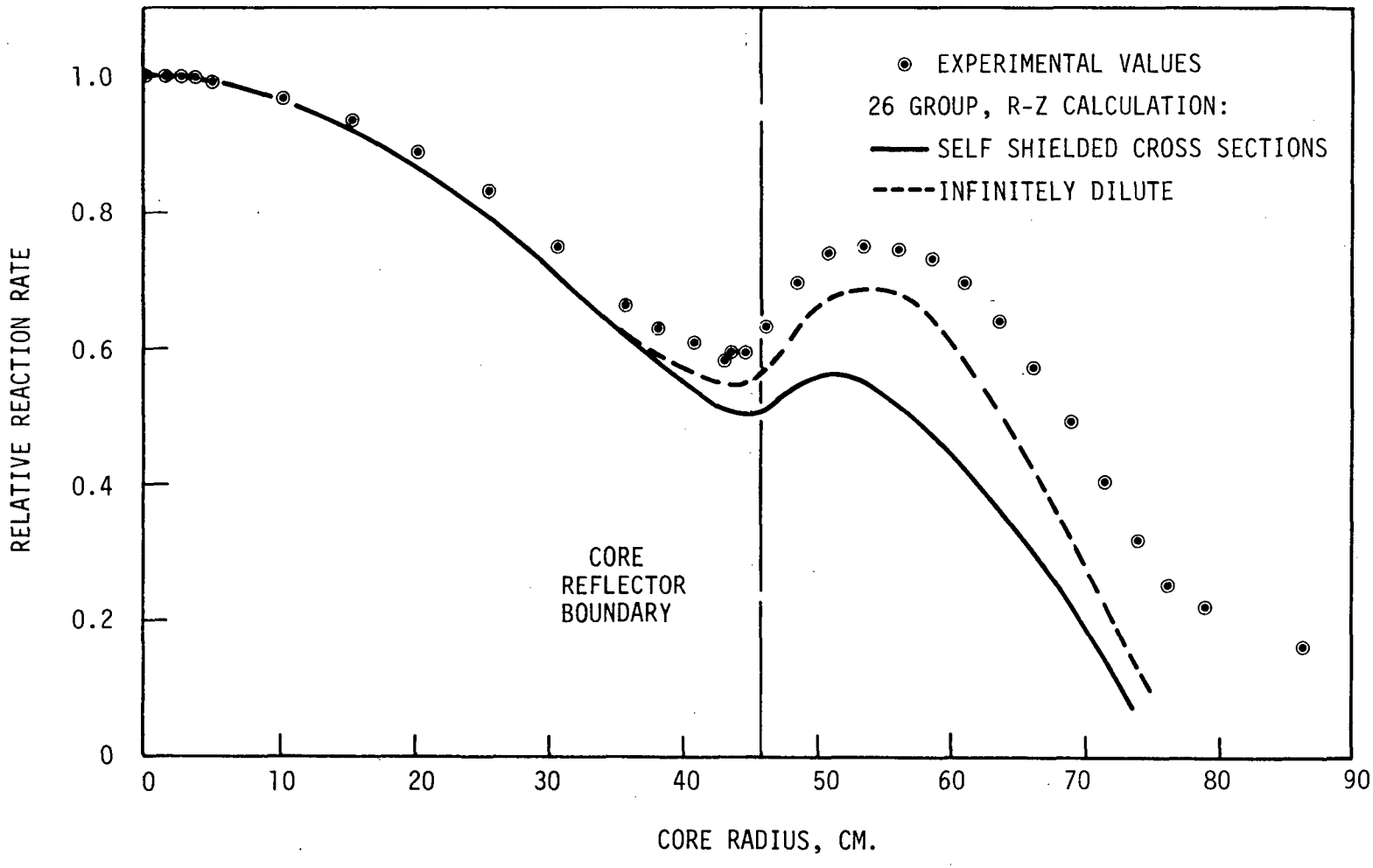

FIGURE 3.15 ^{239}Pu Axial Fission Rate Distribution

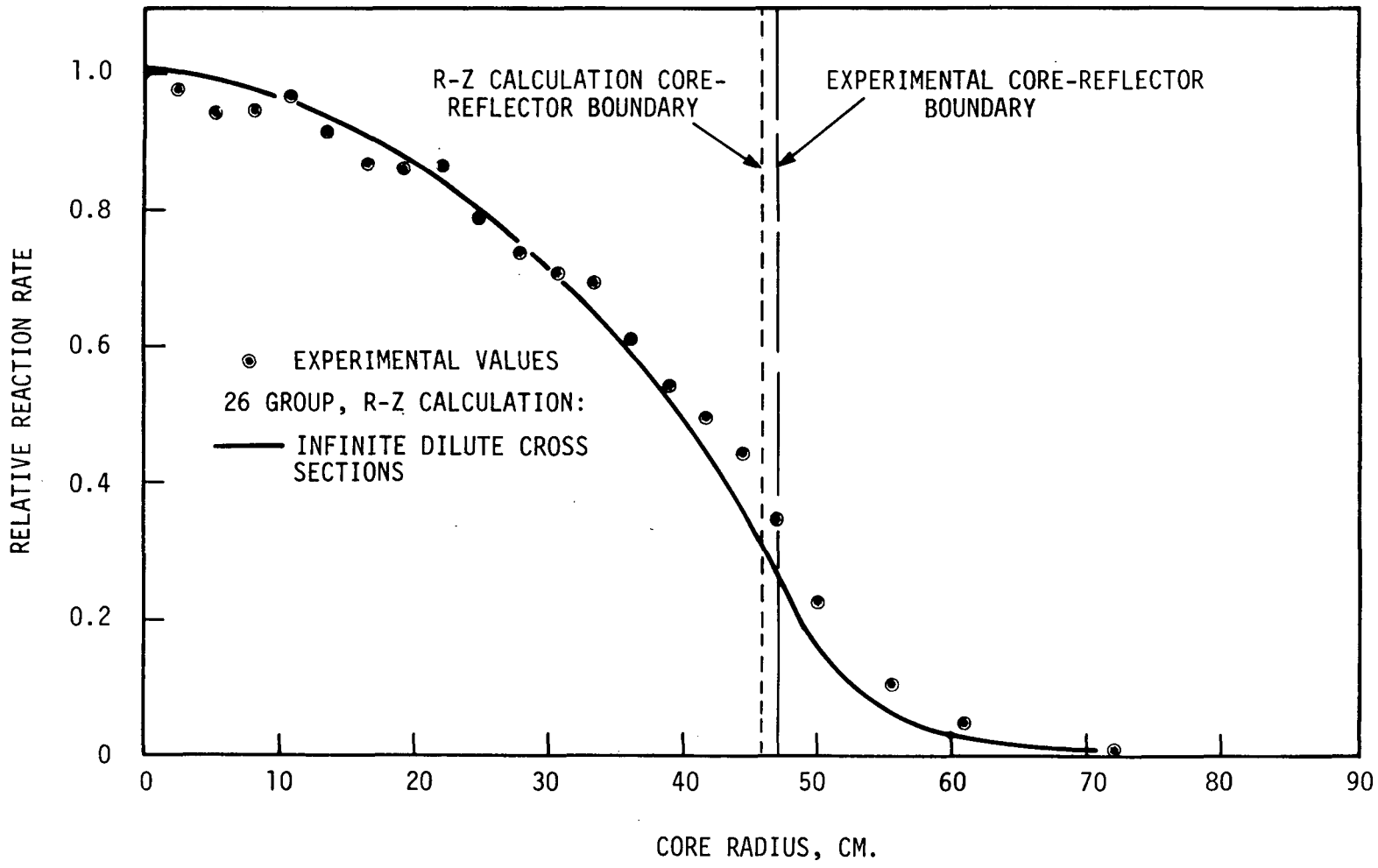

FIGURE 3.16 ^{238}U Radial Fission Rate Distribution

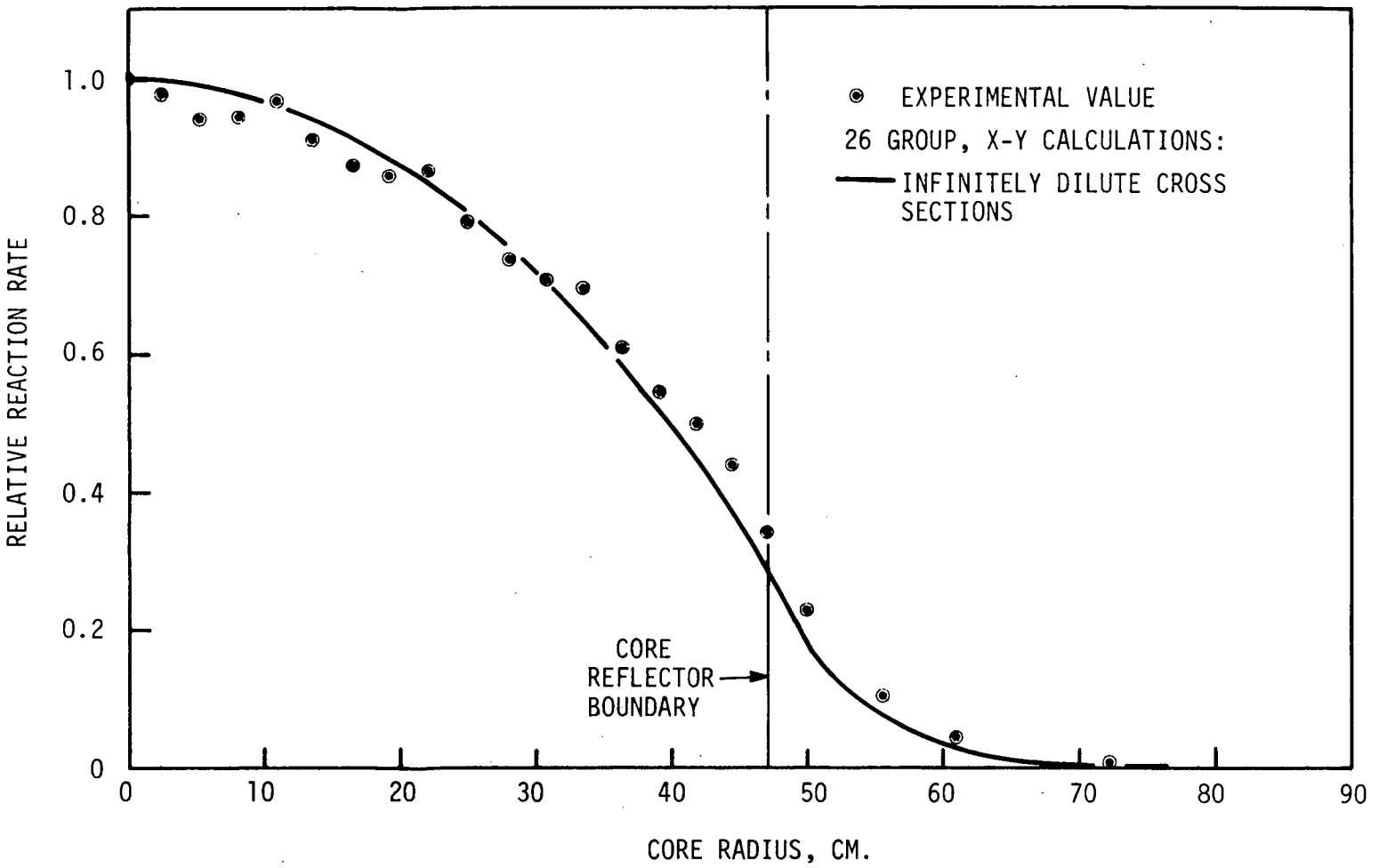

FIGURE 3.17 ^{238}U Radial Fission Rate Distribution

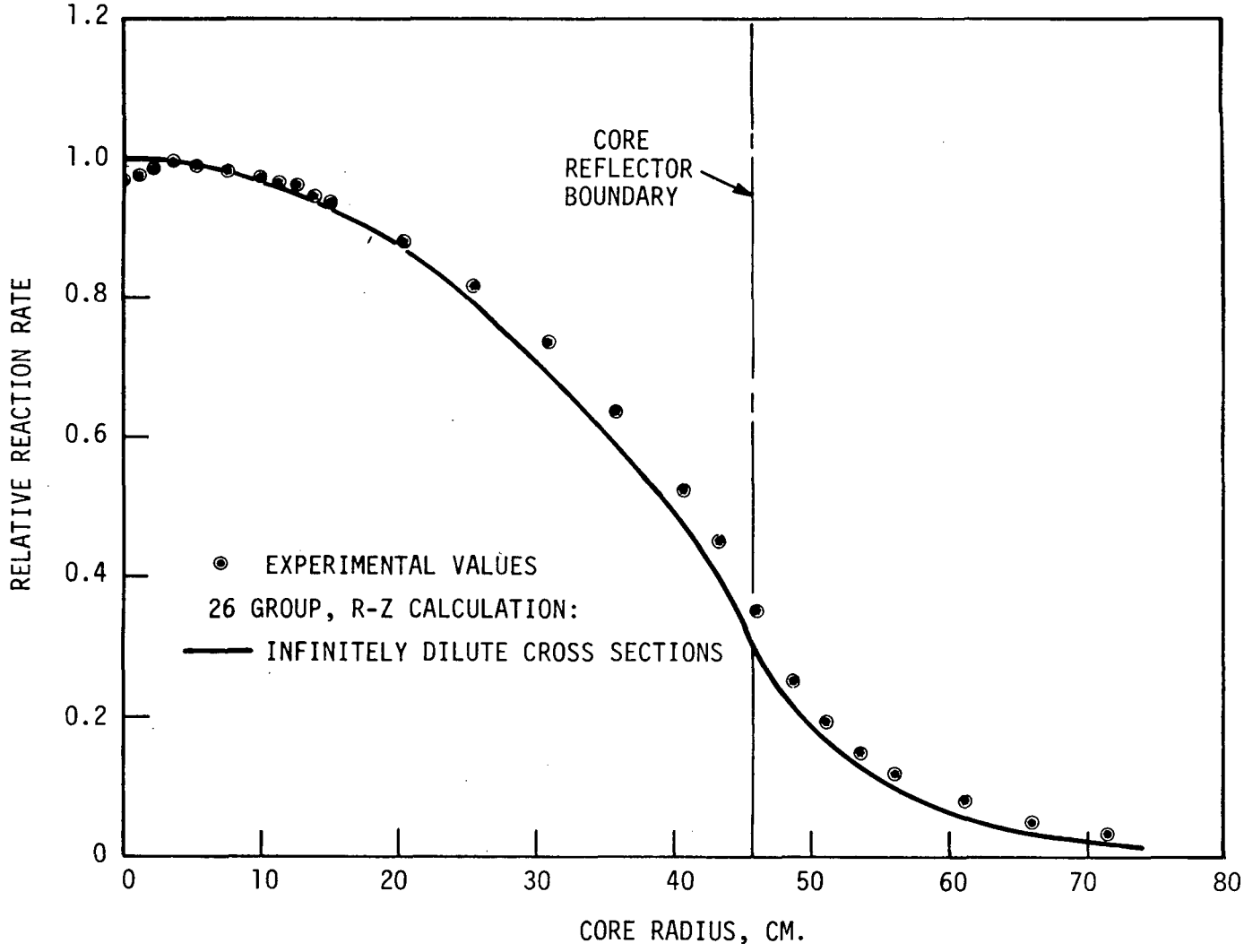

FIGURE 3.18 ^{238}U Axial Fission Rate Distribution

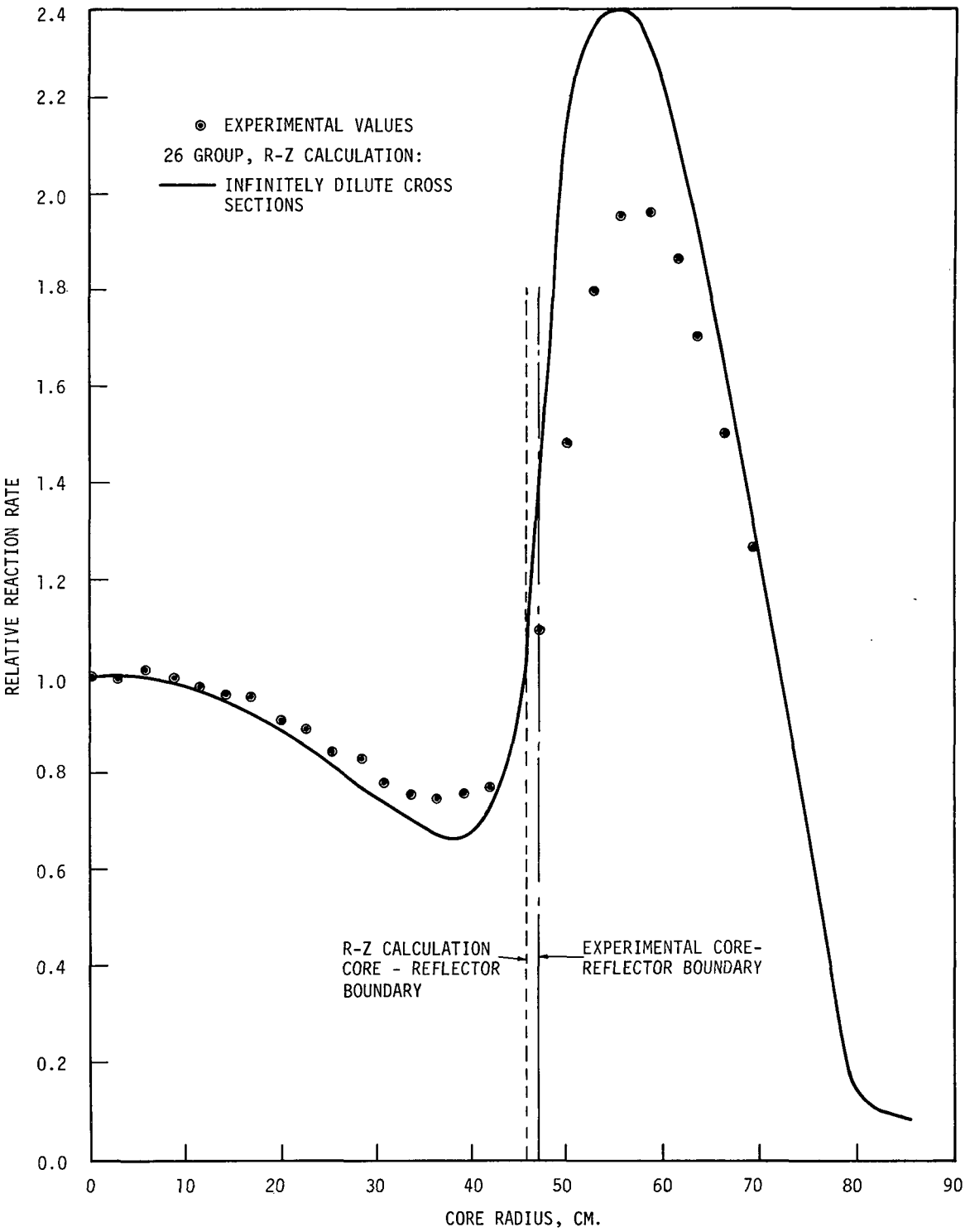

FIGURE 3.19 ^{10}B Radial Absorption Rate Distribution

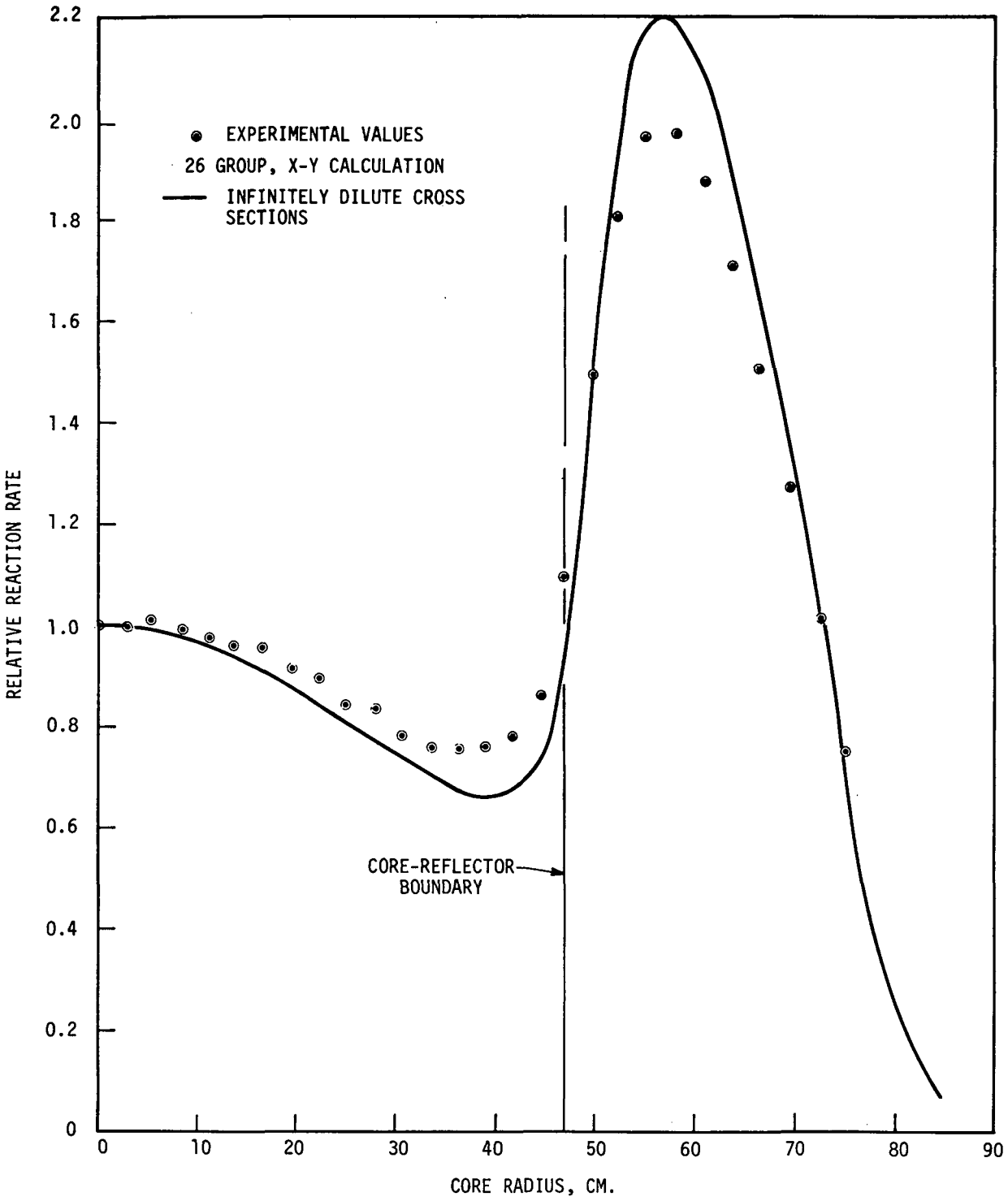

FIGURE 3.20 ^{10}B Radial Absorption Rate Distribution

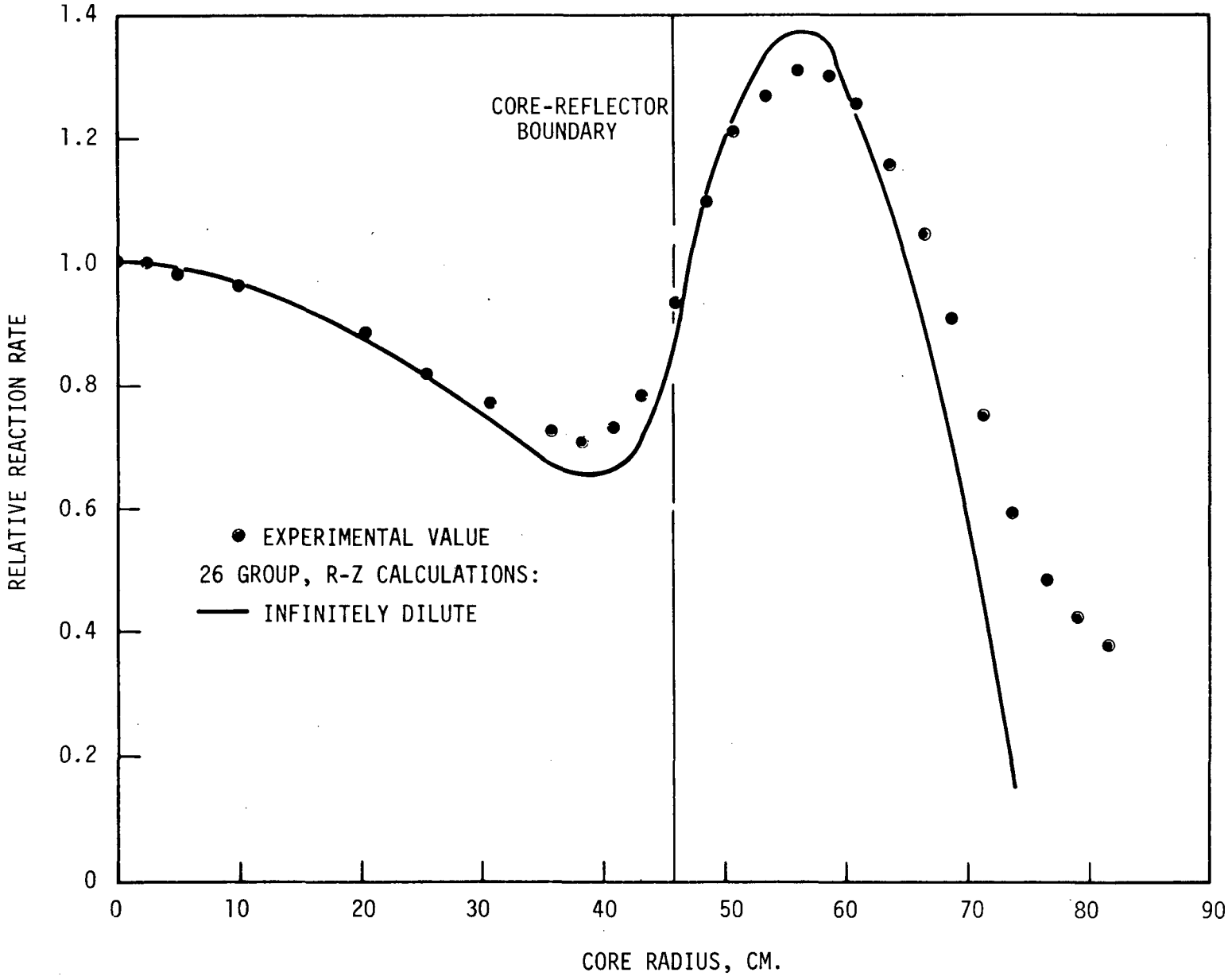

FIGURE 3.21 ^{10}B Axial Absorption Rate Distribution

REFERENCES

1. R. A. Bennett and S. L. DeMyer. Analysis of FTR Phase A Control Rod Experiments in ZPR-III Assembly 48 and 48A, BNWL-967, Battelle-Northwest, Richland, Washington, April 1969.

2. W. R. Young and R. A. Bennett. Analysis of Phase B Critical Experiments, Part 1, ZPR-III Assembly 51, BNWL-1138, Battelle-Northwest, Richland, Washington, January 1970.

3. W. R. Young and R. A. Bennett. Analysis of Phase B Critical Experiments, Part 2, ZPR-III Assemblies 52a, b, c, d, e and f, BNWL-1139, Battelle-Northwest, Richland, Washington, February 1970.

4. W. R. Young and R. A. Bennett. Analysis of FTR Phase B Critical Experiments Part 3, Doppler Effect in ZPR-III Assembly 51, HEDL-TME 71-57, WADCO Corporation, Richland, Washington, 1971.

5. R. A. Bennett, S. L. Engstrom, J. V. Nelson and W. R. Young. "Statistically Significant Biases in the FTR Neutronics Model," Transactions of the American Nuclear Society 1970 Annual Meeting, Volume 13, Number 1, p. 291, Hinsdale, Illinois, 1970.

6. G. R. Keepin. Physics of Nuclear Kinetics, Addison-Wesley Publishing Co., Palo Alto, California, 1965.

7. W. W. Little. Private Communication.

8. C. F. Masters, et al. "The Measurement of Absolute Delayed-Neutron Yields From 3.1 and 14.9 MeV Fission," Nucl. Sci. & Eng., pp. 202-208, 1969.

9. Reactor Development Program Progress Report, ANL-7553, Argonne National Laboratory, Argonne, Illinois, February 1969.

10. Reactor Development Program Progress Report, ANL-7561, Argonne National Laboratory, Argonne, Illinois, March 1969.

11. Reactor Development Program Progress Report, ANL-7577, Argonne National Laboratory, Argonne, Illinois, April-May 1969.

12. J. V. Nelson and S. L. DeMyer. Group Constants for Analysis of FFTF Critical Experiments, BNWL-1044, Battelle-Northwest, Richland, Washington, November 1969.

13. I. I. Bondarenko, et al. Group Constants for Nuclear Reactor Calculations, Consultants Bureau, New York, 1964.

14. R. W. Hardie and W. W. Little, Jr. 1DX, A One Dimensional Diffusion Code for Generating Effective Nuclear Cross Sections, BNWL-954, Battelle-Northwest, Richland, Washington, 1969.

15. W. W. Little, Jr. and R. W. Hardie. 2DB User's Manual, Revision 1, BNWL-831 R1, Battelle-Northwest, Richland, Washington, August 1969.

16. K. D. Lanthrop. DTF-IV, A Fortran IV Program for Solving the Multigroup Transport Equation with Anisotropic Scattering, LA-3373, Los Alamos Scientific Laboratory, Los Alamos, New Mexico, 1965.

17. R. W. Hardie and W. W. Little, Jr. PERT V, A Two Dimensional Code for Fast Reactor Analysis, BNWL-1162, Battelle-Northwest, Richland, Washington, September 1969.

18. L. D. O'Dell, R. W. Hardie and W. W. Little, Jr. A Numerical Comparison of Diffusion and Transport (S_n) Codes for Selected Fast Reactor Configurations, BNWL-992, Battelle-Northwest, Richland, Washington, March 1969.

19. W. W. Little, et al. Analysis of Selected Critical Experiments Using Version II of the Evaluated Nuclear Data File (ENDF/B), BNWL-1348, Battelle-Northwest, Richland, Washington, July 1970.

20. Reactor Development Program Progress Report, ANL-7255, Argonne National Laboratory, Argonne, Illinois, September 1966.

21. Reactor Development Program Progress Report, ANL-7267, Argonne National Laboratory, Argonne, Illinois, October 1966.

22. Reactor Development Program Progress Report, ANL-7460, Argonne National Laboratory, Argonne, Illinois, June 1968.

23. Private Communication, A. Travelli.

24. Reactor Development Program Progress Report, ANL-7581, Argonne National Laboratory, Argonne, Illinois, June 1969.

25. Reactor Development Program Progress Report, ANL-7595, Argonne National Laboratory, Argonne, Illinois, July 1969.

26. Reactor Development Program Progress Report, ANL-7655, Argonne National Laboratory, Argonne, Illinois, December 1969.

27. W. W. Little, Jr. and R. W. Hardie. "Discrepancy Between Measured and Calculated Reactivity Coefficients in Dilute Plutonium Fueled Fast Criticals," Nuclear Science and Engineering, Vol. 28, No. 111, 1967.

28. V. O. Uotinen. "An Analysis of Subcritical Measurements of Peripheral Control Rods in ZPR-3 Assembly 56B," Reactor Physics Quarterly Report, October, November, December 1969, BNWL-1304, February 1970.

29. W. G. Davey and P. I. Amundson. Nuclear Science and Engineering, Vol. 28, No. 111, 1967.

30. S. L. Engstrom, R. A. Bennett, V. O. Uotinen. "Inverse Multiplication in Monitoring of Subcritical Changes in FTR", Transactions of the American Nuclear Society 1970 Annual Meeting, Volume 13, Number 1, p. 325, Hinsdale, Illinois, 1970.

APPENDIX A

CYLINDRICAL REPRESENTATION OF ASSEMBLY 56B, LOADING 56-17

APPENDIX A

CYLINDRICAL REPRESENTATION OF ASSEMBLY 56B, LOADING 56-17

GENERAL EVALUATION

For evaluation of calculational methods, it is advantageous to know the dimensions and fissile mass of a homogeneous, cylindrical representation of an irregular, heterogeneous, cylindrical, critical assembly. The following alterations are necessary to convert loading 56-17 to such a representation:

- Full insertion of the control drawer, which was withdrawn 8.62 inches at 3.74 Ih subcritical,
- Adjustment of the average assembly temperature from 37.6 to 40.0°C.
- Conversion of irregular profile to a circular cylinder,
- Conversion of safety and control drawers to typical core drawers,
- Removal of interface gap between assembly halves,
- Adjustment of core radius to achieve critical.

CONTROL DRAWER INSERTION

Loading 56-17 was measured to have a $k_{eff} = 0.999964$ and a total fissile inventory of $^{239}Pu + ^{241}Pu + ^{235}U$ of 333.415 kg. The control drawer was withdrawn 8.62 inches. Full insertion of this drawer would move 0.477 kg of fissile mass into the core and increase the reactivity by 0.0719% $\Delta k/k$.

TEMPERATURE CORRECTIONS

From temperature change reactivity measurements, made during core edge drawer measurements, an assessment of the temperature coefficient was found to be 2.41 ± 0.03 Ih/°C where the Ih = 1039.08%ρ. The average temperature for loading 56-17 was 37.6°C. The analytical model is at 40°C. The change in reactivity from 37.6 to 40.0°C is a -0.0056% $\Delta k/k$.

CYLINDRICIZATION

With the control drawer fully inserted, the core loading contains 218.5 fuel columns. The equivalent radius for a cylinder of this volume

is 46.179 cm. The process used to estimate the reactivity and mass change brought about by cylindricizing the core involved replacing all fuel drawers, through which the equivalent radius falls, with reflector material; noting the decrease in mass and reactivity; and then replacing fuel for reflector everywhere within the equivalent radius. Figure A-1 is a scale representation of one quarter of the core, giving drawer dimensions and the equivalent radius.

The measured worth of replacing reflector with fuel drawers at various core edge locations is given in Table 3.3. These worths are plotted as a function of distance from core center to drawer center in Figure A-2. An estimation of the center of mass is made for each partial drawer area in which fuel will replace reflector to complete the core within the cylindrical boundary. By extrapolation or interpolation from the curves in Figure A-2, worths of full fuel drawers are associated with the distance from core center to the centers of these fractional drawer areas. The product of this worth and the fractional drawer area used is the worth of that fractional fuel drawer. A tabulation of the worth of the full fuel drawers removed is given in Table A-1. Worths of fractional drawers, filling in the cylindrical area, are tabulated in Table A-2.

TABLE A-1

CORE EDGE DRAWER WORTHS

Drawer	Number of similar drawers in core (N)	Worth of fuel-for-reflector exchange per drawer % Δk/k (W)	Total worth of fuel drawers on core boundary % Δk/k = (N) x (W)
H-15; L-9	16	0.022	0.352
H-16; P-8	8	0.051	0.408
I-12; O-8	16	0.050	0.800
J-11	8	0.023	0.184
K-10	8	0.56	0.448
N-8; H-14	11	0.048	0.528
		Total worth	2.720% Δk/k

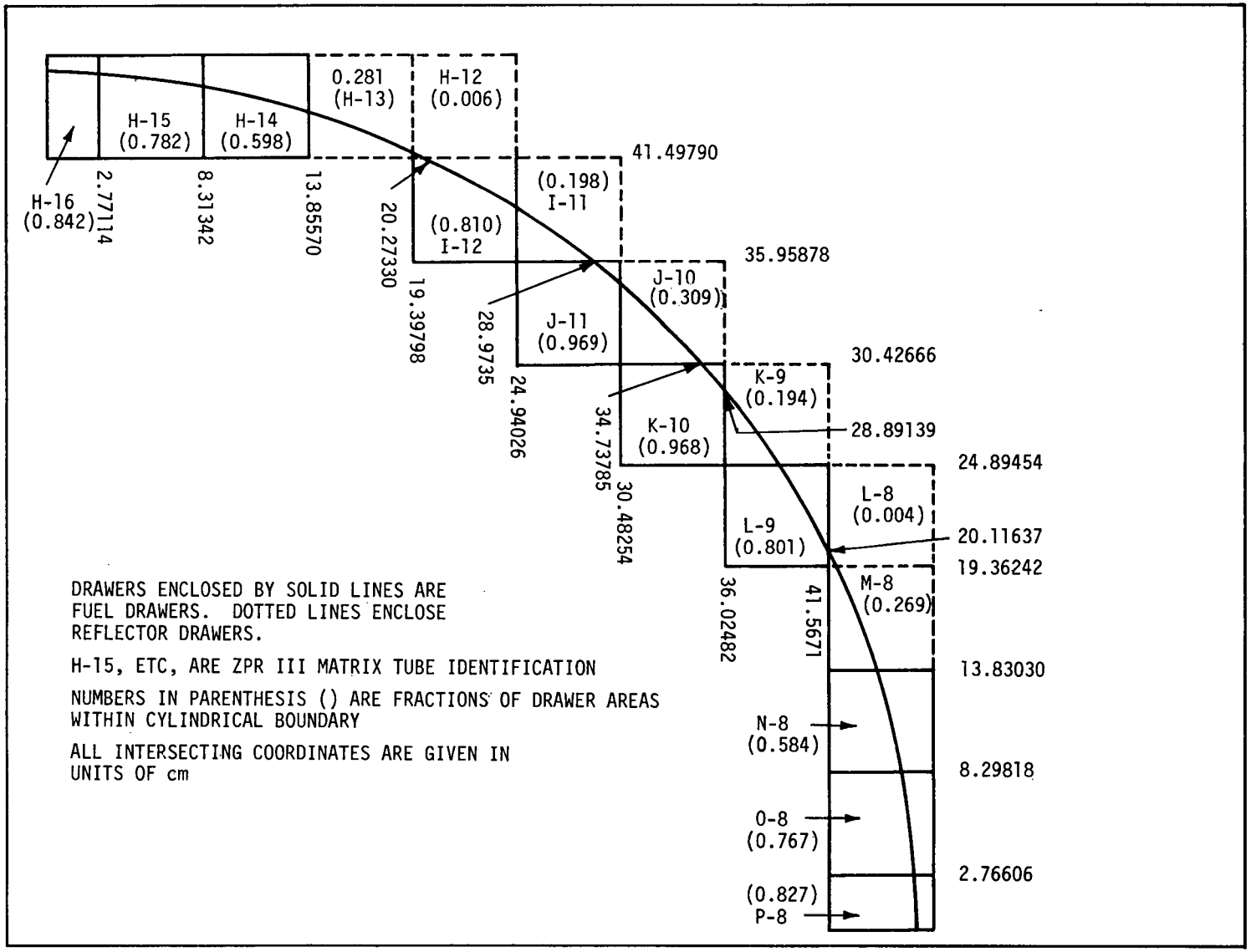

FIGURE A-1 Drawer Areas Effected by Cylindricization

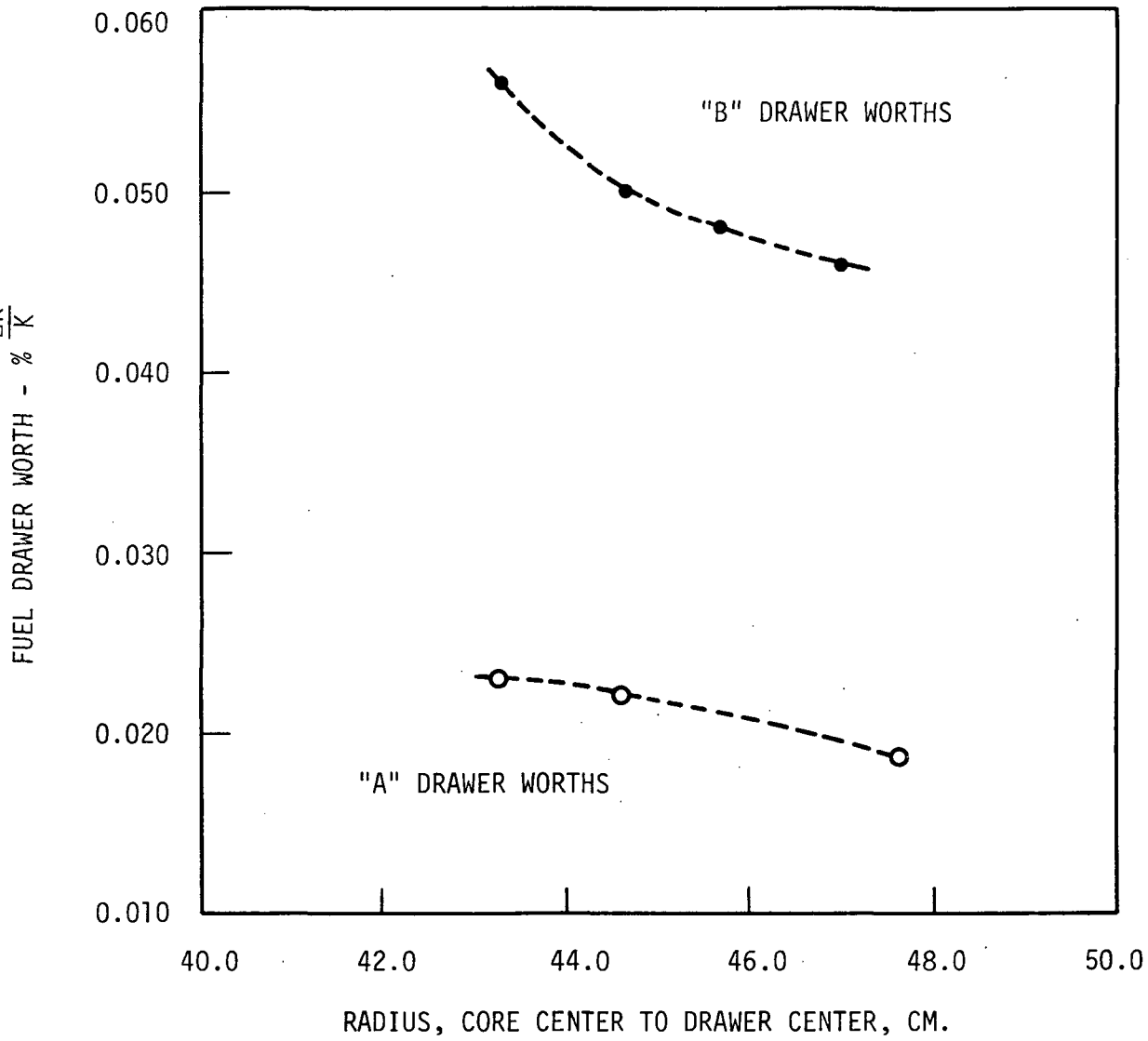

FIGURE A-2. Fuel Drawer Worth as a Function of Core Radius

TABLE A-2

ASSEMBLY 56-B LOADING 56-17, CORE CYLINDRICIZATION AND ADJUSTMENT OF DRAWER WORTHS

Drawers to be Partially Filled with Fuel	Initial Drawer Worth % Δk/k	Drawer Type	Number (N) of Similar Drawers in Core	Fraction (F) of Drawer within Bounds of Equivalent Cylinder	Number of Drawers (N) x Fraction of Drawer (F) = A	Worth (W) of Full Drawer centered at Fractional Drawer Center	Total Worth of Replaced Drawer Area = AXW
X-16, H-16	0.051	B	4	0.8424	3.3696	0.0532	.17926
P-24, P-8	0.051	B	4	0.8271	3.3084	0.0532	.17601
Q,O; 8,24	0.050	B	8	0.7670	6.1360	0.0525	.32214
X,H; 14,18	0.048	B	8	0.5979	4.7832	0.0505	.24155
R,N; 8,24	0.048	B	8	0.5840	4.6720	0.0505	.23594
X,H; 13,19	0.0193	A	8	0.2814	2.2512	0.0213	.04795
T,L; 9,23	0.0220	A	8	0.8014	6.4112	0.0223	.14297
W,I; 11,21	0.019	A	8	0.1984	1.5872	0.0210	.03333
U,K; 9,23	0.019	A	8	0.1940	1.5520	0.0210	.03259
U,K; 10,22	0.056	B	8	0.9683	7.7646	0.0570	.44258
V,J; 10,22	0.046	B	8	0.3086	2.4688	0.0490	.12097
V,J; 11,21	0.023	A	8	0.9692	7.7536	0.0233	.18066
W,I; 12,20	0.050	B	8	0.8152	6.5216	0.0535	.34891
S,M; 8,24	0.046	B	8	0.2737	2.1896	0.0485	.10620
X,H; 15,17	0.022	A	8	0.7820	6.2560	0.0225	.14076

Total Worth = 2.7518

Replaced

While the volume of the X-Y core configuration and the equivalent cylinder are equal, there is a lower fissile mass in the cylinder because it contains a higher ratio of "A" to "B" drawers. However, this decrease in fissile mass is accompanied by a net reactivity increase, since the edge fuel is moved to locations of higher worth. The difference in reactivity and fissile mass between the totals of Tables A-1 and A-2 yields a fissile mass decrease of 0.90 kg and a reactivity increase of 0.032% $\Delta k/k$ as a result of cylindricizing the core.

5. CONVERSION OF SAFETY AND CONTROL DRAWERS TO "B" DRAWERS

Each control and safety drawer contains 0.0381 fewer kg of fissile mass than a "B" drawer. In converting all 18 control and safety drawers to "B" drawers, the fissile mass of the core increases by 0.6858 kg.

The following factors are involved in the calculation of the increase in reactivity resulting from this increase in fissile mass:

- Fractional worth of fissile material to total drawer contents = 0.835 ± 0.042
- Total worth of 18 safety and control drawers = $1.98\%\ \Delta k/k \pm 0.02$
- Fraction of fissile mass to be added to total fissile mass in safety and control drawers = $0.0376 \pm ?$

The resultant reactivity increase, equal to the product of the above three factors, is $0.0622\%\ \Delta k/k \pm 0.0032$.

REMOVAL OF INTERFACE GAP

The two halves of the ZPR-3 facility are separated by a small gap. Removal of the gap would cause a closer proximity of the fuel of the two halves; consequently, a reactivity increase.

For Assembly 48, the reactivity effect was estimated to be 40 ± 20 Ih.* The effect is thought to be smaller in larger cores. Reducing this effect by the ratio of the cross sectional areas of Assemblies 48 and 56B, the resulting reactivity increase would be $0.024 \pm 0.012\%\ \Delta k/k$.

---

*Ih/%ρ = 1039.08

ADJUSTMENT OF CORE RADIUS TO ACHIEVE A CRITICAL CONFIGURATION

A summary of the above mass and reactivity changes is given in Table A-3. A return to critical involves removing a quantity of edge material, uniformally, which will be worth 0.180% $\Delta k/k$. The average worth per kg of edge fuel is 0.043% $\Delta k/k/kg$. Consequently, 4.209 kg of fissile material must be removed. This is equivalent to removing 2.763 columns which yields a critical radius of 45.89 cm.

TABLE A-3

SUMMARY OF MASS AND REACTIVITY CHANGES INVOLVED IN CONVERTING TO A HOMOGENEOUS RIGHT CYLINDER REPRESENTATION OF 56B

	Fissile Mass, kg	Multiplication
Initial Values:	333.415	0.999964 $\pm$ 0.0000015
Changes:	Δkg	$\Delta\rho$, $\%\Delta k/k$
1. Control drawer insertion	0	+0.0719 $\pm$ 0.0007
2. Temperature, 37.6 40.0°C		-0.0056 $\pm$ 0.00007
3. Cylindricization	-0.90	+0.032 $\pm$ 0.0015[(a)]
4. Convert safety and control drawers to "B" drawers	+0.6858	+0.0622 $\pm$ 0.0032[(a)]
5. Remove interface gap		+0.024 $\pm$ 0.012[(a)]
TOTALS:	333.20	1.00181 $\pm$ 0.00013
Return to Critical	-4.209	-0.00181 $\pm$ 0.00004
Critical Configuration =	328.991 kg	1.00000 $\pm$ 0.00014

(a) Uncertainties are estimates based on ability to calculate small correction factors.

APPENDICES B

CALCULATION SUMMARIES

CALCULATION SUMMARIES

The following appendices summarize:

1. Experimental cores and adjustments made in these cores based on experimental measurements producing cores which resemble some calculational possibility. For example, an adjustment is always made for the core gap - as this cannot be constructed in the calculational model.
2. Analytical models used to calculate the adjusted experimental cores. Calculational corrections are added to approximate the best possible calculations. These corrections are based on other calculations, rather than experiment. For example, all initial calculations for Assembly 56B were made using diffusion theory. One pair of calculations was made to find the diffusion - transport theory difference and this difference is added to all calculations.

Uncertainties on experimental k_{eff} and Δk of adjustments are listed in Tables 3.3 and A-9, and are not reproduced here. The uncertainties on all calculated k_{eff} are within $\pm 3\ \varepsilon$ of the absolutely converged k_{eff} where ε is the convergence criterion. As all calculations have been converged to 10^{-5} or better, the uncertainty on any calculated k_{eff} is at least as good as 3×10^{-5}. All corrections to the calculated k_{eff} are based on pairs of calculations, converged to 10^{-5} or better. Hence, the uncertainty on all corrections is 4×10^{-5} or better.

These summaries are not meant to be used or understood apart from the context of the entire report. They provide additional detail to sections of the report where they are referenced and are not meant to be independent.

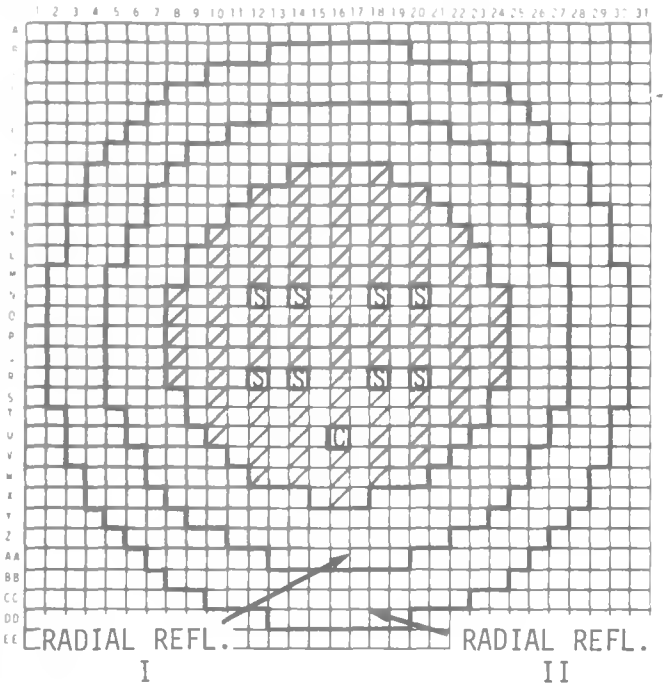

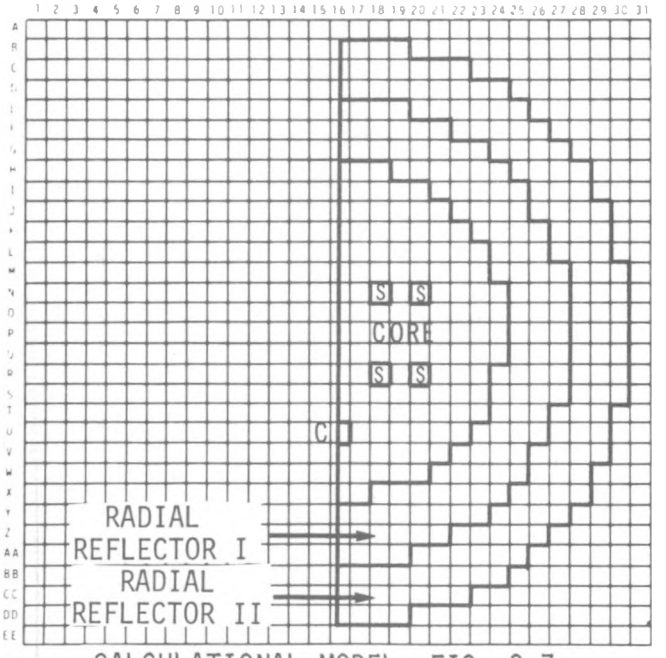

CALCULATIONAL MODEL, FIG. 3.7

CALCULATION #167 I

EXPERIMENTAL ASSEMBLY #56B

EFFECTIVE CORE RADIUS 46.231 cm.

CORE HEIGHT 91.59 cm.

REFLECTOR THICKNESS { RADIAL 34 cm. / AXIAL 27.9 cm.

CRITICAL MASS 334.428 Kg. ($Pu^{239+241}$ + U^{235})

ABBREVIATIONS:

■ _____ IN HALF #1, _____ IN HALF #2

[S] = SAFETY DRAWER

[C] = CONTROL DRAWER

⊘ = ENRICHED DRAWER OF CELL

OTHER: _____

MEASURED K_{eff}, inferred 1.000444

CORE GAP ADJUSTMENT +0.00024

TEMPERATURE " -0.000056

SAFETY ROD POSITION +0.000719

ADJUSTED K_{eff} 1.001347 ± .000120

(see Table 3.3)

CALCULATIONAL MODEL

CODE 2DB GEOMETRY X-Y

DIFFUSION √, if S_N, N = _____

SYMMETRY 1/2 core

SOURCE OF ATOM DENSITIES homogeneous, "X-Y Averaged"

X-SEC. { GROUPS 26 / HOMO./HETERO homogeneous

CORE HT. 0

EFFECTIVE CORE RADIUS 46.231 cm.

REFLECTOR THICKNESS { RADIAL 34.cm. / AXIAL 0

BUCKLING 6.35×10^{-4} $cm.^{-2}$

CALCULATED K_{eff} = 0.98538

CALCULATED MASS = 334.217

DIFFUSION + TRANSPORT S_∞ +0.00634

HOMOG. + HETEROGENEOUS +0.01016

OTHER: (1) Norm. Recip. Wt. +0.00194

(2) Mass Difference +0.00031

CORRECTED DIFFUSION K_{eff} 0.99779

CORRECTED TRANSPORT K_{eff} 1.00413 ± .00009

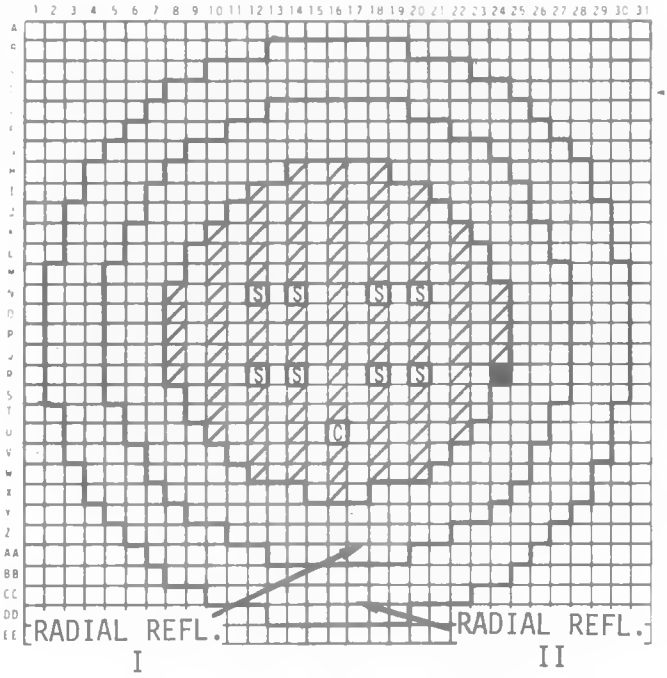

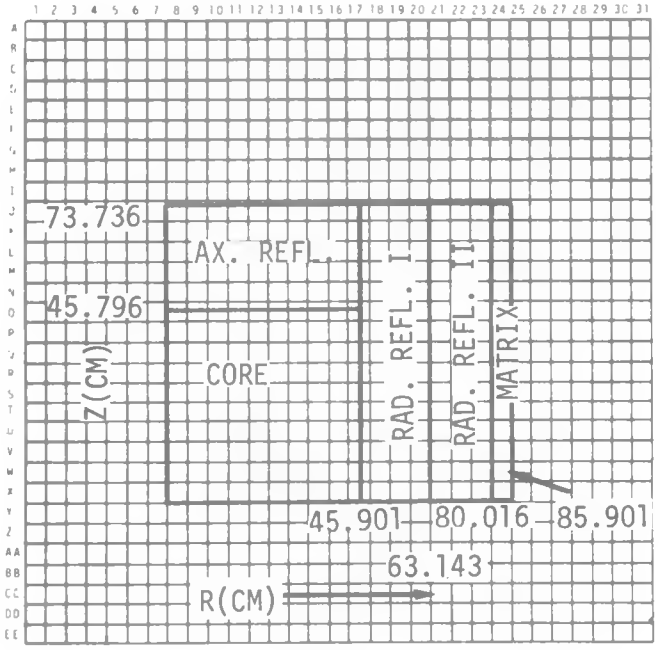

CALCULATIONAL MODEL FIGURE 3.6

CALCULATION # 167-K

EXPERIMENTAL ASSEMBLY # 56B

EFFECTIVE CORE RADIUS 45.89 cm.

CORE HEIGHT 91.59 cm.

REFLECTOR THICKNESS { RADIAL 34 cm. / AXIAL 27.9 cm.

CRITICAL MASS 328.991 kg. ($Pu^{239+241}+U^{235}$)

ABBREVIATIONS:

■ Core IN HALF #1, Refl. IN HALF #2

[S] = SAFETY DRAWER

[C] = CONTROL DRAWER

[⊘] = ENRICHED DRAWER OF CELL

OTHER:

MEASURED K_{eff} 0.999964

CORE GAP ADJUSTMENT

TEMPERATURE " See Appendix A

SAFETY ROD POSITION

ADJUSTED K_{eff} 1.00000 ±.00014 (see Table A-3)

CALCULATIONAL MODEL

CODE 2DB GEOMETRY R-Z

DIFFUSION ✓, if S_N, N =

SYMMETRY 1/2 core

SOURCE OF ATOM DENSITIES homogeneous, "R-Z Averaged"

X-SEC. { GROUPS 26 / HOMO./HETERO homogeneous

CORE HT. 91.59 cm.

EFFECTIVE CORE RADIUS 45.901

REFLECTOR THICKNESS { RADIAL 34.cm. / AXIAL 27.9cm.

BUCKLING 0.0

CALCULATED K_{eff} = 0.98143

CALCULATED MASS = 329.978

DIFFUSION + TRANSPORT S_∞ +0.00634

HOMOG. + HETEROGENEOUS +0.01016

OTHER: (1) Norm. Recip. Wt. +0.00194

(2) Mass & Core Radius Difference -0.00126

CORRECTED DIFFUSION K_{eff} 0.99227

CORRECTED TRANSPORT K_{eff} 099861 ±.00008

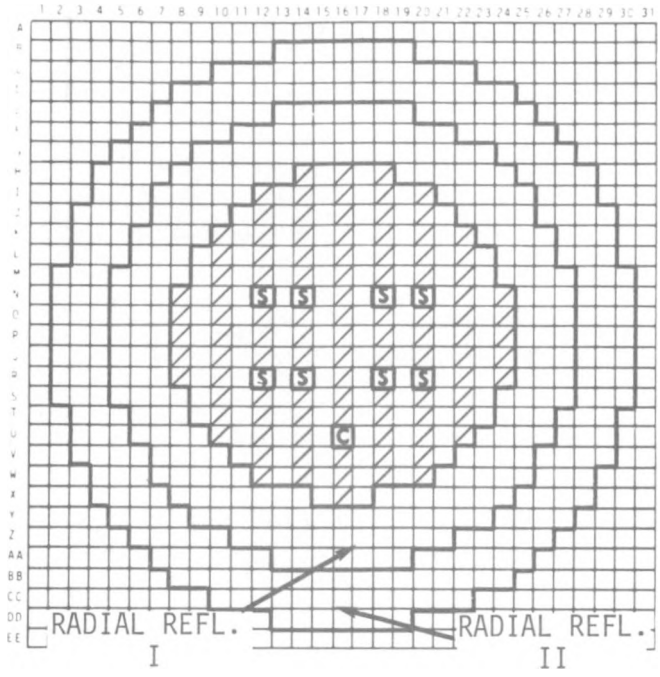

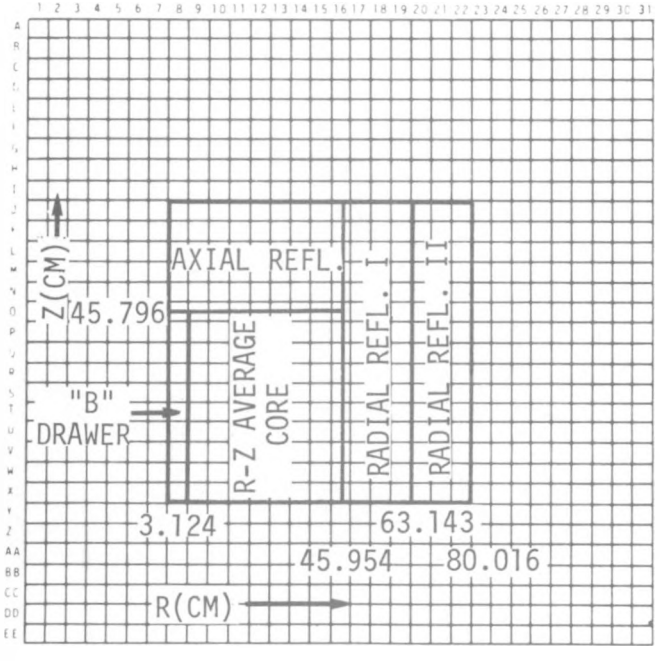

CALCULATIONAL MODEL, FIGURE 3.10

CALCULATION #167-M

EXPERIMENTAL ASSEMBLY # 56B

EFFECTIVE CORE RADIUS 45.954 cm.

CORE HEIGHT 91.59 cm.

REFLECTOR THICKNESS { RADIAL 34 cm. / AXIAL 27.9 cm.

CRITICAL MASS 329.015 Kg. ($Pu^{239+241}_{+U^{253}}$)

ABBREVIATIONS:

■ _____ IN HALF #1, _____ IN HALF #2

[S] = SAFETY DRAWER

[C] = CONTROL DRAWER

⊘ = ENRICHED DRAWER OF CELL

OTHER: _____

MEASURED K_{eff} _____

CORE GAP ADJUSTMENT _____

TEMPERATURE " _____

SAFETY ROD POSITION _____

ADJUSTED K_{eff} _____

CALCULATIONAL MODEL

CODE 2DB GEOMETRY R-Z

DIFFUSION ✓, if S_N, N = _____

SYMMETRY 1/2 core

SOURCE OF ATOM DENSITIES homogeneous,

"R-Z Averaged" in core, "B" in center zone

X-SEC. { GROUPS 13 / HOMO./HETERO homogeneous

CORE HT. 91.59 cm

EFFECTIVE CORE RADIUS 45.954 cm.

REFLECTOR THICKNESS RADIAL 34 cm. / AXIAL 27.9 cm.

BUCKLING 0.0

CALCULATED K_{eff} =	0.97988
CALCULATED MASS =	331.18 Kg.
DIFFUSION + TRANSPORT S_∞	+0.00634
HOMOG. + HETEROGENEOUS	+0.010106
	+0.00194
OTHER: Norm. Recip. Wt. mass difference	-0.00320
CORRECTED DIFFUSION K_{eff}	0.98878
CORRECTED TRANSPORT K_{eff}	0.99512 ±.00008

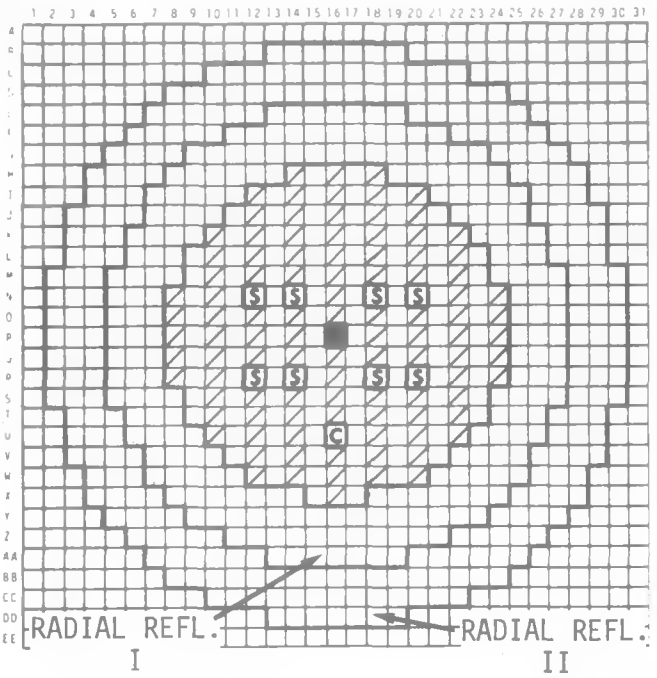

SEE FIGURE,
APPENDIX B-3

CALCULATION #167-N,O

EXPERIMENTAL ASSEMBLY #

EFFECTIVE CORE RADIUS 45.954 cm.

CORE HEIGHT ~~91.59 cm.~~

REFLECTOR THICKNESS { RADIAL 34 cm. / AXIAL 27.9 cm.

CRITICAL MASS

ABBREVIATIONS:

■ N-B4C o-Ax. IN HALF #1, Same IN HALF #2

[S] = SAFETY DRAWER

[C] = CONTROL DRAWER

⧄ = ENRICHED DRAWER OF CELL

OTHER:

MEASURED K_{eff}

CORE GAP ADJUSTMENT

TEMPERATURE "

SAFETY ROD POSITION

ADJUSTED K_{eff}

CALCULATIONAL MODEL

CODE 2DB GEOMETRY R-Z

DIFFUSION ✓, if S_N, N =

SYMMETRY 1/2 core

SOURCE OF ATOM DENSITIES homog., "R-Z Av."

in core, Ax. Ref. or Cent. B_4C in central zone

X-SEC. { GROUPS 13 / HOMO./HETERO homogeneous

CORE HT. 91.59 cm.

EFFECTIVE CORE RADIUS 45.954 cm

REFLECTOR THICKNESS { RADIAL 34 cm. / AXIAL 27.9 cm.

BUCKLING 0.0

CALCULATED K_{eff} = N=0.96265 / O-0.97422

CALCULATED MASS =

DIFFUSION + TRANSPORT S_∞ +0.00634

HOMOG. + HETEROGENEOUS +0.01016

OTHER: Norm. Recip. wt. +0.00194

mass difference (seeB-3) -0.00320

CORRECTED DIFFUSION K_{eff} N=0.97155 / O=098312

CORRECTED TRANSPORT K_{eff} N=0.97789 ±.00008 / O=0,98946 ±.00008

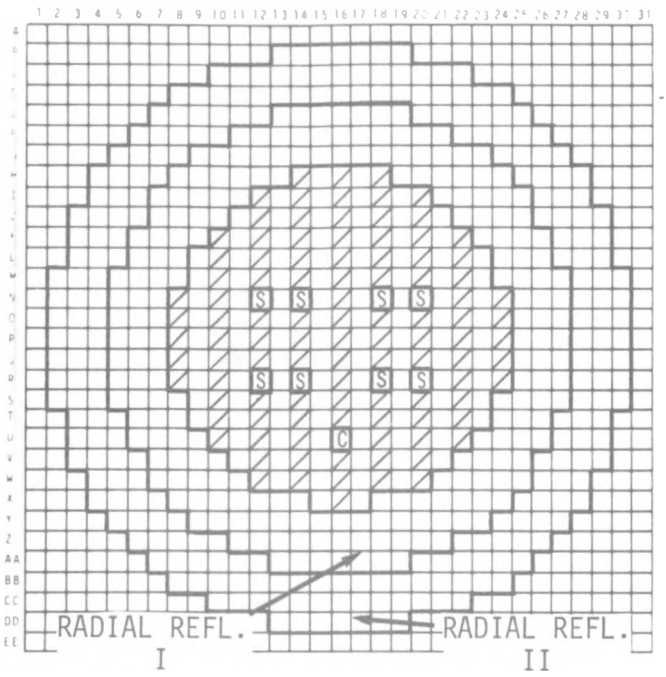

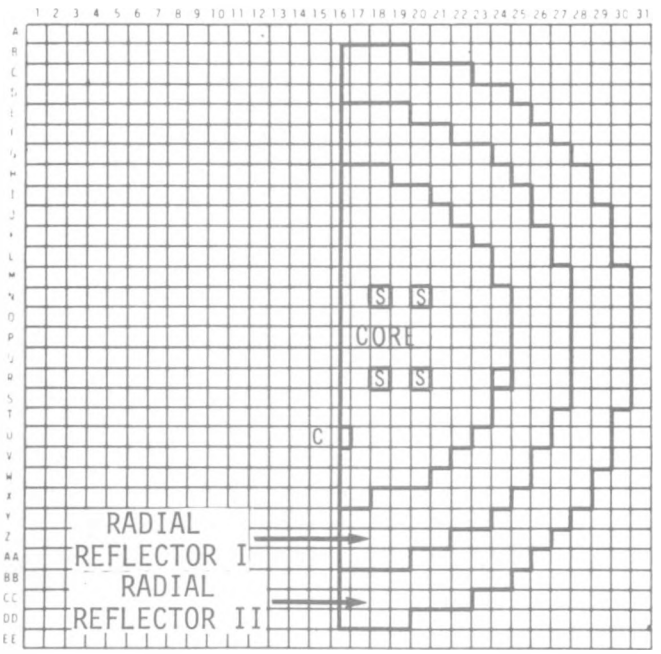

CALCULATIONAL MODEL, FIGURE 3.7

CALCULATION #168-A

EXPERIMENTAL ASSEMBLY # 56B

EFFECTIVE CORE RADIUS 46.231 cm.

CORE HEIGHT 91.59 cm.

REFLECTOR THICKNESS { RADIAL 34 cm. / AXIAL 27.9 cm.

CRITICAL MASS 334.428 kg. ($Pu^{239+241}+U^{235}$)

ABBREVIATIONS:

■ _____ IN HALF #1, _____ IN HALF #2

[S] = SAFETY DRAWER

[C] = CONTROL DRAWER

⧄ = ENRICHED DRAWER OF CELL

OTHER: _____

MEASURED K_{eff} inferred 1.000444

CORE GAP ADJUSTMENT +0.00024

TEMPERATURE " ~~-0.000056~~

SAFETY ROD POSITION +0.000719

ADJUSTED K_{eff} 1.001347±.00012

CALCULATIONAL MODEL

CODE 2DB GEOMETRY XY

DIFFUSION ✓, if S_N, N = _____

SYMMETRY 1/2 core

SOURCE OF ATOM DENSITIES homogeneous,

"X-Y Averaged"

X-SEC. { GROUPS 13 / HOMO./HETERO homogeneous,

CORE HT. 0.0

EFFECTIVE CORE RADIUS 46.231 cm.

REFLECTOR THICKNESS { RADIAL 34 cm. / AXIAL 0.0

BUCKLING $6.35 \times 10^{-4} cm^{-2}$

CALCULATED K_{eff} = 0.98384

CALCULATED MASS = 334.217

DIFFUSION + TRANSPORT S∞ +0.00634

HOMOG. + HETEROGENEOUS +0.01016

OTHER: (1)Norm. Recip. Wt. +0.00194

(2) 26g. → 13 gr. B_z^2 ~~-0.00196~~

(3) mass difference +0.00031

CORRECTED DIFFUSION K_{eff} ~~0.99429~~

CORRECTED TRANSPORT K_{eff} 1.00063 ±.00009

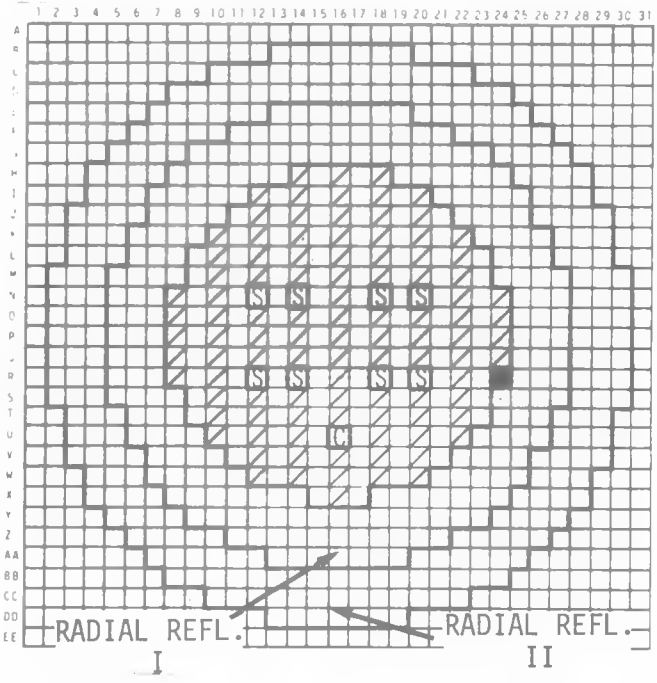

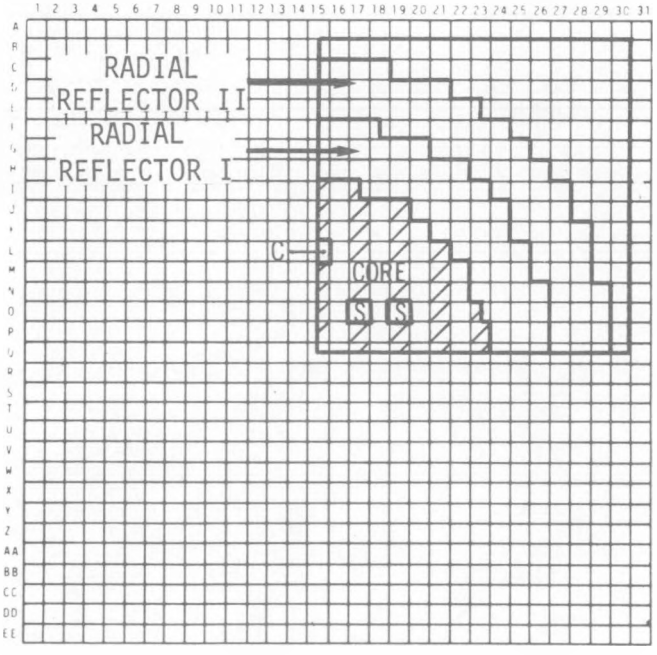

CALCULATION #168C

EXPERIMENTAL ASSEMBLY #56B

EFFECTIVE CORE RADIUS 46.179 cm.

CORE HEIGHT 91.59 cm

REFLECTOR THICKNESS { RADIAL 34cm. / AXIAL 27.9cm.

CRITICAL MASS 333.415 Kg. ($Pu^{239+241}+U^{235}$)

ABBREVIATIONS:

■ core IN HALF #1, refl. IN HALF #2

[S] = SAFETY DRAWER

[C] = CONTROL DRAWER

⊘ = ENRICHED DRAWER OF CELL

OTHER:

MEASURED K_{eff}	0.999964
CORE GAP ADJUSTMENT	+0.00024
TEMPERATURE "	-0.000056
SAFETY ROD POSITION	+0.000719
ADJUSTED K_{eff}	1.000867 ±.00012

CALCULATIONAL MODEL

CODE 2DB GEOMETRY X-Y

DIFFUSION ✓, if S_N, N =

SYMMETRY 1/4 core

SOURCE OF ATOM DENSITIES homogeneous, "X-Y Averaged"

X-SEC. { GROUPS 13 / HOMO./HETERO homogeneous

CORE HT. 0.0

EFFECTIVE CORE RADIUS 46.179 cm.

REFLECTOR THICKNESS { RADIAL 34 cm. / AXIAL 0.0

BUCKLING 6.35×10^{-4} cm^{-2}

CALCULATED K_{eff} =	0.98358
CALCULATED MASS =	333.503 Kg.
DIFFUSION + TRANSPORT S_∞	+0.00634
HOMOG. + HETEROGENEOUS	+0.01016
OTHER: (1) Norm.Recip.wt.	+0.00194
(2) 26g. → 13g. B_z^2	-0.00196
(3) mass difference	-0.00013
CORRECTED DIFFUSION K_{eff}	0.99359
CORRECTED TRANSPORT K_{eff}	0.99993 ±.00009

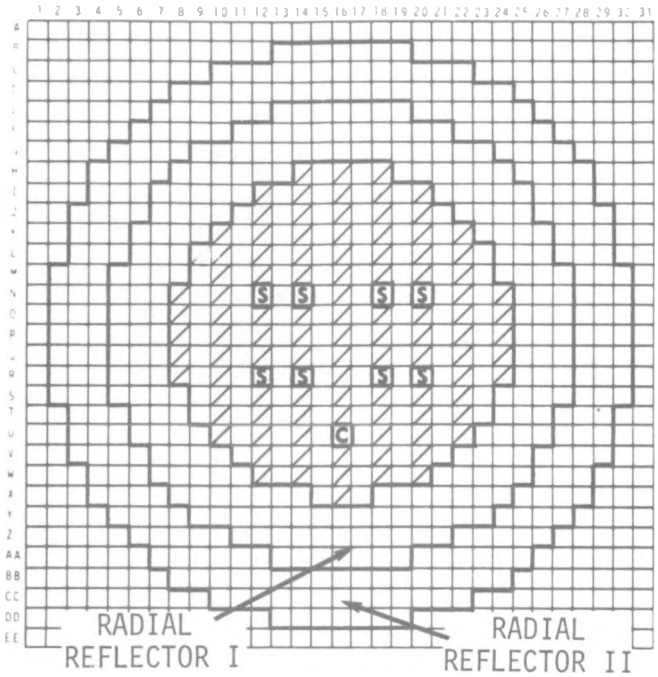

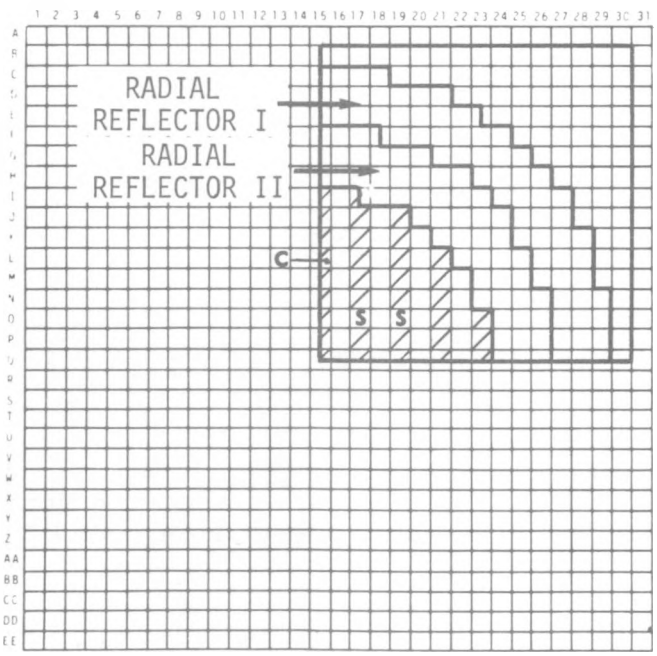

CALCULATIONAL MODEL, FIGURE 3.8

FINE MESH

CALCULATION #168 K1

EXPERIMENTAL ASSEMBLY #56B

EFFECTIVE CORE RADIUS 46.231 cm.

CORE HEIGHT 91.59 cm.

REFLECTOR THICKNESS { RADIAL 34 cm. / AXIAL 27.9 cm.

CRITICAL MASS 334.428 kg. ($Pu^{239+241}+U^{235}$)

ABBREVIATIONS:

■ _____ IN HALF #1, _____ IN HALF #2

[S] = SAFETY DRAWER

[C] = CONTROL DRAWER

⊘ = ENRICHED DRAWER OF CELL

OTHER: _____

MEASURED K_{eff}, inferred 1.000444

CORE GAP ADJUSTMENT +0.00024

TEMPERATURE " -0.000056

SAFETY ROD POSITION +0.000719

ADJUSTED K_{eff} 1.001347 ±0.00012

CALCULATIONAL MODEL

CODE 2DB GEOMETRY X-Y

DIFFUSION ✓, if S_N, N = _____

SYMMETRY 1/4 core

SOURCE OF ATOM DENSITIES homogeneous

"X-Y Averaged"

X-SEC. { GROUPS 13 groups / HOMO./HETERO homogeneous

CORE HT. 0.0

EFFECTIVE CORE RADIUS 46.231 cm.

REFLECTOR THICKNESS { RADIAL 34 cm. / AXIAL 0.0

BUCKLING 6.35×10^{-4} cm.$^{-2}$

CALCULATED K_{eff} = 0.97894

CALCULATED MASS = 334.54 kg

DIFFUSION + TRANSPORT S_∞ +0.00634

HOMOG. + HETEROGENEOUS +0.01016

OTHER: Norm. Recip. Wt. +0.00194

26g.→13g. B_E^2 -0.00196

Mass diffusion -0.00016

CORRECTED DIFFUSION K_{eff} 0.98892

CORRECTED TRANSPORT K_{eff} 0.99526 ±.00009

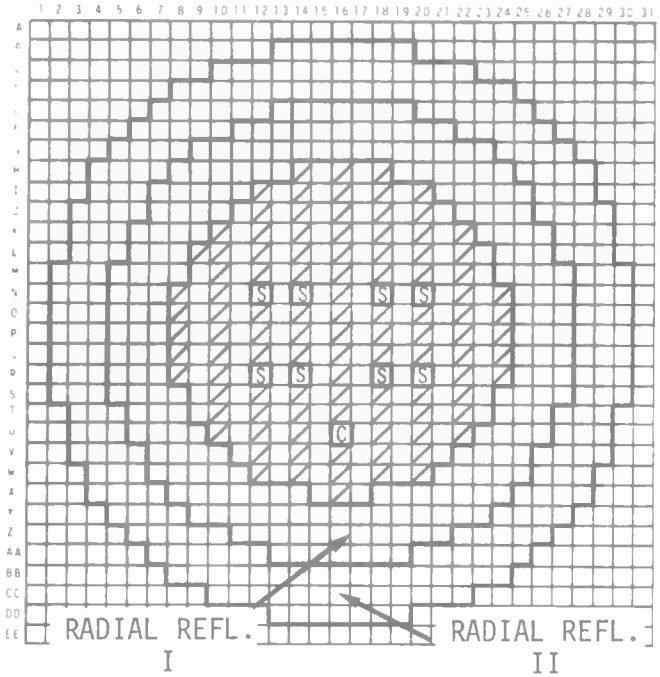

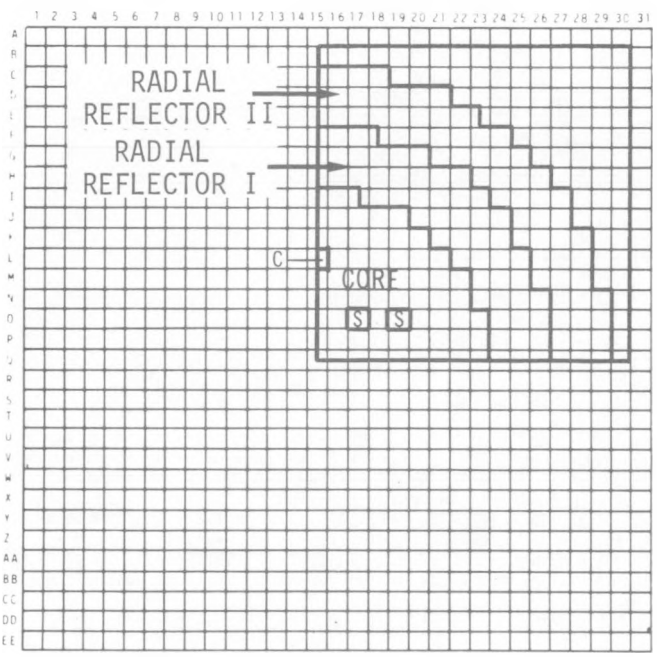

CALCULATIONAL MODEL, FIGURE 3.8
FINE MESH

CALCULATION #168 K-2

EXPERIMENTAL ASSEMBLY # 56B

EFFECTIVE CORE RADIUS 46.281 cm.

CORE HEIGHT 91.59 cm.

REFLECTOR THICKNESS { RADIAL 34 cm. / AXIAL 27.9 cm.

CRITICAL MASS 334.428 Kg. ($Pu^{239+241}+U^{235}$)

ABBREVIATIONS:

■ _____ IN HALF #1, _____ IN HALF #2

[S] = SAFETY DRAWER

[C] = CONTROL DRAWER

⊘ = ENRICHED DRAWER OF CELL

OTHER: _____

MEASURED K_{eff}, inferred 1.000444

CORE GAP ADJUSTMENT +0.00024

TEMPERATURE " -0.000056

SAFETY ROD POSITION +0.000719

ADJUSTED K_{eff} 1.001347 ± .00012

CALCULATIONAL MODEL

CODE 2DB GEOMETRY X-Y

DIFFUSION ✓, if S_N, N = _____

SYMMETRY 1/4 core

SOURCE OF ATOM DENSITIES homogeneous, "X-Y Averaged"

X-SEC. { GROUPS 13 / HOMO./HETERO homogeneous

CORE HT. 0.0

EFFECTIVE CORE RADIUS 46.231 cm.

REFLECTOR THICKNESS { RADIAL 34 cm. / AXIAL 0.0

BUCKLING 6.35×10^{-4} cm^{-2}

CALCULATED K_{eff} = 0.98377

CALCULATED MASS = 334.257kg.

DIFFUSION + TRANSPORT S_∞ +0.00634

HOMOG. + HETEROGENEOUS +0.01016

OTHER: (1) Norm.Recip.Wt. +0.00194

(2) 26g. → 13g. B_o^2 -0.00196

(3) Mass Difference +0.00025

CORRECTED DIFFUSION K_{eff} 0.99416

CORRECTED TRANSPORT K_{eff} 1.00050 ± 0.00009

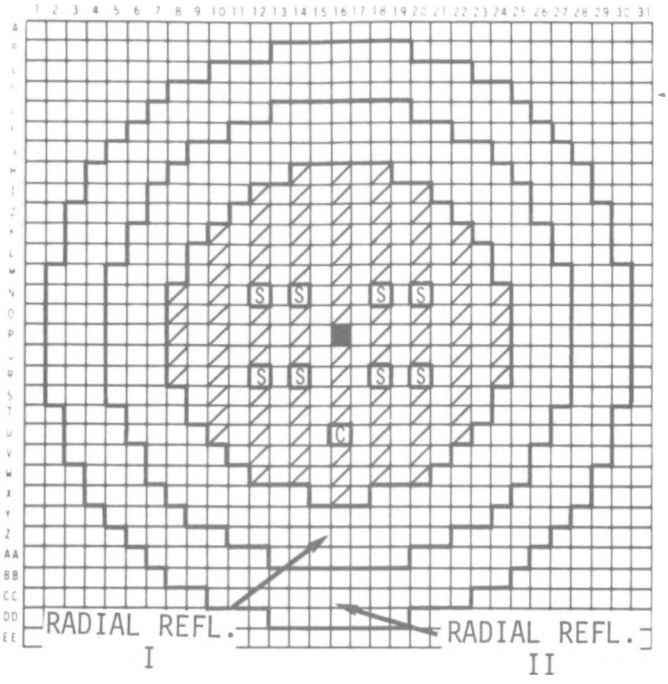

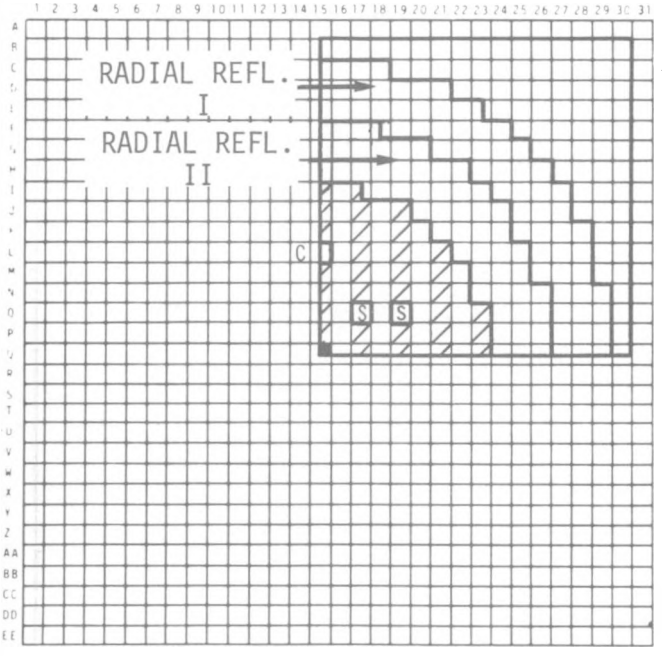

CALCULATIONAL MODEL, FIGURE 3.8
FINE MESH

CALCULATION #168-L

EXPERIMENTAL ASSEMBLY # 56B

EFFECTIVE CORE RADIUS 46.231 cm.

CORE HEIGHT 91.59 cm.

REFLECTOR THICKNESS { RADIAL 34 cm. / AXIAL 27.9 cm.

CRITICAL MASS

ABBREVIATIONS:

Ax. Refl. IN HALF #1, Same IN HALF #2

[S] = SAFETY DRAWER

[C] = CONTROL DRAWER

[⊘] = ENRICHED DRAWER OF CELL

OTHER:

MEASURED K_{eff}

CORE GAP ADJUSTMENT

TEMPERATURE "

SAFETY ROD POSITION

ADJUSTED K_{eff}

CALCULATIONAL MODEL

CODE 2DB GEOMETRY X-Y

DIFFUSION ✓, if S_N, N =

SYMMETRY 1/4 core

SOURCE OF ATOM DENSITIES

Striped zoned Atom densities

X-SEC. { GROUPS 13 / HOMO./HETERO homogeneous

CORE HT. 0.0

EFFECTIVE CORE RADIUS 46.231 cm.

REFLECTOR THICKNESS RADIAL 34 cm. / AXIAL 0.0

BUCKLING 6.35×10^{-4} cm^{-2}

CALCULATED K_{eff} =	0.97315
CALCULATED MASS =	
DIFFUSION + TRANSPORT S∞	+0.00634
HOMOG. + HETEROGENEOUS	+0.01016
OTHER: (1) Norm.Recip.Wt.	+0.00194
(2) 26g. → 13g. See B-7	-0.00196
(3) Mass Difference	-0.00016
CORRECTED DIFFUSION K_{eff}	0.98313
CORRECTED TRANSPORT K_{eff}	0.98847 ± 00009

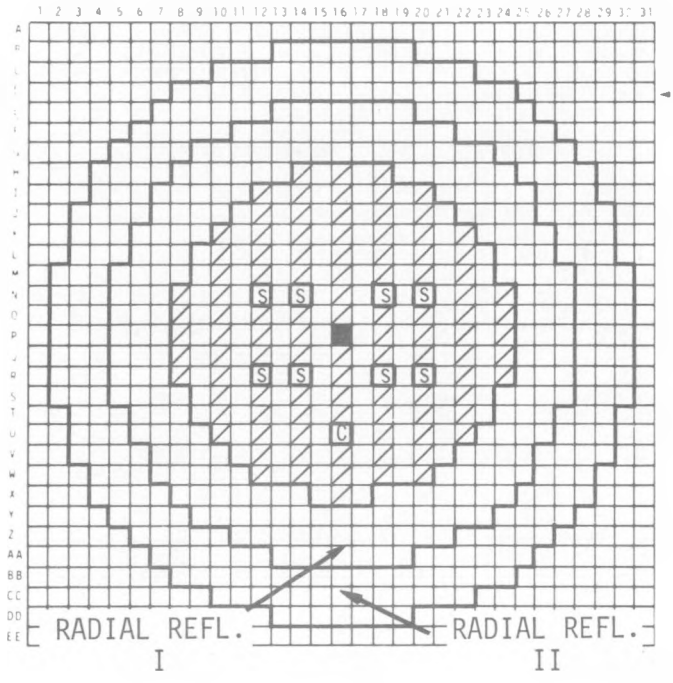

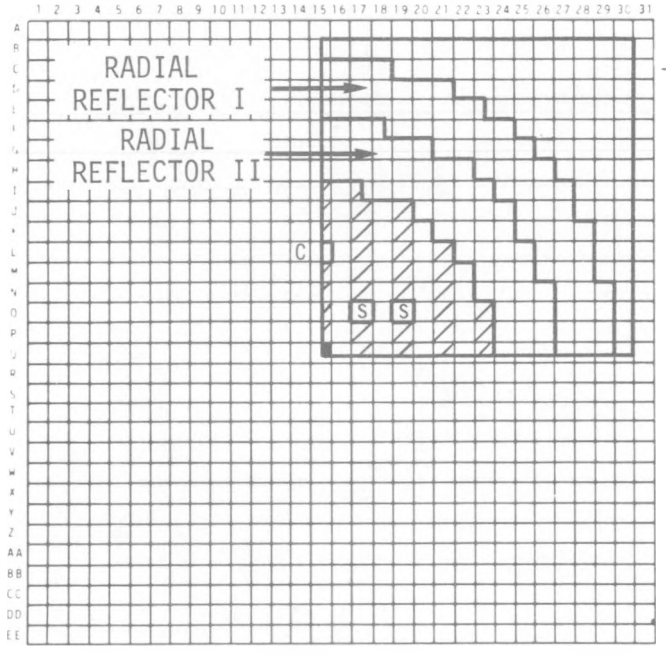

CALCULATIONAL MODEL, FIGURE 3.8
FINE MESH

CALCULATION #167M

EXPERIMENTAL ASSEMBLY #

EFFECTIVE CORE RADIUS 46.23/cm.

CORE HEIGHT 91.59 cm.

REFLECTOR THICKNESS { RADIAL 34 cm. / AXIAL 27.9 cm.

CRITICAL MASS

ABBREVIATIONS:

■ B_4C IN HALF #1, Same IN HALF #2

[S] = SAFETY DRAWER

[C] = CONTROL DRAWER

⧄ = ENRICHED DRAWER OF CELL

OTHER:

MEASURED K_{eff}

CORE GAP ADJUSTMENT

TEMPERATURE "

SAFETY ROD POSITION

ADJUSTED K_{eff}

CALCULATIONAL MODEL

CODE 2DB GEOMETRY X-Y

DIFFUSION ✓, if S_N, N =

SYMMETRY 1/4 core

SOURCE OF ATOM DENSITIES

Striped Zoned Atom Densities

X-SEC. { GROUPS 13 / HOMO./HETERO homogeneous

CORE HT. 0.0

EFFECTIVE CORE RADIUS 46.231 cm.

REFLECTOR THICKNESS { RADIAL 34 cm. / AXIAL 0.0

BUCKLING 6.35×10^{-4}

CALCULATED K_{eff} = 0.96183

CALCULATED MASS =

DIFFUSION + TRANSPORT S_∞ +0.00634

HOMOG. + HETEROGENEOUS +0.01016

OTHER: Norm. Recip. Wt. +0.00194

(2) 26g. → 13gr. B_z^2 -0.00196

(3) Mass Difference (See B-7) -0.00016

CORRECTED DIFFUSION Keff 0.97181

CORRECTED TRANSPORT K_{eff} ~~0.97815 ±.00009~~

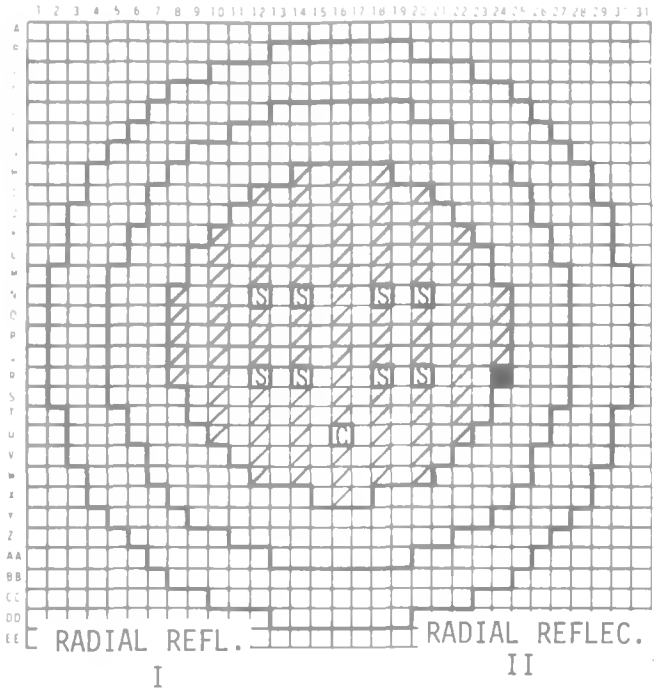

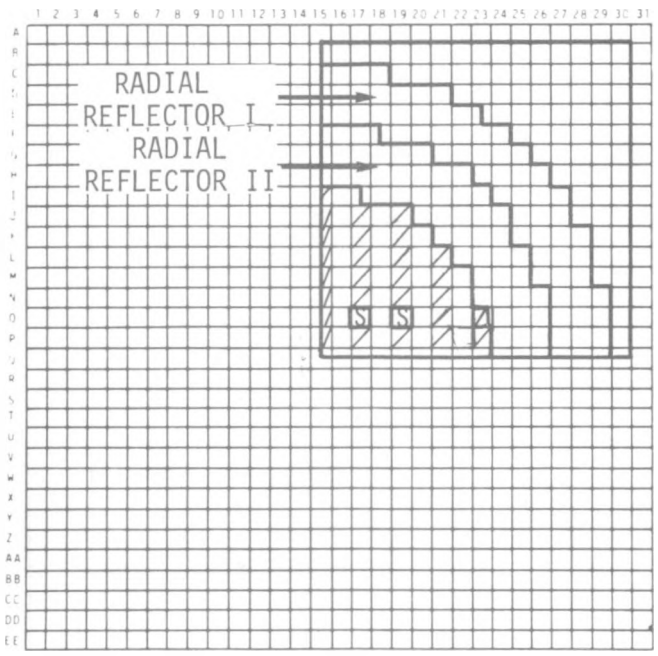

CALCULATIONAL MODEL, FIGURE 3.8
FINE MESH

CALCULATION #168Q

EXPERIMENTAL ASSEMBLY # 56B

EFFECTIVE CORE RADIUS 46.179 cm.

CORE HEIGHT 91.59 cm.

REFLECTOR THICKNESS { RADIAL 34 cm. / AXIAL 27.9 cm.

CRITICAL MASS 333.415 kg. ($Pu^{239+241}+U^{235}$)

ABBREVIATIONS:

■ core IN HALF #1, Refl. IN HALF #2

[S] = SAFETY DRAWER

[C] = CONTROL DRAWER

⊘ = ENRICHED DRAWER OF CELL

OTHER:

MEASURED K_{eff}	0.999964
CORE GAP ADJUSTMENT	+0.00024
TEMPERATURE "	-0.000056
SAFETY ROD POSITION	+0.000719
ADJUSTED K_{eff}	1.000867 ±.00012

CALCULATIONAL MODEL

CODE ~~2DB~~ GEOMETRY X-Y

DIFFUSION ✓, if S_N, N =

SYMMETRY 1/4 core

SOURCE OF ATOM DENSITIES

striped zone atom densities

X-SEC. { GROUPS 13 / HOMO./HETERO homogeneous

CORE HT. 0.0

EFFECTIVE CORE RADIUS 46.179 cm.

REFLECTOR THICKNESS { RADIAL 34 cm. / AXIAL 0.0

BUCKLING 6.35×10^{-4} $cm.^{-2}$

CALCULATED K_{eff} =	0.97847
CALCULATED MASS =	333.513
DIFFUSION + TRANSPORT S∞	+0.00634
HOMOG. + HETEROGENEOUS	+0.01016
OTHER: (1)norm.recip.wt.	+0.00194
(2) 26g. → 13g B_z^2	-0.00196
(3) mass difference	-0.00014
CORRECTED DIFFUSION K_{eff}	0.98847
CORRECTED TRANSPORT K_{eff}	0.99481 ±.00009

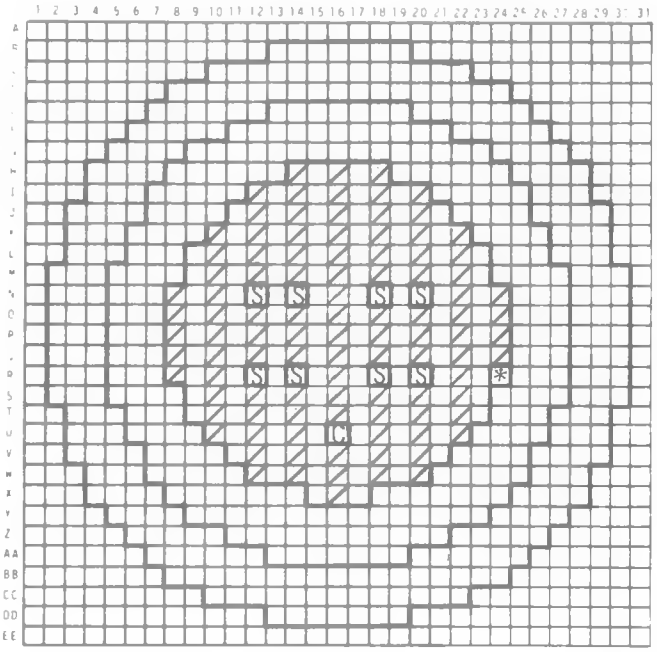

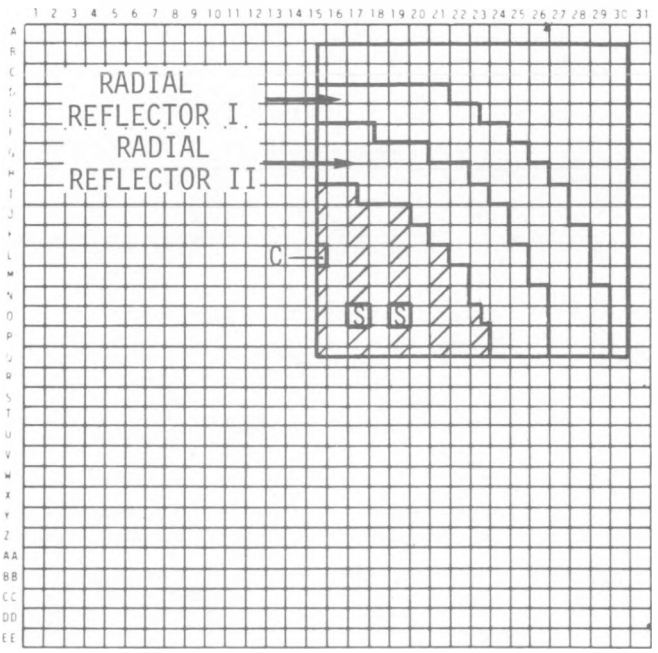

CALCULATIONAL MODEL, FIGURE 3.8
FINE MESH

CALCULATION #168R

EXPERIMENTAL ASSEMBLY # 56B

EFFECTIVE CORE RADIUS 46.179 cm.

CORE HEIGHT 91.59 cm.

REFLECTOR THICKNESS { RADIAL 34 cm. / AXIAL 27.9 cm.

CRITICAL MASS 333.415 Kg ($Pu^{239+241}+U^{235}$)

ABBREVIATIONS:

■ core IN HALF #1, refl. IN HALF #2

[S] = SAFETY DRAWER

[C] = CONTROL DRAWER

⊘ = ENRICHED DRAWER OF CELL

OTHER: Measured (interpolated) worth of fuel-radial ref. Exch. in drawer 2-R-8 0.048 % $\frac{\Delta K}{K}$

CORE GAP ADJUSTMENT

TEMPERATURE "

SAFETY ROD POSITION

ADJUSTED K_{eff}

CALCULATIONAL MODEL

CODE 2DB GEOMETRY X-Y

DIFFUSION ✓, if S_N, N =

SYMMETRY 1/4 core

SOURCE OF ATOM DENSITIES

striped zoned atom densities

X-SEC. { GROUPS 13 / HOMO./HETERO homogeneous

CORE HT. 0.0

EFFECTIVE CORE RADIUS 46.179 cm.

REFLECTOR THICKNESS RADIAL 34 cm. / AXIAL 0.0

BUCKLING 6.35×10^{-4} $cm.^{-2}$

CALCULATED K_{eff} = 0.97459

CALCULATED MASS =

DIFFUSION + TRANSPORT S_∞ +0.00634

HOMOG. + HETEROGENEOUS +0.01016

OTHER: (1) norm.recip.wt. +0.00194

(2) 26g. → 13gr. B_z^2 -0.00196

(3) mass difference (See B-7) -0.00016

CORRECTED DIFFUSION K_{eff} 0.98457

CORRECTED TRANSPORT K_{eff} ~~0.99091 ±.00009~~

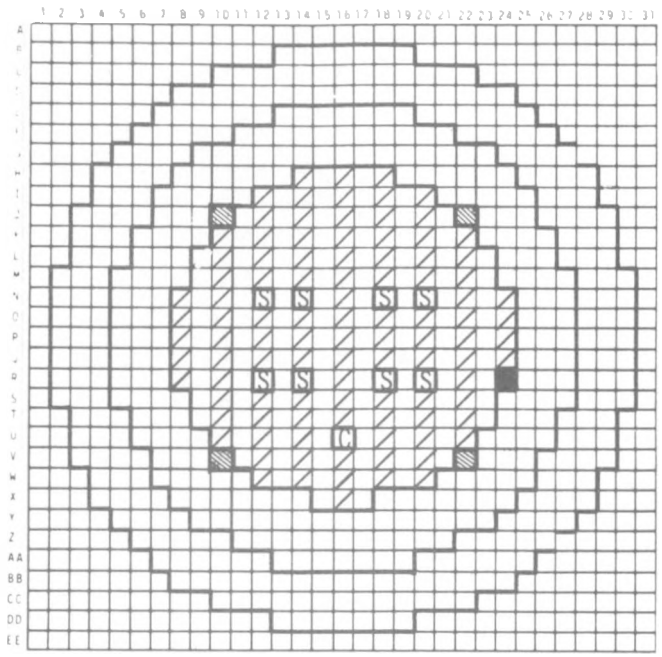

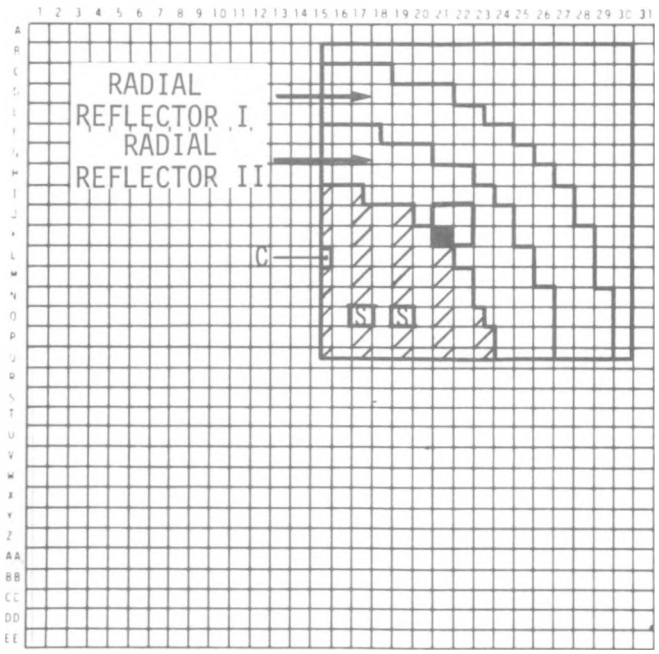

CALCULATIONAL MODEL, FIGURE 3.8
FINE MESH

CALCULATION #168 S

EXPERIMENTAL ASSEMBLY #

EFFECTIVE CORE RADIUS

CORE HEIGHT

REFLECTOR THICKNESS RADIAL
AXIAL

CRITICAL MASS

ABBREVIATIONS:

■ core IN HALF #1, refl. IN HALF #2

[S] = SAFETY DRAWER

[C] = CONTROL DRAWER

⧄ = ENRICHED DRAWER OF CELL

▨ = Nat. B_4C, Na.

OTHER: measured worth of radial refl. B_4C exchange; counter #1 -0.932% $\frac{\Delta K}{K}$

CORE GAP ADJUSTMENT

TEMPERATURE "

SAFETY ROD POSITION

ADJUSTED K_{eff}

CALCULATIONAL MODEL

CODE 2DB GEOMETRY

DIFFUSION ✓, if S_N, N =

SYMMETRY 1/4 core

SOURCE OF ATOM DENSITIES

Striped zone-atom densities

X-SEC. { GROUPS 13
HOMO./HETERO homogeneous

CORE HT. 0.0

EFFECTIVE CORE RADIUS

REFLECTOR THICKNESS RADIAL 34 cm
AXIAL 0.0

BUCKLING 6.35×10^{-4} cm^{-2}

CALCULATED K_{eff} = 0.96942

CALCULATED MASS =

DIFFUSION + TRANSPORT S_∞ +0.00634

HOMOG. + HETEROGENEOUS +0.01016

OTHER: (1)norm. recip. wt. +0.00194
(2)26g. → 13g. B^2 -0.00196
(3)mass difference (see B-11) -0.00014

CORRECTED DIFFUSION K_{eff} 0.97942

CORRECTED TRANSPORT K_{eff} 0.98576 +.00009

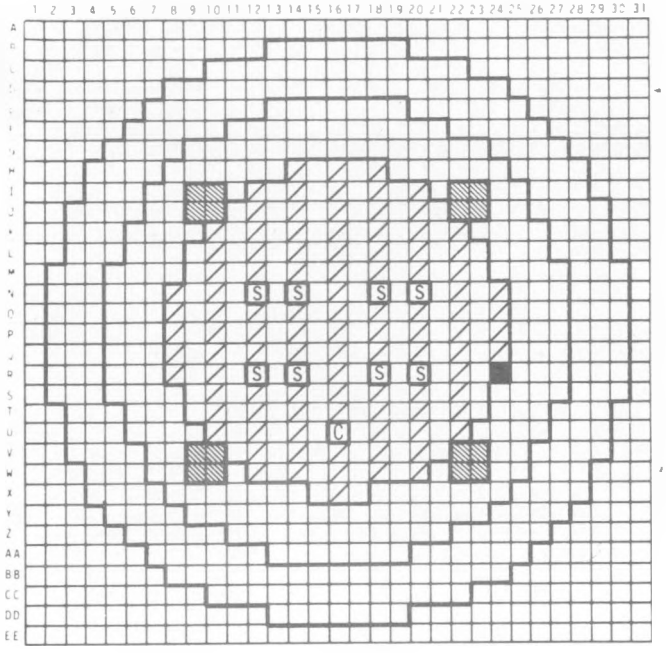

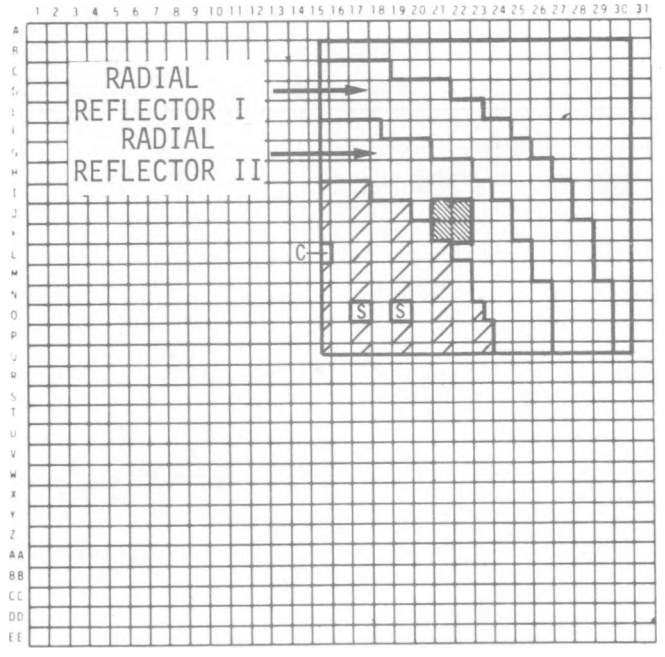

CALCULATIONAL MODEL, FIGURE 3.8
FINE MESH

CALCULATION # 168 T

EXPERIMENTAL ASSEMBLY # 56B

EFFECTIVE CORE RADIUS _____

CORE HEIGHT _____

REFLECTOR THICKNESS RADIAL _____
AXIAL _____

CRITICAL MASS _____

ABBREVIATIONS:

■ core IN HALF #1, refl. IN HALF #2

[S] = SAFETY DRAWER

[C] = CONTROL DRAWER

▨ = ENRICHED DRAWER OF CELL

▩ = Nat. B_4C, Na.

OTHER: measured worth of radial refl. - B_4C exchange, counter #1 -1.736% $\frac{\Delta K}{K}$

CORE GAP ADJUSTMENT _____

TEMPERATURE " _____

SAFETY ROD POSITION _____

ADJUSTED K_{eff} _____

CALCULATIONAL MODEL

CODE 2DB GEOMETRY X-Y

DIFFUSION ✓, if S_N, N = _____

SYMMETRY 1/4 core

SOURCE OF ATOM DENSITIES _____

Striped zone-atom densities

X-SEC. { GROUPS 13
HOMO./HETERO homogeneous

CORE HT. 0.0

EFFECTIVE CORE RADIUS _____

REFLECTOR THICKNESS RADIAL 34.cm.
AXIAL _____

BUCKLING 6.35×10^{-4} cm.$^{-2}$

CALCULATED K_{eff} = .96126

CALCULATED MASS =

DIFFUSION + TRANSPORT S_∞ +0.00634

HOMOG. + HETEROGENEOUS +0.01016

OTHER: norm recip. wt. +0.00194
26g. → 13g. B_2 -0.00196
mass difference (see B-11) -0.00014

CORRECTED DIFFUSION K_{eff} 0.97126

CORRECTED TRANSPORT K_{eff} 0.97760 ±.00009

APPENDIX B-15

The inferred calculated value of k_{eff} of Assembly 56B containing a full fuel column in location R-8 using a calculational model which has 1/4 core, X-Y geometry, homogeneous core zoning, 13 group cross sections and a coarse mesh structure in 2DB is 0.98395.

Although this exact calculation was not made, two calculations having nearly the above description were made. In one, location R-8 was 1/2 filled with fuel and in the second, R-8 was 7/8 filled with fuel.

1. R-8 7/8 filled with fuel k_{eff} = 0.98358 (Appendix B-6)
2. R-8 1/2 filled with fuel k_{eff} = 0.98246

From these calculations it can be inferred that the k_{eff} of a similar calculation, in which location R-8 is totally filled with fuel is 0.98395. Although the last 1/8 of the quarter core R-8 drawer, being further from the core center, will be worth less per 1/8 than the preceeding 3/8 of a drawer, from the worth vs. distance curves of Figure A-2 of Appendix A, it is clear that this worth decrease is negligible and, consequently was not taken into account.

Inferred k_{eff}, calculated:	0.98395
Diffusion - transport:	+0.00634
Homogeneous - heterogeneous:	+0.01016
Normal reciprocal weight:	+0.00194
26 gr. - 13 gr. B_Z^2:	-0.00196
Mass correction (see B-8)	+0.00025
Corrected diffusion k_{eff} =	0.99434
Corrected transport k_{eff} =	1.00068 $\pm$ .00009

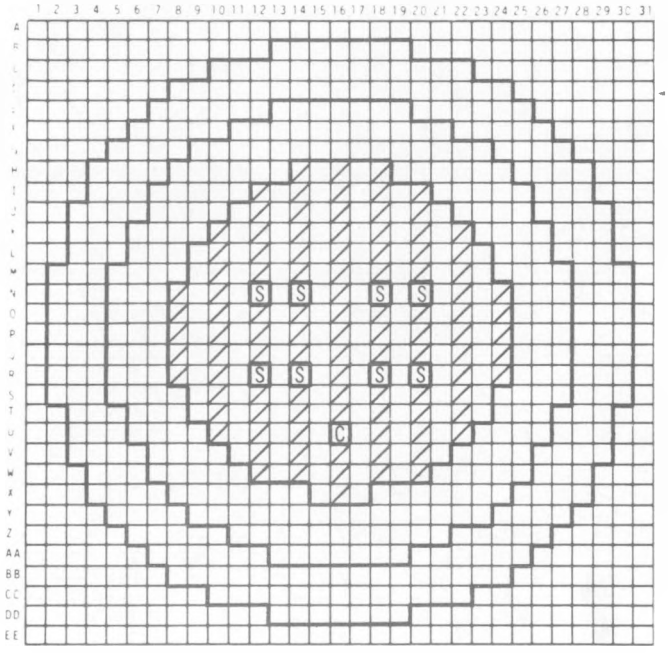

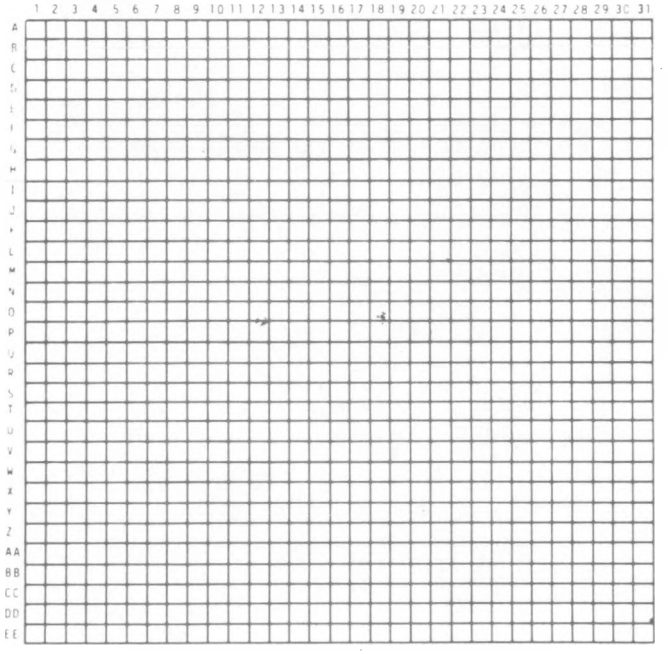

See Figure
Appendix B-3

CALCULATION #167.7A

EXPERIMENTAL ASSEMBLY # 56B

EFFECTIVE CORE RADIUS 45.954 cm.

CORE HEIGHT 91.59 cm

REFLECTOR THICKNESS { RADIAL 34 cm. / AXIAL 27.9 cm

CRITICAL MASS 329.015 Kg. ($Pu^{239+241}+U^{235}$)

ABBREVIATIONS:

■ _____ IN HALF #1, _____ IN HALF #2

[S] = SAFETY DRAWER

[C] = CONTROL DRAWER

⊘ = ENRICHED DRAWER OF CELL

OTHER: _____

MEASURED K_{eff} _____

CORE GAP ADJUSTMENT _____

TEMPERATURE " _____

SAFETY ROD POSITION _____

ADJUSTED K_{eff} _____

CALCULATIONAL MODEL

CODE 2DB GEOMETRY R-E

DIFFUSION ✓, if S_N, N = _____

SYMMETRY 1/2 core

SOURCE OF ATOM DENSITIES homogeneous

"R-Z Averaged"

X-SEC. { GROUPS 26 / HOMO./HETERO homogeneous

CORE HT. 91.59 cm.

EFFECTIVE CORE RADIUS 45.954

REFLECTOR THICKNESS { RADIAL 34 cm / AXIAL 27.9 cm

BUCKLING 0.0

CALCULATED K_{eff} = 0.98307

CALCULATED MASS = 331.18 kg

DIFFUSION + TRANSPORT S∞ +0.00634

HOMOG. + HETEROGENEOUS +0.01016

OTHER: norm.recip.wt. +0.00194

mass difference -0.00320

CORRECTED DIFFUSION K_{eff} 0.99197

CORRECTED TRANSPORT K_{eff} 0.99831 ±.00008

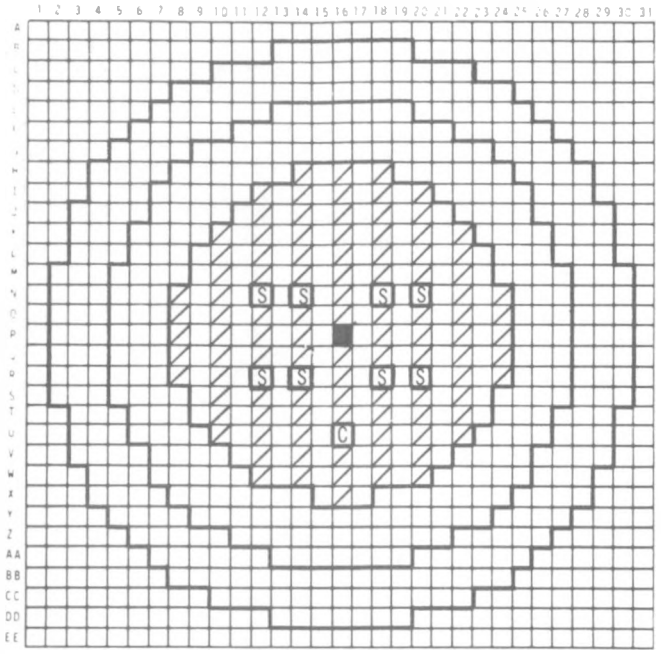

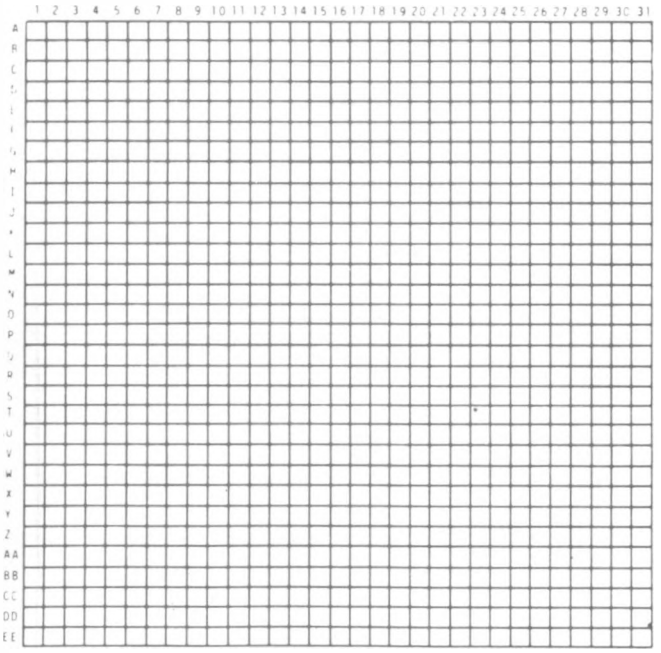

See Figure
Appendix B-3

CALCULATION #167.7-B

EXPERIMENTAL ASSEMBLY # 56B

EFFECTIVE CORE RADIUS 45.954 cm.

CORE HEIGHT 91.59 cm.

REFLECTOR THICKNESS { RADIAL 34 cm.
AXIAL 27.9 cm.

CRITICAL MASS

ABBREVIATIONS:

■ Ax.Ref IN HALF #1, Ax. Ref. IN HALF #2

[S] = SAFETY DRAWER

[C] = CONTROL DRAWER

[⧄] = ENRICHED DRAWER OF CELL

OTHER:

MEASURED K_{eff}

CORE GAP ADJUSTMENT

TEMPERATURE "

SAFETY ROD POSITION

ADJUSTED K_{eff}

CALCULATIONAL MODEL

CODE 2DB GEOMETRY RZ

DIFFUSION ✓, if S_N, N =

SYMMETRY 1/2 core

SOURCE OF ATOM DENSITIES homogeneous;

"R-Z Averaged"

X-SEC. { GROUPS 26
HOMO./HETERO homogeneous

CORE HT. 91.59 cm.

EFFECTIVE CORE RADIUS 45.954 cm.

REFLECTOR THICKNESS RADIAL 34.cm.
AXIAL 27.9 cm

BUCKLING 0.0

CALCULATED K_{eff} = 0.97743

CALCULATED MASS =

DIFFUSION + TRANSPORT S_∞ +0.00634

HOMOG. + HETEROGENEOUS +0.01016

OTHER: norm recip.wt. ~~+0.00194~~

mass difference (see B-16) -0.00320

CORRECTED DIFFUSION K_{eff} 0.98633

CORRECTED TRANSPORT K_{eff} 0.99267 ±.00008

APPENDIX C

CONTROL ROD HETEROGENEITY

APPENDIX C

CONTROL ROD HETEROGENEITY

Rectangular bars of boron carbide used in the FTR Critical Experiments to represent control rods of interest, are usually arranged in patterns that require extremely detailed two dimensional transport calculations in order to represent them precisely. In fact, as much as is possible, diffusion theory homogeneous approximations of the rods are made for calculations. This is known to introduce errors in the calculations.[1] As a prelude to a detailed two dimensional transport analyses of actual rod configurations, a series of comparisons of cylindrical calculations of rod worths have been made.

A single cylindrical control rod, diameter of 3.12 cm, was represented at the center of a cylindrical reactor closely approximating the early FTR Critical, ZPR-III, Assembly 51. Four B_4C arrangements were compared:

1. A homogeneous cylinder of B_4C-Na-SS. R = 3.12 cm.
2. A small ring of B_4C, IR = 1.43 cm, OR = 2.02 cm, imbedded in a homogeneous cylinder of Na and SSt, OR = 3.12 cm.
3. A large ring of B_4C, IR = 2.78 cm, OR = 3.12 cm, surrounding a homogeneous cylinder of Na and SSt.
4. A solid B_4C cylinder R = 1.43 cm, centered in a homogeneous cylinder of Na and SSt, R = 3.12 cm.

For each physical configuration the mass of B_4C, Na, and SS was identically the same. Three enrichments of B^{10} in boron were used to comprise a set of worths. In Table C-1, the % difference in worth given by the exact transport model and alternate models are given for each rod configuration.

To illustrate the contents of Table C-1, the homogeneous diffusion approximation of the solid highly enriched B_4C cylinder overestimates the rod worth by 26.7%.

TABLE C-I

% DIFFERENCE APPROXIMATIONS VS. PRECISE TRANSPORT MODEL

Enrichment	Approximate Model	Rod Configuration: Solid B_4C Cylinder	Rod Configuration: Small Ring	Rod Configuration: Large Ring
Natural (19.2% B^{10})	Transport Homog.	+ 6.22	+ 1.19	-3.03
	Diffusion Homog.	+ 6.02	+ 0.99	-3.22
	Diffusion Heter.	+ 3.32	+ 1.58	0.00
Intermediate (56.1% B^{10})	Transport Homog.	+19.00	+ 5.26	-2.78
	Diffusion Homog.	+21.25	+ 7.27	-0.93
	Diffusion Heter.	+11.61	+ 4.76	+2.31
Highly Enriched (90.7% B^{10})	Transport Homog.	+19.74	+ 7.69	-2.67
	Diffusion Homog.	+26.68	+11.21	+0.53
	Diffusion Heter.	+10.58	+ 7.25	+3.74

In general these calculations illustrate that the sign of the disagreement between the worths given by the approximate models depends upon the extent of the moderating material internal to the rod and upon the degree of enrichment. One may make at least two conclusions:

1. Calculated worths of FTR enriched control rod designs should be determined with transport theory using at least approximate physical models, i.e., B_4C annuli to represent hexagonal arrays of rods.
2. Rod configurations used in critical experiments should be evaluated in detail with good transport approximations. The latter was illustrated in one isolated instance in the analysis of ZPR-III 48 central rod experiments.[1]

APPENDIX D

SPECIFIC ISOTOPES USED IN 56B ANALYSIS

APPENDIX D

SPECIFIC ISOTOPES USED IN 56B ANALYSIS

Isotope Name	Order on Tape #U0509
M3 Pu^{239}	1
Pu^{240}	2
M2 Pu^{241}	49
M2 U^{235}	3
M1 U^{238}	4
O	6
M2 Fe	8
Cr	7
Ni	9
Na	10
Mo	35
Si	24
E4 Mn	65
B^{10}	16
B^{11}	17
C	18